UNIVERSITÀ DEGLI STUDI DI PADOVA
Second Cycle Degree in Environmental Engineering
ICEA Department

Master Thesis
Elisa Burigo

PHOTOCATALYTIC DEGRADATION OF PETROLEUM HYDROCARBONS: LAB SCALE TESTS ON CONTAMINATED SOIL SAMPLES

Supervisors
Prof. Roberto Raga
Prof. Roberta Bertani

Academic Year 2013-2014

LIST OF CONTENTS

LIST OF TABLES

LIST OF FIGURES

1. INTRODUCTION AND THESIS OBJECTIVES

1.1 INTRODUCTION

In recent years, increasing ecological problems, connected with the presence of hydrocarbons in the natural environment are observed.

Hydrocarbons are a class of persistent organic pollutants that are ubiquitous in the environment (Zhang, 2008).

They are considered as hazardous pollutants due to their toxicity and carcinogenicity, and they are classified as compounds with significant human health risk (Zhang, 2008). Anthropogenic activities are their principal sources and the result is the rise of the presence of contaminated sites.

A serious problem connected with remediation of soil contaminated with hydrocarbons is currently faced in Italy.

The objective of this thesis is to perform an innovative method in order to remediate soils contaminated by hydrocarbons. The client is RE.AL.Service spa, a company that deals with contaminated sites remediation, environmental investigation and ecological emergency. The company asks the laboratory of Padua University to investigate the use of the photocatalysis as remediation method for hydrocarbons contaminated soils. It gave to the laboratory 2 samples of soils contaminated by an unknown mixture of hydrocarbons.

The content of the thesis will be the analysis of the feasibility and the efficiency of photocatalytic degradation of hydrocarbons on soil surfaces using TiO_2 under UV irradiation.

Processes which successfully remove and eliminate hydrocarbons from the environment are biological or chemical processes but the former often are ineffective on recalcitrant compounds and need long time and the latter may cause secondary contamination. Hence, it is necessary to search for alternative methods: photocatalysis could be an effective method, easy to perform and clean.

Heterogeneous photocatalysis of organic pollutants using TiO_2 under UV irradiation and/or solar light has demonstrated successful performance in various remediation system of polluted soil (Dong, 2010). The addition of small amounts of TiO_2 enhanced the photodegradation of p,p'-DDT on soil surfaces significantly (Dong, 2010). The photocatalytic

treatment using TiO_2 combined with solar light was very efficient in the destruction of pesticide Diuron in the top 4cm of contaminated soils (Dong, 2010).

Up to now only some research has been performed on hydrocarbons photodegradation. Photocatalytic degradation of hydrocarbons has essentially been studied in different liquid media and in gas phase but little is known about the photochemical behaviour of them on soil surfaces especially in the presence of real polluted soils.

1.2 THESIS OBJECTIVES

In this study the experiments were conducted to investigate the photocatalytic degradation of hydrocarbons present in real polluted soil samples kindly provided by RE.AL Company to the laboratory.

The results of the photocatalytic degradation of hydrocarbons on soil surfaces with the addition of TiO_2 under UV irradiation are reported in this thesis and the possibility of heterogeneous photocatalysis in remediation of hydrocarbons contaminated soils is discussed. Thus, the work focuses on the possible usefulness of photocatalytic processes for the degradation of the mixture of hydrocarbons present in the soil samples.

The main aims to be developed with the present experimental work are presented below.

- Characterization of the catalyst and soil sample.

- Optimization of experimental conditions.

- Analysis of the efficiency of photocatalytic process for the remediation of contaminated soil in particular with hydrocarbons: first attempt to evaluate the effect on photodegradation of the content of catalyst, the presence of a solvent and the use of hydrogen peroxide.

- Development of an experimental procedure for the analysis of the pollutants present in a soil sample.

2. PHOTOCATALYSIS

2.1 DESCRIPTION OF THE PROCESS

Photocatalysis is a degradation process in which a substance, the photocatalyst, changes the speed of a chemical reaction by the action of light.

This phenomenon was discovered in 1972 by Fujishima and Honda, who wanted to split water by the action of sunlight (photelectrolysis), in analogy to what plants do with photosynthesis. For the purpose, they have built a circuit consisting of two electrochemical electrodes immersed in water: a single crystal of TiO_2 and a counter electrode of Pt. After the electrode surface of TiO_2 was illuminated with a radiation wavelength less than 415 nm, they noted a flow of current from counter-electrode platinum to TiO_2 electrode through an external circuit. From the direction of current flow, they concluded that the reaction of oxidation occurs on TiO_2 electrode while the reducing one on the counter electrode platinum. So, according to the experiment conducted by Fujishima and Honda, the water can be split into oxygen and hydrogen using UV-visible light and without applying an external voltage.

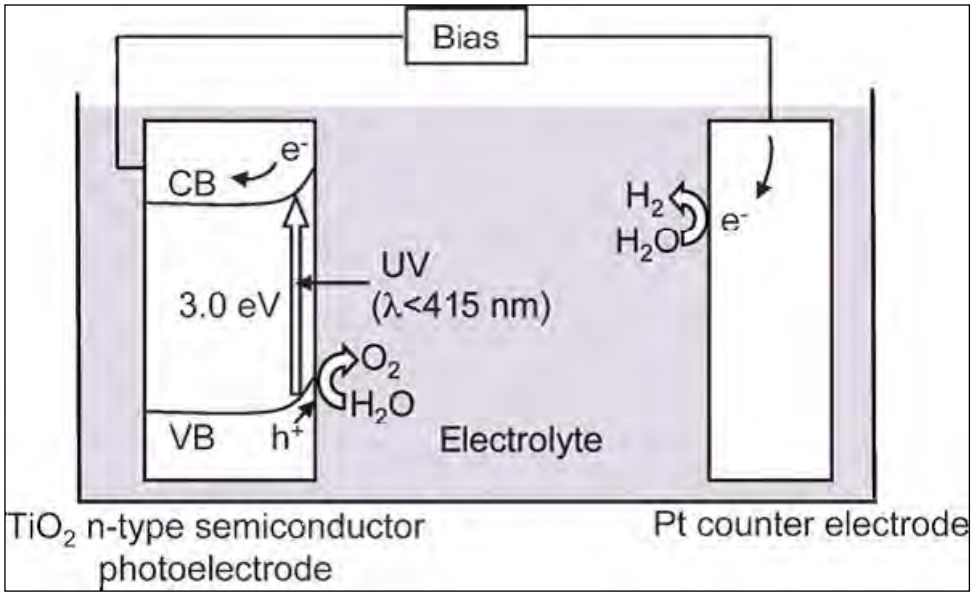

Figure 1: schematic diagram of an electrochemical photocell consisting of TiO2 and Pt electrodes in an aqueous electrolyte. When TiO_2 is irradiated with UV light, electrons and holes are generated. e- reduces water to form H_2 on a Pt counter electrode while h+ oxidize water to form O_2 on the TiO_2 electrode (Kudo, 2009)

$TiO_2 + 2\ h\nu \rightarrow 2\ e^- + 2\ h^+$ (1)

$H_2O + 2\ h^+ \rightarrow ½\ O_2 + 2\ H^+$ (on TiO_2 electrode) (2)

$2\ H^+ + 2\ e^- \rightarrow H_2$ (on Pt electrode) (3)

The overall reaction is:

$H_2O + 2\ h\nu \rightarrow ½\ O_2 + H_2$ (4)

The mechanism of photocatalysis is similar: it uses light energy to make photocatalysts active.

The photocatalysts, after being illuminated by light with the appropriate wavelength, induce the formation of strong oxidizing agents that decompose the organic matter present. Photocatalysis is an accelerator of the oxidation processes already active in nature. The substances which modify the rate of a chemical reaction, through the action of light, are semiconductors.

By definition, a semiconductor is a material with a band structure characterized by a valence band (VB) almost full, separated from the conduction band (CB), almost empty. In semiconductors, the energy difference between the valence band and the conduction band (Energy gap Eg) is approximately less than or equal to 4eV (figure 2). Being the gap small enough, a large number of electrons can be thermally excited from the valence band to the conduction one.

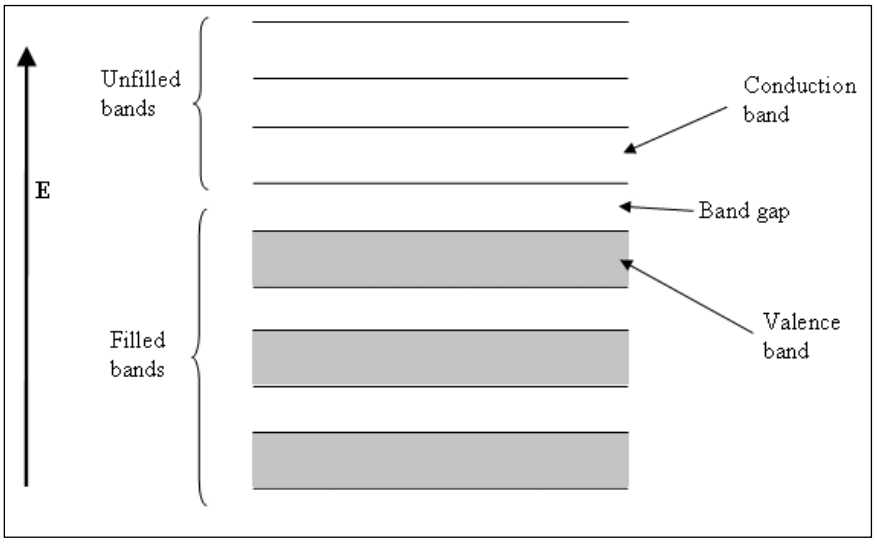

Figure 2: band structure of a semiconductor (Tobaldi, 2009)

Figure 3 shows a schematic representation of the photoexcitation of a semiconductor solid particle by exposure to light radiation with energy above the band gap energy. The excitation, produced by the absorption of a photon is shown by the star symbol. This is followed by the transition of an electron from the valence band to the conduction band: the electron-hole pair is formed and transported to the surface by processes C and D. These e^- and h^+ reduce and oxidize respectively chemical species on the surface of photocatalyst, unless they recombine to give no net chemical reaction but heat (Kaneko, 2002). Processes A and B represent electron-hole pair recombination processes at the surface and in the bulk, respectively.

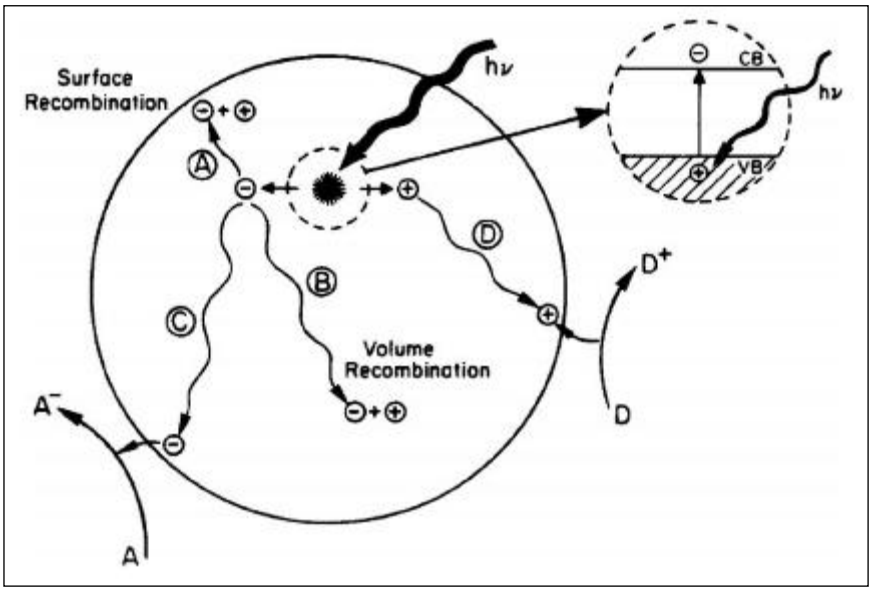

Figure 3: schematic photoexcitation in a semiconductor particle followed by later events (Yates, 2009)

The main reactions involved in photcatalytic process are:

$$\text{semicoductor} + h\nu \rightarrow e^- + h^+ \quad (5)$$

$$e^- + h^+ \rightarrow \text{heat} \quad (6)$$

$$e^- + O_2 \rightarrow O_2^{\bullet -} \quad (7)$$

after the superoxide radical generation:

$$O_2^{\bullet -} + H_2O \rightarrow HO_2 + OH^- \quad (8)$$

$$HO_2 + e^- \rightarrow HO_2^- \quad (9)$$

At the end hydroxyl radicals are formed:

$$OH^- + h^+ \rightarrow OH^{\bullet} \quad (10)$$

The reaction (5) is related to the formation of the photogenerated electron-hole pair in the semiconductor after irradiation, reaction (6) to the recombination of electron-hole pairs on the surface of the particles. The average life time is estimated on the order of a couple of hundred nanoseconds (Graetzel, 1983), in this period of time the electron and hole can reduce, or oxidize, the chemical species adsorbed on the surface of the photocatalytic material.

Because the photocatalytic effect is effective, it is necessary that the reaction (6) is suppressed or at least reduced, in order to favor the reactions (8-10), so that the formed radicals attack the adsorbed organic substrate, beginning in this way the process of photo-oxidation. The species that are formed are strongly oxidizing for example the hydroxyl radicals.

Lacuna h^+ can oxidize the donor molecules (for example, organic substances) or hydroxyl groups on the surface forming OH• radical (the chemical species with the higher oxidizing power), while the electrons can reduce the acceptor molecules, including oxygen which originates the superoxide radical O2• $^-$. These species, very reactive, in their turn may react by oxidizing other molecules, for example organic compounds (Hoffmann, Martin et al. 1995).

The efficiency of the oxido-reduction processes depends, besides the process of charge transfer at the interface, also on the ability of adsorption of substances to degrade on the surface of the photocatalyst particle: this is a critical point of the process, because the radicals that are formed, as extremely reactive, have a short life time and, therefore, have a short diffusion radius in the eventual solution present. Similarly, it is important that the process of desorption of the degraded molecule is fast, so as to let free the active site for a new molecule.

In addition, the effect magnitude depends on the energy of the incident photons, not on their intensity, which means that even a few photons having the necessary energy, are able to stimulate the photocatalytic activity (Tobaldi, 2009).

The photocatalytic reaction, occurring between the photocatalyst and the species adsorbed on its surface, follows a Langmuir- Hinshelwood kinetic, where the reaction rate R is proportional to the extent of overlap of the absorbed species, θ, according to this equation:

$R = dc/dt = k*\theta = k*KC/(1+KC)$

Where k is the reaction constant, K is the adsorption coefficient of the reactant and C the reactant concentration. When the concentration of reactant is low, KC is negligible and the reaction can be modelled as a pseudo first order kinetic.

2.2 THE CATALYST: TiO_2

Photodegradation reactions occur in the presence of nanosized semiconductors: an ideal catalyst must have some minimum requirements: high crystallinity and a larger surface area (Kaneko, 2002) that correspond to a higher rate of surface reaction of e^- and h^+. If the specific surface increases (without changing the surface properties) also the rate increases because it's higher the amount of substrates adsorbed on the photocatalyst.

The most common photocatalyst is titanium dioxide TiO_2 and it is the catalyst used in this thesis work. One of the most important aspects of environmental photocatalysis is the availability of the semiconductor such as TiO_2, which is close to being an ideal photocatalyst in several aspects (Kaneko, 2002): for example it is relatively inexpensive, available in nature, chemically stable, not harmful and with a more efficient photoactivity (Kaneko, 2002).

Feature of the process is the maintenance by the titanium dioxide of its properties: the photocatalysis process takes place without the support is degraded, and a continuous and constant effectiveness over time is guaranteed. The molecule of TiO_2 takes part as catalyst, and not directly to the chemical conversion processes.

Titanium dioxide can crystallize in different polymorphs: anatase, rutile, brookite. The brookite (B in figure 4) has an orthorhombic structure, the other two forms, anatase (A in Figure 4) and rutile (C in Figure 4), which are the most widespread in nature, instead have a tetragonal structure.

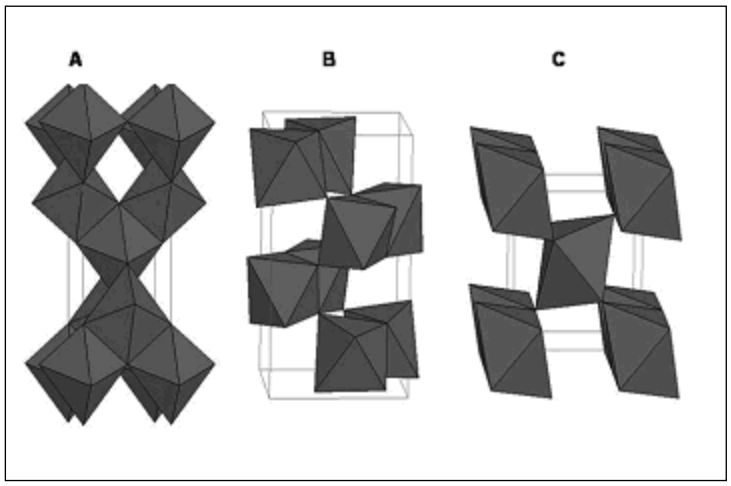

Figure 4: polymorphic forms of titanium oxide, (A) anatase, (B) brookite, (C) rutile. (Battiston, 2010)

The three structures are derived from different polymorphic distortion of the unit base of octahedral symmetry TiO_6, where each titanium atom is at the center of a slightly distorted octahedron whose vertices are occupied by oxygen atoms (Battiston, 2010).

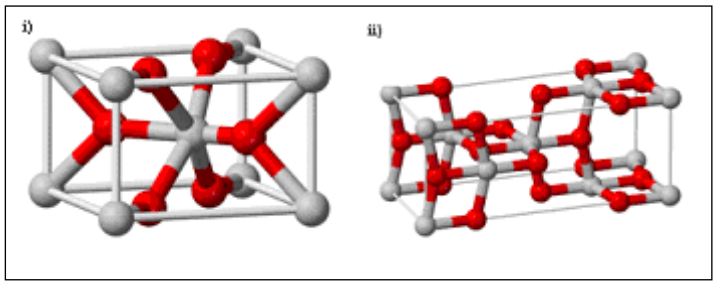

Figure 5: structure of: i) rutile e ii) anatase ; Ti atoms are grey, O atoms are red.

Table 1: some properties of titanium dioxide

	Rutile	**Anatase**	**Brookite**
Molecular Weight (g mol -1)	79.89	79.89	79.89
Crystallyne structure	tetragonal	tetragonal	orthorhombic
Density (g cm-3)	4.2743	3.895	4.123
Eg (eV) in single crystal	3	3.2	/

The phases of interest for photocatalysis are anatase and rutile.

Despite the rutile has lower band gap energy, 3.0 eV in the case of a single crystal, anatase, with band gap energy of 3.2 eV in the case of a single crystal, seems to show the highest photocatalytic activity (Rocca, 2004). The anatase possesses, in fact, a more negative

conduction band of 0.2 eV which provides a greater efficiency in the reduction of oxygen, a higher electron mobility, a lower dielectric constant, a lower density and a low tendency to adsorb permanently oxygen, is also able to accommodate a large number of hydroxyl groups on the surface (Carp, Huisman et al. 2004).

As reported in the literature, the mixture of anatase and rutile exhibits a greater photocatalytic activity compared to the pure anatase, thanks of the combination of the respective energy gap (Eg).

Increasing the efficiency of photocatalytic titanium oxide is one of the main goals of scientific research that has as its object this particular material. It is possible, in fact, acting on different aspects that make up the overall photocatalytic process as, for example, the capacity of absorption and desorption of the molecules on the photocatalyst, the rate of charge transfer at the interface and the absorption spectrum of the material. Titanium dioxide may be doped with different elements especially metal ions such as, for example, the alkaline earth metals Ca^{2+}, Sr^{2+} and Ba^{2+}, transition metals V^{+}, Cr^{+}, Mn^{+}, Fe^{+} (Yamashita H., Harada et al. 2001), Fe^{3+}, Cr^{6+}, Mn^{2+}, Cr^{3+}, Co^{2+}, Co^{3+}, Mo^{5+} (Brezová, Blazkova et al. 1997; Dvoranová, Brezová et al. 2002; Carp, Huisman et al., 2004) and Al^{3+} (Teodorescu, Blanchin et al . 1999), Ga^{3+}, In^{3+} (Wang, Cheng et al. 1999), Ag^{+} (Herrmann, Tahiri et al. 1997), Ru^{3+} (Choi, Termin et al. 2002), Nd^{5+} (Wang, Cheng et al. 1999) , Sb^{5+} (Moon, Takagi et al., 2001) and rare earths (La^{3+}, $Ce3^{+}$, Er^{3+}, Pr^{3+}, Gd^{3+}, Nd^{3+}, Sm^{3+}) (Carp, Huisman et al. 2004).

The photocatalyst used for this study is TiO_2 P25 developed by the company Evonik Degussa. The powder was studied with a trasmission electron microscopy (TEM) and with XRD. The images given by TEM are reported in figure 6: the nominal size of the nanoparticles is about 21 nm and agrees with the features included in the product card present in Evonik database. The specific surface area is about 50±15m2/g (Evonik).

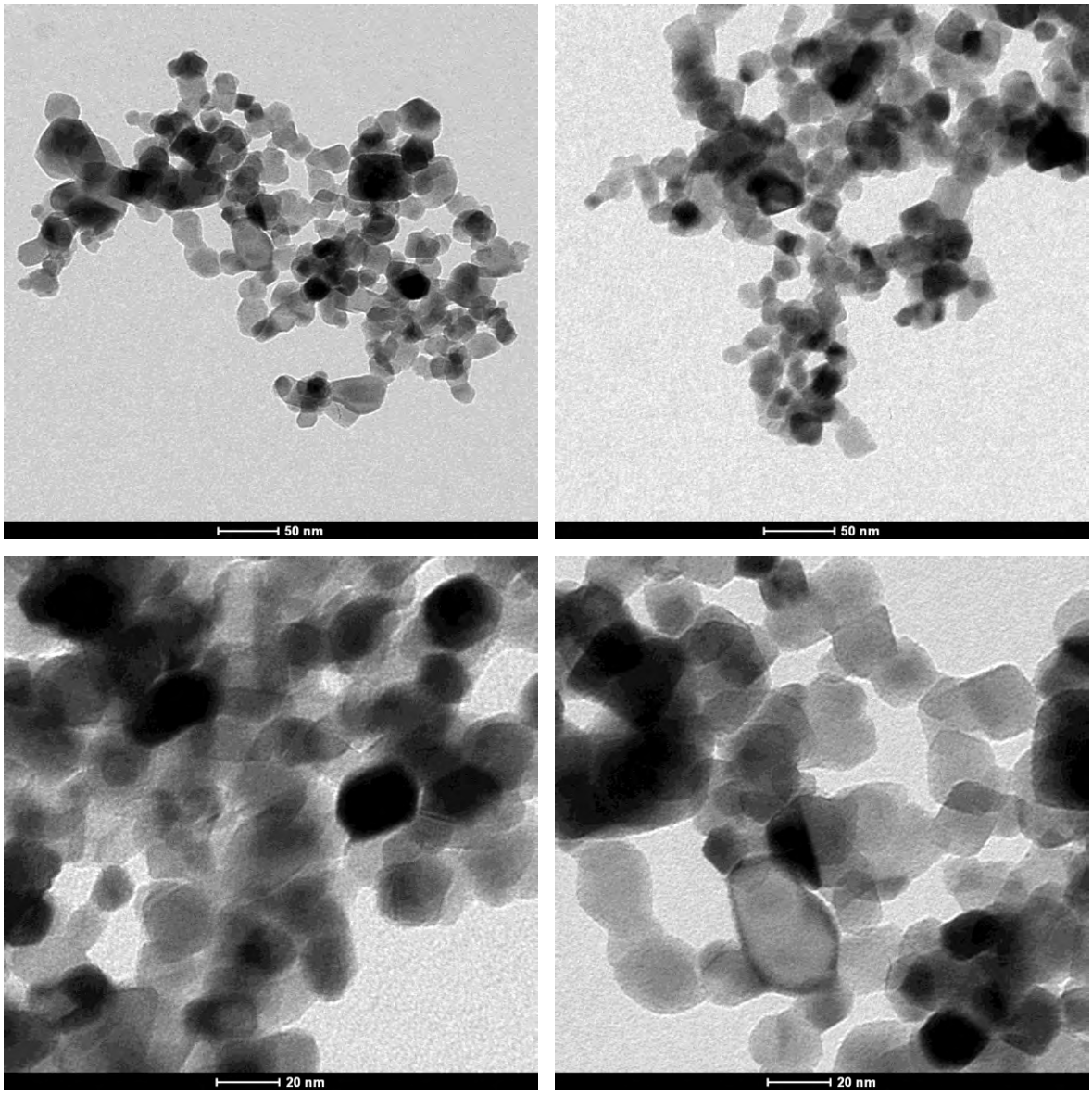

Figure 6: TEM images of TiO_2 P25

The composition of TiO_2 and the ratio between anatase and rutile is evaluated with XRD: it is well known that P25 is composed of anatase and rutile crystallites, but it seems that nobody knows the exact crystalline composition, presumably due to a lack of methodology for determination of crystalline contents in nanometer-sized particulate samples (Ohtani B. et al., 2010).

In figure 7 and in table 2 the diffractogram and the main peaks are reported. Blu line is the difractogram of TiO2 P25 powder, red line regarding anatase phase and green line rutile phase. Peak at 25.30 and 27.45 are related to the main crystallographic plane and respectively the former to anatase and the latter to rutile. Comparing the intensity values

the content of rutile is about 15.8%, in agreement with Evonik product card. The amorphous phase is difficult to quantify but seems to be a small amount.

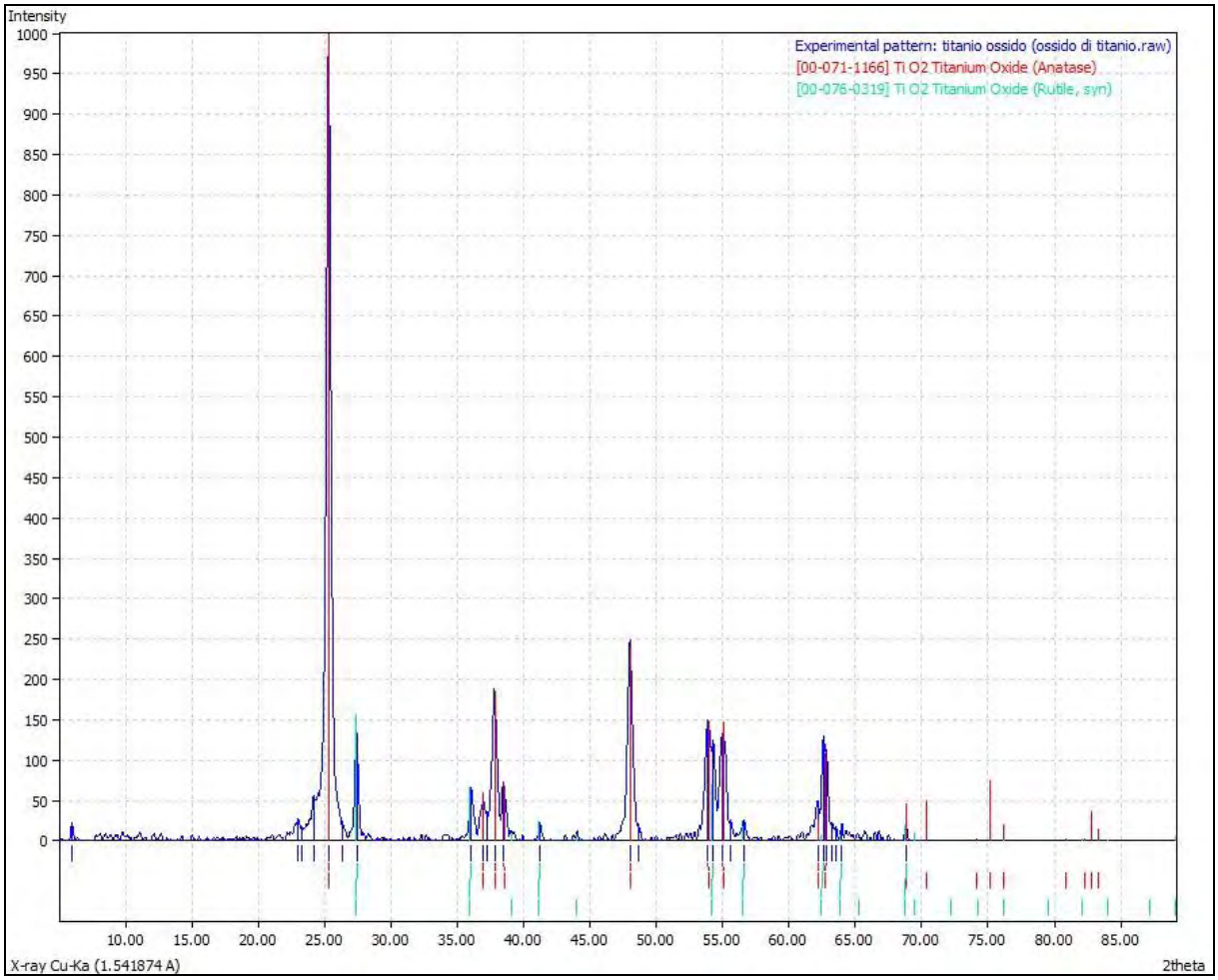

Figure 7: X-ray diffractometer (XRD) pattern of TiO_2 Degussa P25: Blu line is the difractogram of TiO2 P25 powder, red line regarding anatase phase and green line rutile phase.

Table 2: XRD peaks of TiO_2

2theta	intensity
25.3	995.43
27.45	153.73
36.04	78.45
37.8	192.52
38.5	85.27
48.03	276.48
53.98	160.29
54.26	139.09
54.99	140.36
56.66	35.2
62.83	129.76
68.97	72.51

3. STATE OF THE ART IN THE THESIS FIELD

This chapter will give a global vision of the nowadays knowledge about the topic treated in this thesis, reporting the main scientific articles found in literature.

There will be present a brief review of the main experimental works and researches performed in the field of photocatalysis applied to contaminated soil in order to describe the state of the art in this new application.

3.1 *"Photocatalytic degradation of polycyclic aromatic hydrocarbons on soil surfaces using TiO_2 under UV light"*

"Photocatalytic degradation of polycyclic aromatic hydrocarbons on soil surfaces using TiO2 under UV light" is a scientific article written by Lihong Zhang, Peijun Li, Zongqian Gong and Xuemei Li.

They have studied the photocatalytic degradation of phenantrene (PHE), pyrene (PYRE) and benzopyrene (BaP) on soil surfaces in the presence of TiO_2 using ultraviolet light source. The soil samples were spiked in laboratory with methanol solutions of PHE, PYRE and BaP, respectively, mixed thoroughly and then air-dried for the evaporation of methanol. The effects of various factors, as TiO_2, soil pH, humic acids, and UV wavelength, on the degradation performance of polycyclic aromatic hydrocarbons (PAHs) were studied.

Photodegradation studies were performed in a chamber as shown in figure 8: in parallel two arrays of nine UV lamps were fixed in the top and in the middle of the chamber, respectively, with a distance of 150mm from the soil samples. The UV irradiation intensity was 1071 $\mu W/cm^2$. The UV lamps can be changed for wavelength variation. Petri dishes containing 5g of experimental soil samples were placed on the shelves for photoirradiation. Chamber temperature was 30°C maintained by refrigerator heater and fans.

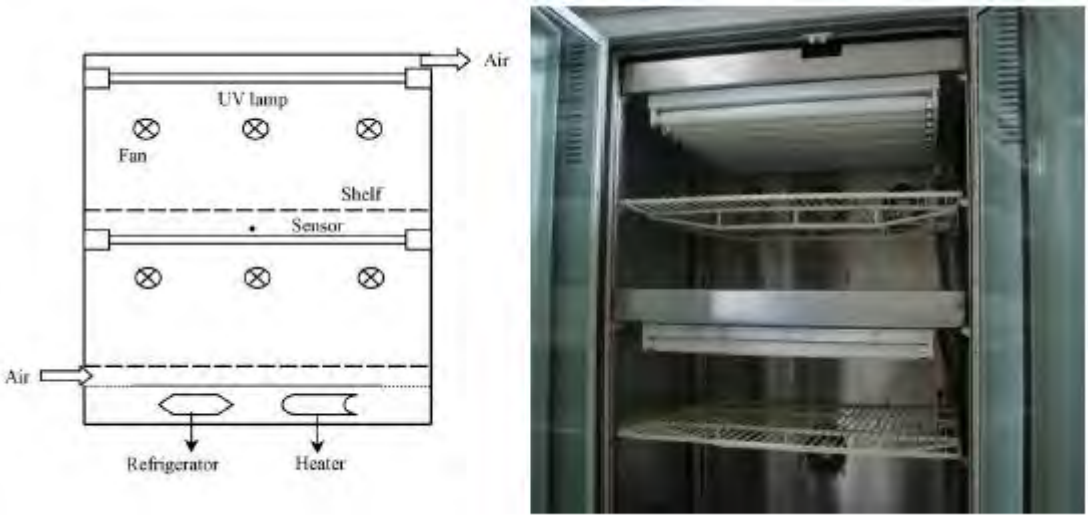

Figure 8: schematic experimental design and chamber for photodegradation of PAHs on soil surfaces

The results show that photocatalytic degradation of PAHs follows the pseudo-first order kinetics. Catalyst TiO_2 accelerated the photodegradation of the hydrocarbons significantly, with their half-lives being reduced drastically compared with the degradation of natural soil without catalysts.

***Table** 3: Kinetic parameters of PAH photocatalytic degradation on soil surfaces at different catalyst concentration*

PAHs	Photo-reactive conditions	k (1×10^{-3} h^{-1})	$t_{1/2}$ (h)	r^2
PHE	Natural soil sample	1.3	533.2	0.92
	TiO_2 (0.5 wt.%)	5.3	130.8	0.93
	TiO_2 (1 wt.%)	5.4	128.4	0.93
	TiO_2 (2 wt.%)	6.0	115.5	0.93
	TiO_2 (3 wt.%)	5.1	135.9	0.94
PYRE	Natural soil sample	1.1	630.1	0.94
	TiO_2 (0.5 wt.%)	3.6	192.5	0.94
	TiO_2 (1 wt.%)	3.7	187.3	0.96
	TiO_2 (2 wt.%)	3.7	187.3	0.97
	TiO_2 (3 wt.%)	3.6	192.5	0.94
BaP	Natural soil sample	1.9	363.2	0.91
	TiO_2 (0.5 wt.%)	6.7	103.3	0.96
	TiO_2 (1 wt.%)	7.2	95.9	0.97
	TiO_2 (2 wt.%)	7.8	89.3	0.96
	TiO_2 (3 wt.%)	7.3	95.0	0.96

In acidic or alkaline conditions, the photocatalytic degradation rates were greater than those in neutral conditions.

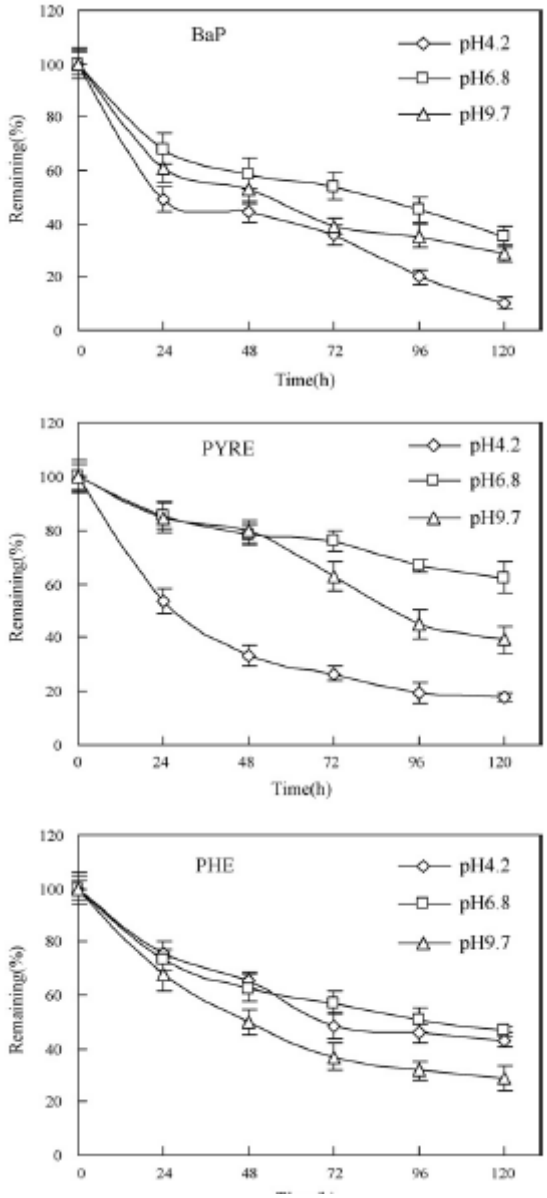

Figure 9: Effect of soil pH on photocatalytic degradation of PAHs on soil surfaces using TiO_2 under UV light

Humic acids (HA) significantly enhanced the PAHs degradation by sensitizing radicals capable of oxidizing PAHs but when the concentration of HA increased from 5 to 40 mg/Kg the rate decreased due to shielding effect of HA, which protested PAHs from incident radiation, thus retarded the photodegradation.

Table 4: Effect of humic acid concentrations on photocatalytic degradation of PAHs on soil surfaces in the presence of TiO_2 under UV light

PAHs	Humic acid (mg kg^{-1})	k (h^{-1})	$t_{1/2}$ (h)	r^2
PHE	0	0.0060	115.5	0.93
	5	0.0113	61.3	0.94
	10	0.0102	68.0	0.95
	20	0.0088	78.8	0.93
	40	0.0071	97.6	0.93
PYRE	0	0.0037	187.3	0.97
	5	0.0179	38.7	0.96
	10	0.0151	45.9	0.96
	20	0.0132	52.5	0.94
	40	0.0119	58.2	0.98
BaP	0	0.0078	89.3	0.96
	5	0.0236	29.4	0.96
	10	0.0212	32.7	0.96
	20	0.0194	35.7	0.98
	40	0.0180	38.5	0.98

The authors concluded that the synergic effect of UV irradiation and TiO_2 catalyst led to the most efficient degradation of PAHs in contaminated soil. Meanwhile some important parameters needed to be monitored in order to control the degradation.

3.2 *"Photocatalytic degradation of phenantrene and pyrene on soil surfaces in the presence of nanometer rutile TiO_2 under UV-irradiation"*

"Photocatalytic degradation of phenantrene and pyrene on soil surfaces in the presence of nanometer rutile TiO_2 under UV-irradiation" is a sceintific article written by Dianbo Dong, Peijun Li, Xiaojun Li, Chengbin Xu, Dawei Gong, Yinqiu Zhang, Qing Zhao and Peng Li. They investigated the photocatalytic degradation on soil surfaces in the presence of nanometer rutile TiO_2 . The soil samples are spiked artificially with phenantrene and pyrene and loaded with different dosages of nanometer rutile TiO_2 (0, 1, 2, 3, 4 wt %).

Photodegradation experiments were conducted in a chamber with UV lamps fixed at the top as shown in figure 10. In all experiments 5g of soil samples were evenly spread on Petri dishes and located in the photodegradation chamber. The height of the lamps above the soil samples was 100mm and the temperature within the chamber was held constant at 25°C using a heater and a fan throughout all the experiments.

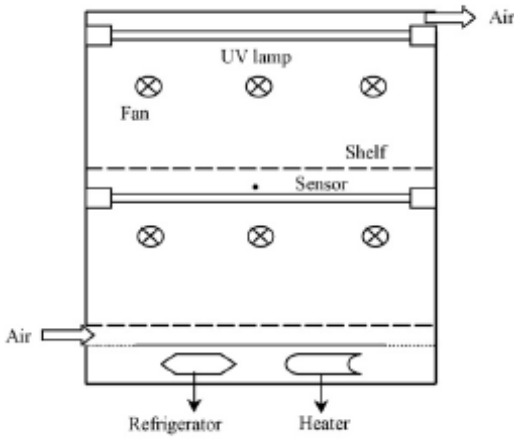

Figure 10: schematic experimental design and chamber for photodegradation of PAHs on soil surfaces

After the exposure to UV irradiation for 25 hours the authors concluded that the optimal catalyst dosage was 2 wt%. In addition they evaluated the effects of different dosages of H_2O_2 (30% content) and humic acids and different light intensity. The degradation of the pollutants increased along with increasing H_2O_2, light intensity and humic acids.

Table 5: Kinetic parameters for the photocatalytic degradation of phenanthrene and pyrene on soil surfaces at different TiO_2 dosages

Compound	Catalyst dosage (wt%)	$k(h^{-1}) \pm$ S.D.	$t_{1/2}$ (h)
Phenanthrene	0	0.0131 ± 0.00014	52.90
	1	0.0137 ± 0.00007	50.59
	2	0.0147 ± 0.00035	47.15
	3	0.0142 ± 0.00021	48.81
	4	0.0139 ± 0.00017	49.86
Pyrene	0	0.0151 ± 0.00007	45.90
	1	0.0162 ± 0.00035	42.78
	2	0.0175 ± 0.00014	39.61
	3	0.017 ± 0.00021	40.77
	4	0.0163 ± 0.00007	42.52

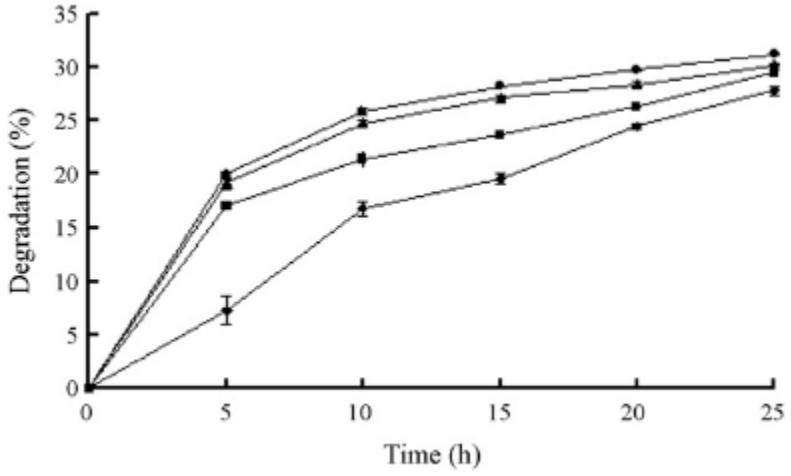

Figure 11: Effect of H_2O_2 on phenanthrene degradation: w/w (♦) 0%, (■) 10%, (▲) 20%, (●) 30%

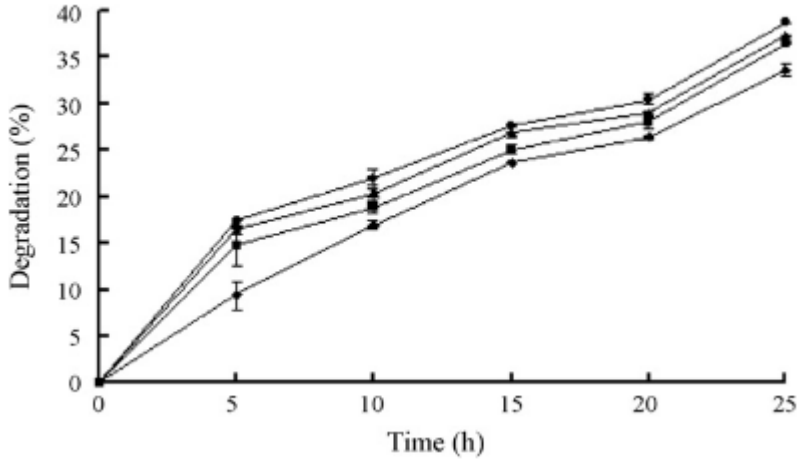

Figure 12: Effect of H_2O_2 on pyrene degradation: w/w (♦) 0%, (■) 10%, (▲) 20%, (●) 30%

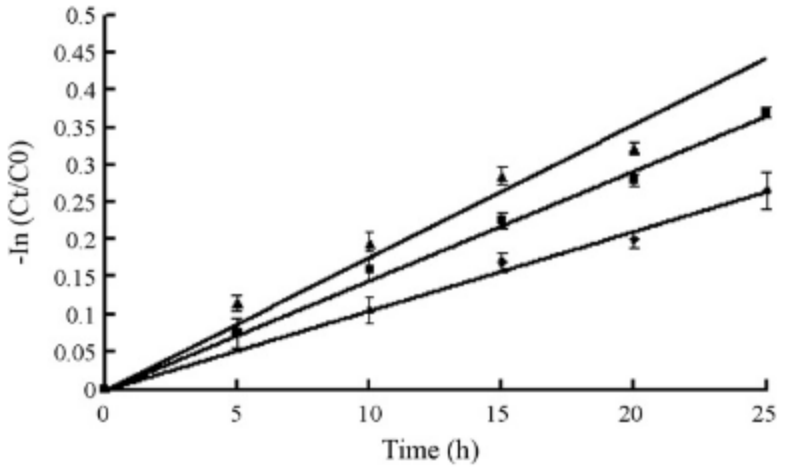

Figure 13: Degradation kinetics of phenanthrene on soil surfaces under different light intensities: (♦) 119 μW/cm², (■) 238 μW/cm², and (▲) 357 μW/cm².

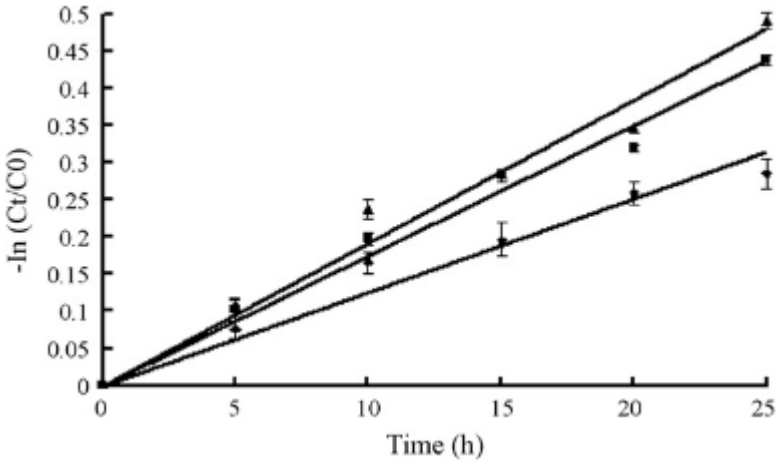

Figure 14: Degradation kinetics of pyrene on soil surfaces under different light intensities: (♦) 119 μW/cm², (■) 238 μW/cm², and (▲) 357 μW/cm².

The authors concluded that the obtained results demonstrate that the phenantrene and pyrene on soil surfaces can be decomposed by the method of photocatalytic degradation in the presence of nanometer rutile TiO_2.

3.3 *"Photocatalytic purification of soil contaminated with oil using modified TiO_2 powders"*

"Photocatalytic purification of soil contaminated with oil using modified TiO_2 powders" is a scientific article written by Maciej Hamerski, Joanna Grzechulska and Antoni Waldemar Morawski. The authors implemented the photocatalysis on TiO_2 for the purification of contaminated soil polluted by oil. In this case the experiments were done applying direct solar light and the catalyst was modified with barium, potassium and calcium to found the more efficient type of doped-TiO_2. All the samples were taken from the open terrain. The experiments were conducted only in sunny days. All samples were accurately mixed and moistoned with water one time per hour, to create the best conditions for a photocatalytic process. Total time of exposure of the samples amounted to 10, 20, 30 and 40 hours. The results of these experiments are presented in figures 15-16.

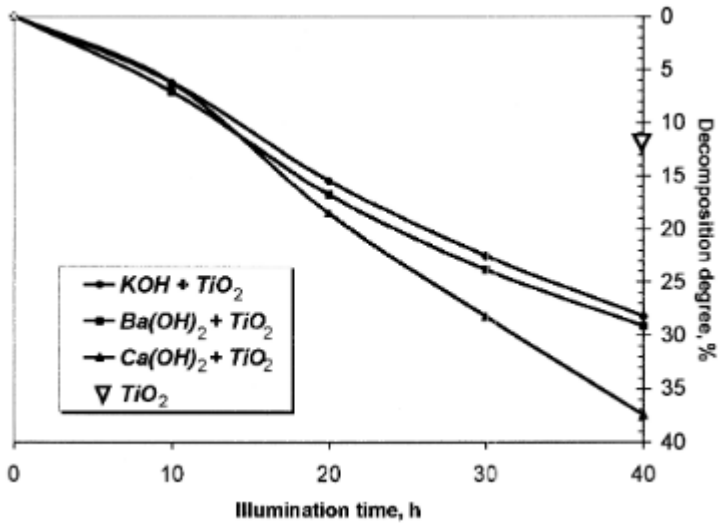

Figure 15: Oil decomposition degree as a function of illumination time

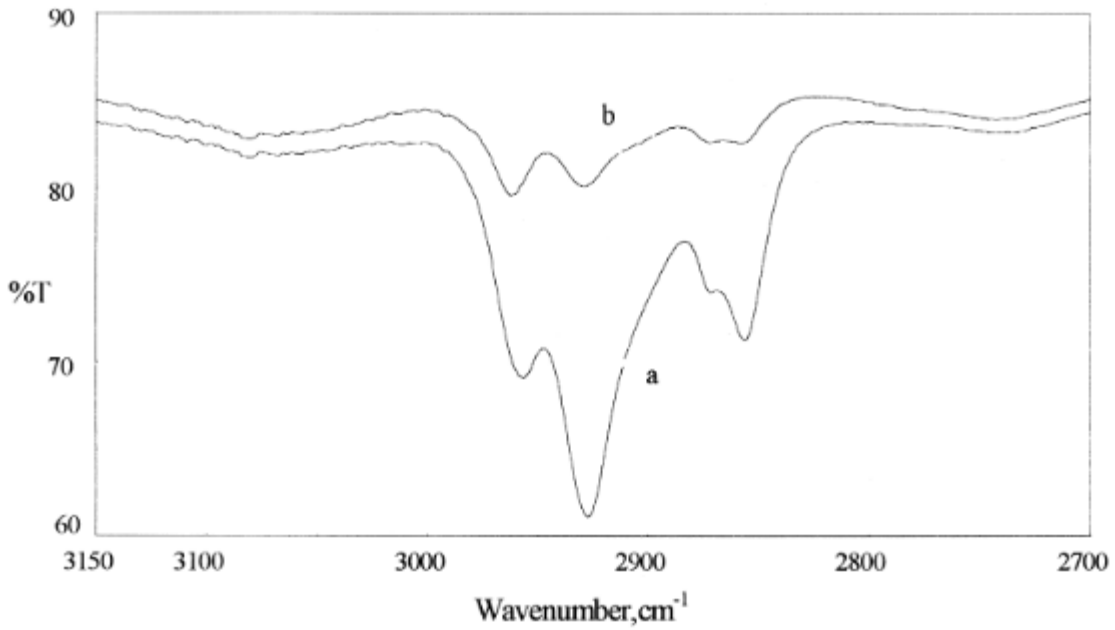

Figure 16: Exemplary FTIR spectra of oil from studied samples: (a) Before the photocatalytic reaction; (b) After the photocatalytic eaction.

The decomposition of oil pollutants during radiation was observed for all the samples and the best degree of oil decomposition was obtained in the case of the catalyst modified with calcium. Moreover the highest degree of oil decomposition was observed during the first hours of the experiment: it can be concluded that it is caused because the reactions occur only on the surface knowing that the sunlight cannot penetrate into the soil.

It is possible to note that the studies conducted up to now confirm the effectiveness of photocatalysis as a method of degradation of hydrocarbons in soil. But all the researches are made on clean soils that were contaminated in the laboratory with specially known mixtures of pollutants. Therefore the contaminants are less deeply adsorbed in the soil particles and easily to degrade. The aim of this work is to investigate if photocatalysis is efficient for real contaminated soil under the laboratory conditions described in chapter 7.

4. MAIN PARAMETERS OF PHOTOCATALYSIS

In this experimental study the main parameters that control the photocatalysis were:

- TiO_2 dosage: the dosage of catalyst is an important parameter in photocatalytic degradation process. In literature to determine the optimal dosage of photocatalyst, various dosage of TiO_2 (0, 1, 2, 3 and 4 wt %) were used to investigate the photocatalytic activity of TiO_2 toward degrading the phenatrene and pyrene on soil surfaces. Adequate dosage of TiO_2 increases the generation rate of electron-hole pairs; thus, the formation of superoxide radical anion ($O_2^{\bullet -}$) for enhancing the photodegradation (Dong, 2010). However, an excess dosage decreases the light penetration via increasing the depth of soil and hence reduces photocatalytic rate (Dong, 2010).
- Light intensity: UV light intensity is an important factor in the photocatalytic degradation. Under the higher light intensity, the enhancement is considerably higher because that electron-hole formation is predominant and, hence, electron-hole recombination is negligible (Dong, 2010). To adjust the irradiation intensity it is possible to work on the UV lamps power, on the number of the lamps but also on the distance between the sample and the light sources.
- Moisture percentage: the presence of humidity in the sample is one of the main parameters to be considered in order to increase the efficiency of photodegradation processes. In fact an increase of the moisture of the sample corresponds to an increase of the photocatalytic rate because the mobility of the catalysts is higher with a consequent greater contact between contaminants and active sites of catalyst. The presence of a carrier is necessary to bring together the substrate onto the catalyst surface and this is normally achieved by increasing the amount of water in this medium. Additionally water molecules can further react in the surface of the catalyst by oxidation in the hole (h+) and generate OH° radicals, thus increasing the rate of degradation (Higarashi, 2002).
- Time of exposure
- Initial concentration of pollutants

In the thesis work the main parameters will be evaluated and discussed each time under the laboratory conditions.

5. INSTRUMENTAL METHODS

FT-IR: Fourier transform infrared spectrometer

The FT-IR spectroscopy is a vibrational absorption spectroscopy: when a molecule is struck by an IR beam of appropriate wavelength, this induces a variation in the level of vibrational energy by lengthening or shortening the chemical bond (stretching), or by changing the 'bond angle (bending). This absorption is characteristic of each functional group, which allows to use this phenomenon for qualitative analysis.

Gruppo	n (cm^{-1}) stretching
O-H	3650-2500
N-H	3550-3050
C-H	3040-2840
C ≡ C	2260-2100
C=O	1850-1630
C=C	1690-1590
C-O	1300-1060
C-C	1200-800

Figure 17: characteristic bands of the main functional groups

In this study a FT-IR PerkinElmer Spectrum100 was used and for the interpretation and analysis of the spectra the OMNIC program was adopted.

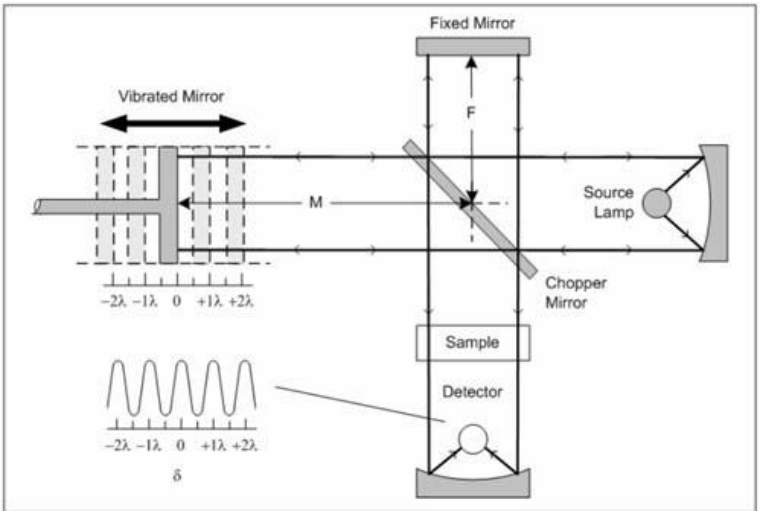

Figure 18: general scheme of FT-IR device

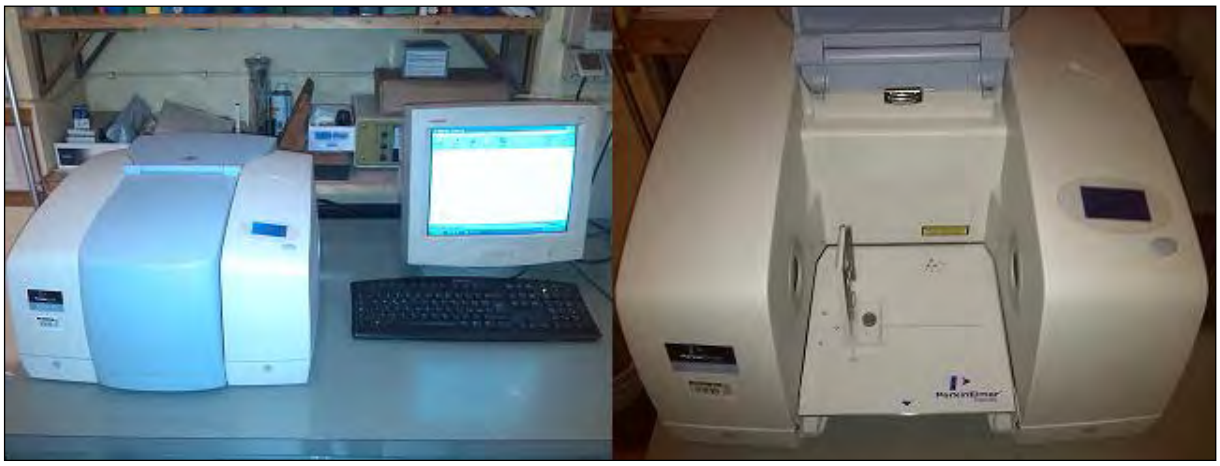

Figure 19: FT-IR PerkinElmer Spectrum100

EXTRACTIONS WITH SOLVENTS

Extraction is a separation process consisting in the separation of a substance from a matrix. The hydrocarbons present in the soil are extracted with different solvents. The extraction depends on the polarity (affinity) of the solvent. The soil sample is put in a flask with a predefined quantity of solvent and then the mixture is mixed with a magnetic stirrer. After the desired time of mixing, the mixture is filtered with a filtering round paper (pore size 4 - 7 µm) (Whatman filter n° 597) in order to separate the liquid phase from the solid one. The extracted hydrocarbons will be present in the liquid ready for further quantitative analysis.

Figure 20: extraction steps: mixing, filtering, drying

ROTAVAPOR

Rotavapor is a device used for the removal of solvents from samples by evaporation. The main components of a rotary evaporator are:

- an evaporation flask containing the solution to be evaporated
- a thermostatic bath, in which plunges the evaporation flask to keep the solution to a suitable temperature
- a vacuum system, to substantially reduce the pressure within the evaporator system
- a motorized mechanism, able to put in rotation the evaporation flask
- an inclined condenser that provides to knock down the vapors which developed
- a condensate-collecting flask at the bottom of the condenser, to catch the distilling solvent after it re-condenses.

The flasks, the capacitor and connecting elements between these are made of glass, and the entire system mounted must guarantee a perfect vacuum seal.

The device used for the research was a rotavapor BÜCHI Waterbath B-480.

Figure 21: rotavapor BÜCHI Waterbath B-480

SEM: scanning electron microscope

The scanning electron microscope (SEM) is a type of electronic microscope that uses a focused electron beam to analyze a small square area of the sample by moving along subsequent parallel lines. Some electrons are reflected (scattering) and some others penetrate the surface of the sample and are absorbed by the atoms producing electrically excited ions; these ions can return at their fundamental state through secondary electrons emissions (fluorescence). These emissions can be detected and analyzed in order to obtain information on the typology and composition of the sample. In particular the measurement of secondary electrons allows to study the morphology of the sample while the measurement of backscattered electrons in addition to producing an image of the sample gives information on its composition because their emission is related to the atomic number of the elements present.

For this thesis was used an Environmental SEM model XL-30 (Philips) which differs from SEM because the chamber where the sample is placed can work at low void pressure instead of high void pressure as in SEM and it's closer to the column of electrons beam.

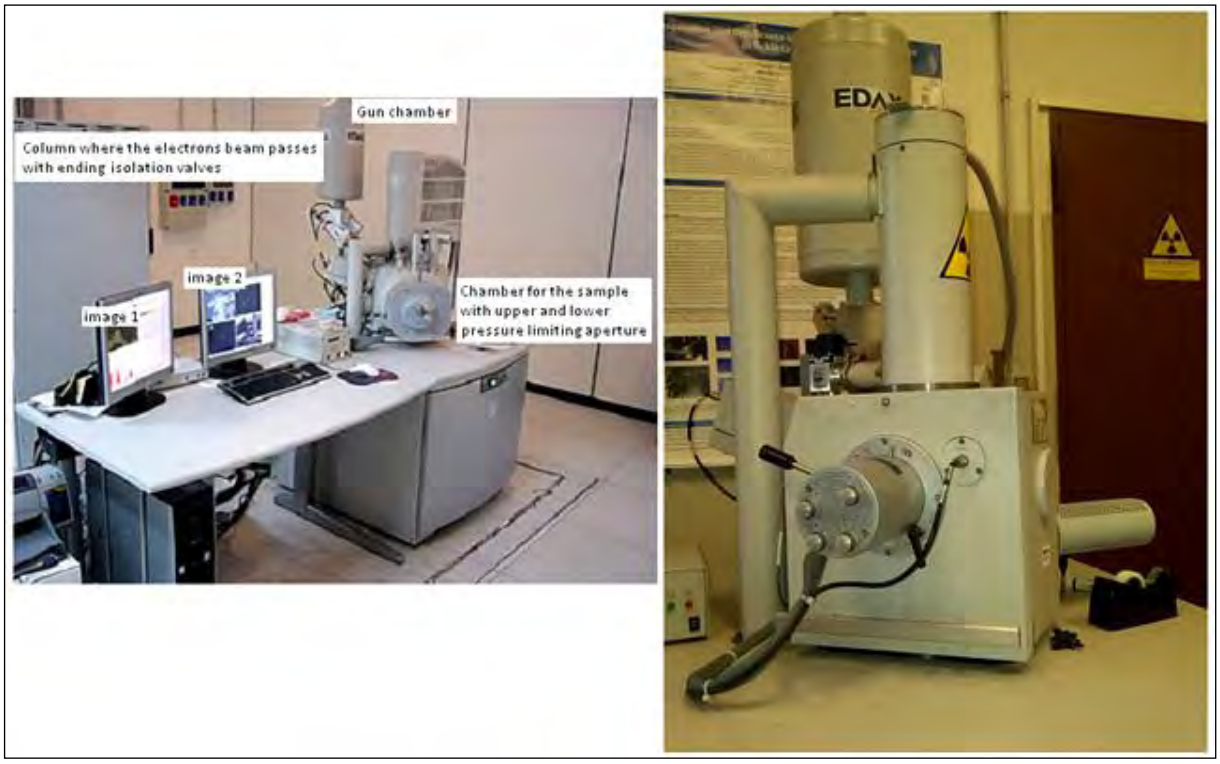

Figure 22: Environmental SEM model XL-30 (Philips)

GC-MS: Gas chromatography–mass spectrometry

Gas chromatography–mass spectrometry (GC-MS) is an analytical method that combines the features of gas-liquid chromatography and mass spectrometry to identify different substances within a test sample. The difference in the chemical properties between different molecules in a mixture and their relative affinity for the stationary phase of the column will promote separation of the molecules as the sample travels the length of the column. The molecules are retained by the column and then elute (come off) from the column at different times (called the retention time), and this allows the mass spectrometer downstream to capture, ionize, accelerate, deflect, and detect the ionized molecules separately.

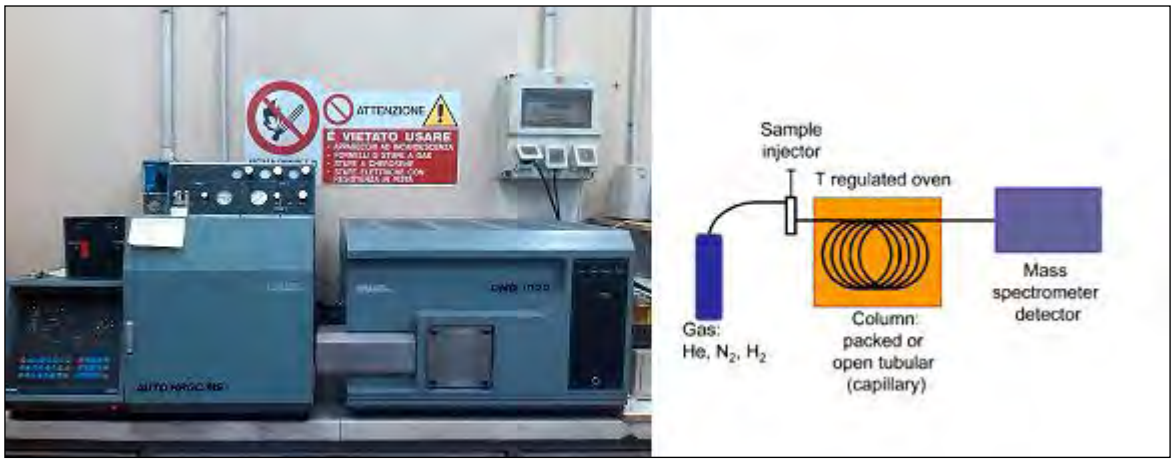

Figure 23; Carlo Erba GC-MS and general operational scheme

The GC-MS analysis was carried out using a Carlo Erba Instruments AUTO / HRGC / MS 1000 MS, as a gas chromatograph coupled to a mass spectrometer detector Carlo Erba Instruments MS QMD 1000. The interpretation of the chromatogram was performed with the aid of the program management of the instrument, equipped with the NIST and Wiley libraries.

UV-VIS spectrophotometer

An UV-VIS spectrophotometer is used for the measurement of transmittance of solutions allowing to estimate the concentration of a substance from a reading of absorbance (at a fixed wavelength). This mechanism exploits the Lambert-Beer law that states the direct proportionality between absorbance and concentration.

The instrument used was a Perkin Elmer Lambda 25, a dual beam spectrophotometer: inside there are two slots for cells: one for the cuvette containing the solvent alone and the other for the cuvette containing the sample solution. An electronic system performs matching on automatically each absorption wavelength of the two cells and subtracts the value of the absorption of the solvent to that of the solution. So the value of the absorption of the solute is got.

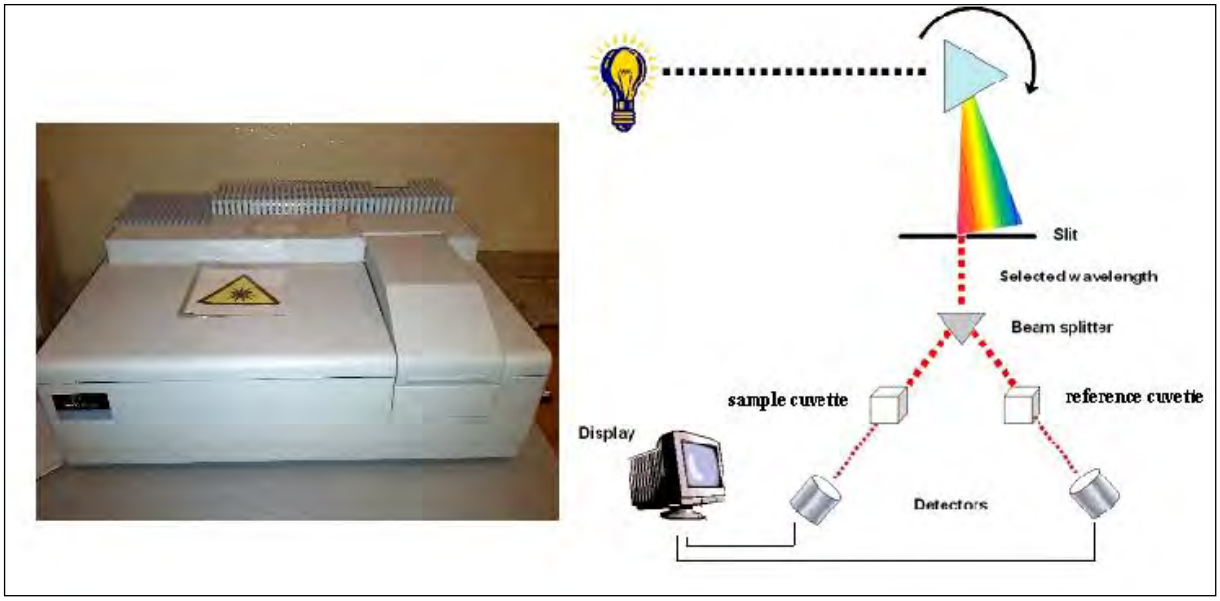

Figure 24: Perkin Elmer Lambda 25 and general operational scheme

X-RAY DIFFRACTION device

The X-ray diffraction (XRD) is a non-destructive technique used for the qualitative and quantitative analysis of crystalline materials in solid state. Using this analytical technique it is possible record the X-rays diffracted by crystalline materials. Each material produces a diffraction spectrum that forms a fingerprint making possible the identification of an unknown material for comparison with a library of spectra of known substances. Basically

the X-ray diffraction is obtained as a reflection of a beam of X-rays from a family of atomic planes parallel and equidistant, following Bragg's law.

$$2d \text{ sen } \theta = n\lambda$$

$$d = \lambda / 2\text{sen } \theta$$

d is the spacing between diffracting planes, θ is the incident angle, n is any integer, and λ is the wavelength of the beam.

When a beam of monochromatic X-rays with a wavelength (wavelength of the radiation that is produced by an X-ray tube) is incident on a lattice plane with an angle θ there is a diffraction if the path of the rays reflected by successive planes (with a distance d) and a multiple of the wavelength. The study of the intensity of diffraction at various angles (setting by the device) allows to identify the symmetry of the crystal and the size of its unit cell.

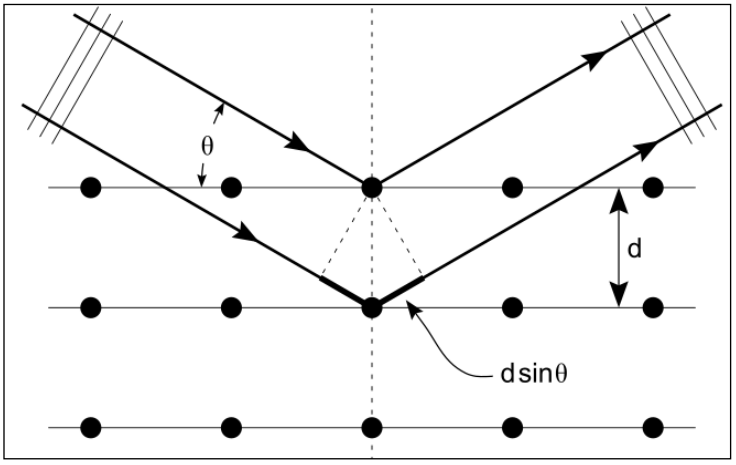

Figure 25: scheme of X-ray diffraction

6. CHARACTERIZATION OF THE SAMPLE

The soil given by the client was contaminated with an unknown mixture of hydrocarbons. Various analysis were made in order to investigate and analyse the mixture of pollutants present in the sample and the nature of soil:

- FT-IR
- Extractions with different solvents and subsequent GC-MS analysis
- SEM
- XRD

The spectrum given by the FT-IR analysis of the soil sample is reported in figure 26. The characteristics infrared bands for hydrocarbons are between 2800 and 3000 cm^{-1}.

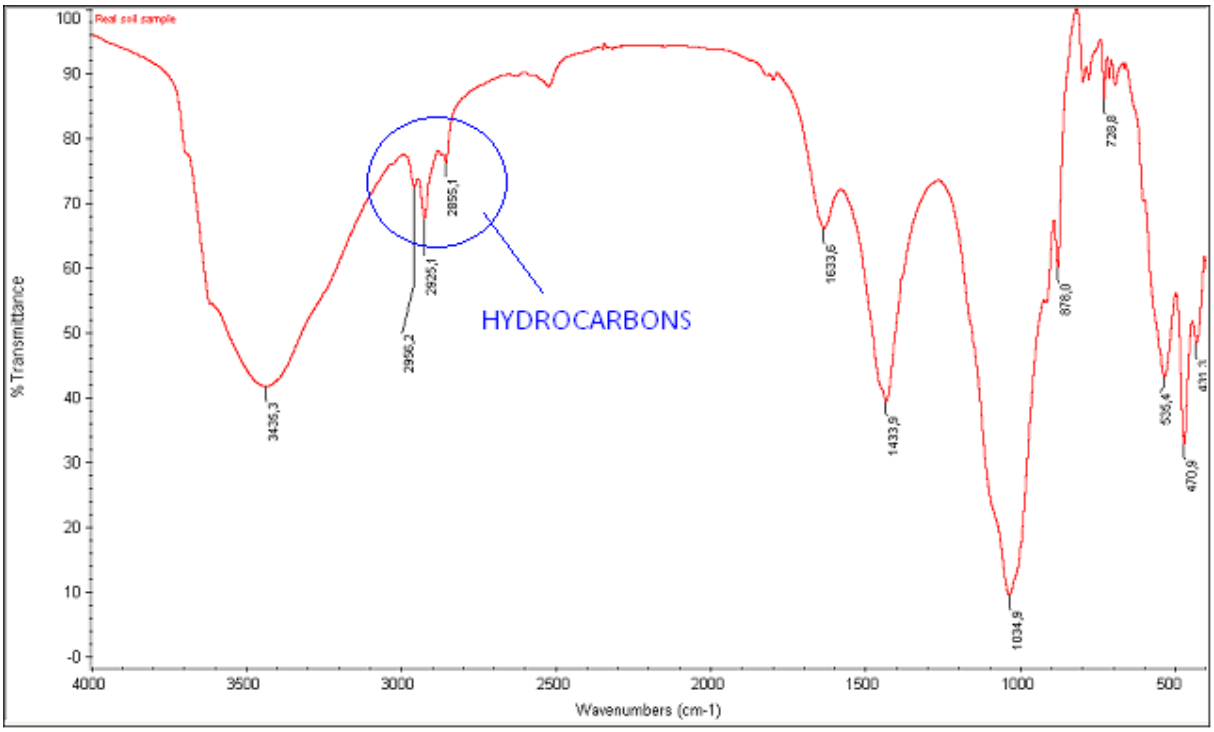

Figure 26: FT-IR of Real sample

The series of 3 extractions was made with 3 different solvents of different polarity: first hexane, second dichloromethane and third acetone. It was used 100g of sample in 200ml of

solvent. The objective of the extractions was to try to extract all the hydrocarbons from the polluted sample for the subsequent identification of each kind of compound and the analysis of the clean soil matrix. In figure 27 is reported the IR spectrum of the liquid resulting from the extraction in hexane.

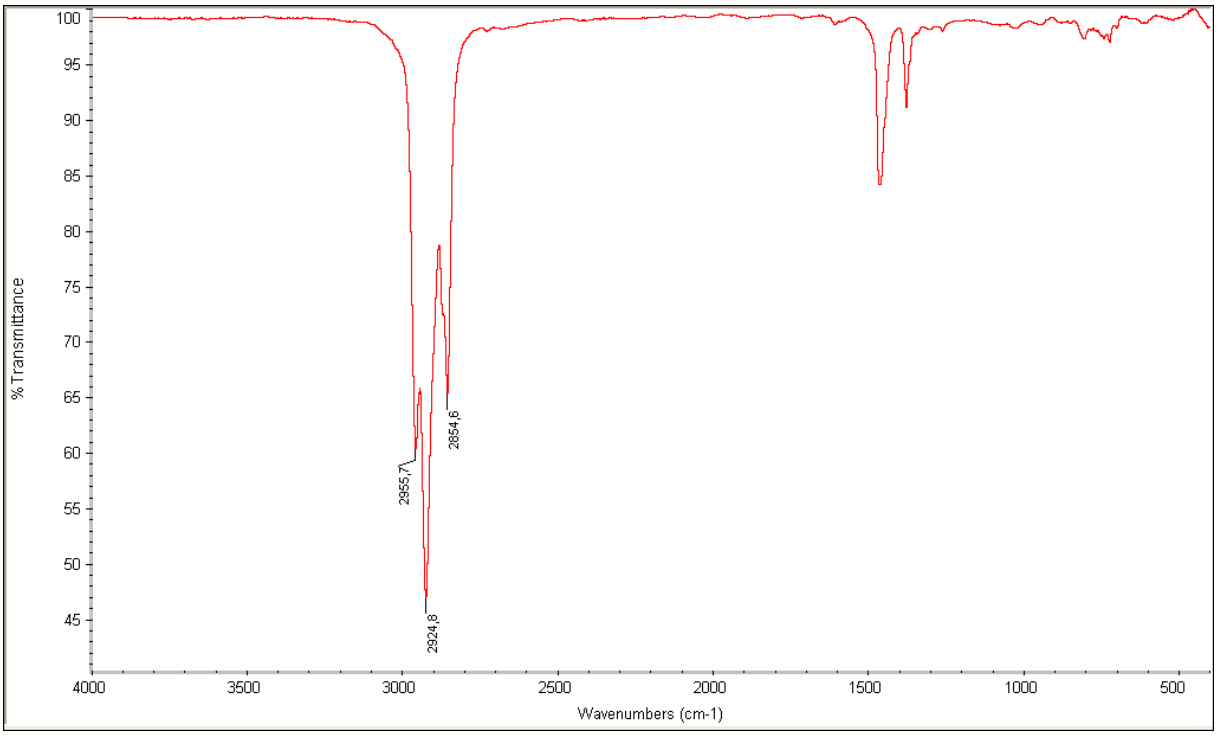

Figure 27: FT-IR of liquid resulting from the extraction in hexane

The liquid extracted was then dried with a RotaVapor and analysed with GC-MS. Below in figure 28 is reported the result of the GC-MS analysis regarding the extraction with hexane.

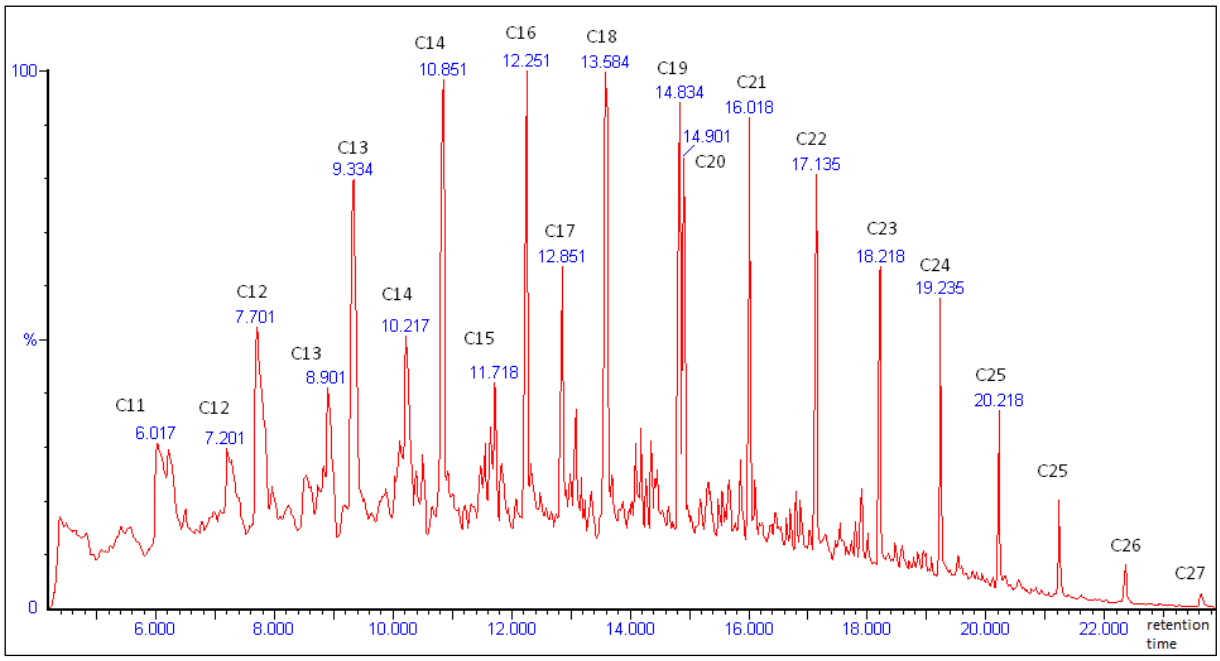

Figure 28: chromatograph of the real polluted soil (RE.AL soil sample) after the extraction in hexane

For each peak the mass spectrum was analysed in order to identify the types of pollutants present in the sample. The following section shows the mass spectra of each peak.

Peak at 6.017: Aliphatic hydrocarbon C_{11}

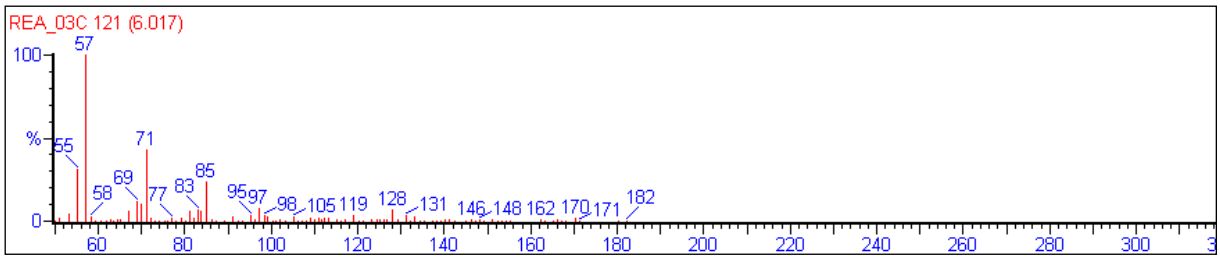

Peak at 7.201: Aliphatic hydrocarbon iso-C_{12}

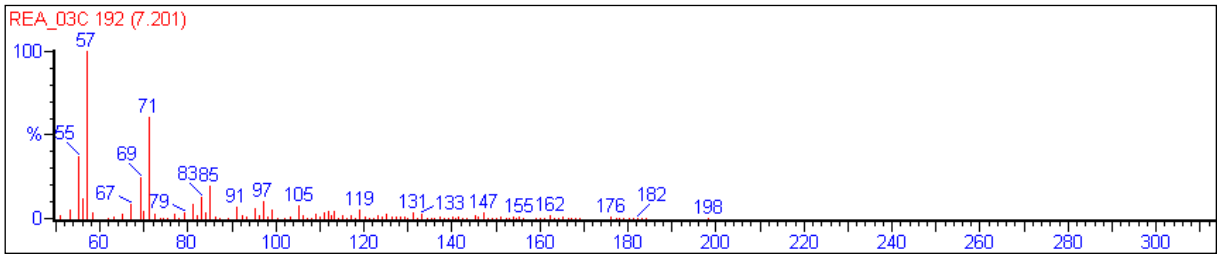

Peak at 7.701: Aliphatic hydrocarbon C_{12}

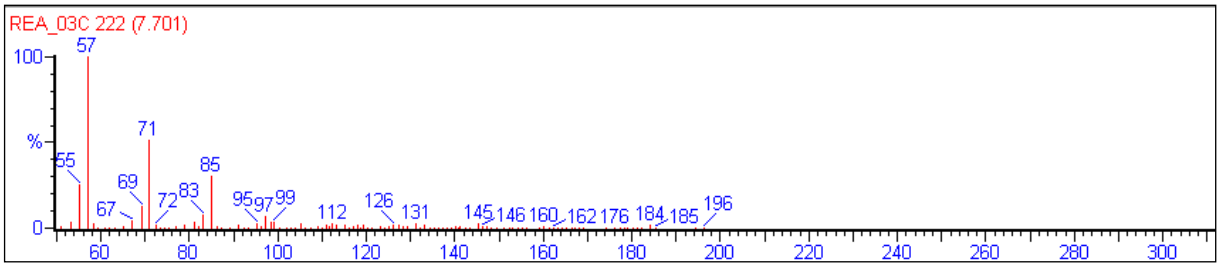

Peak at 8.901: Aliphatic hydrocarbon iso-C_{13}

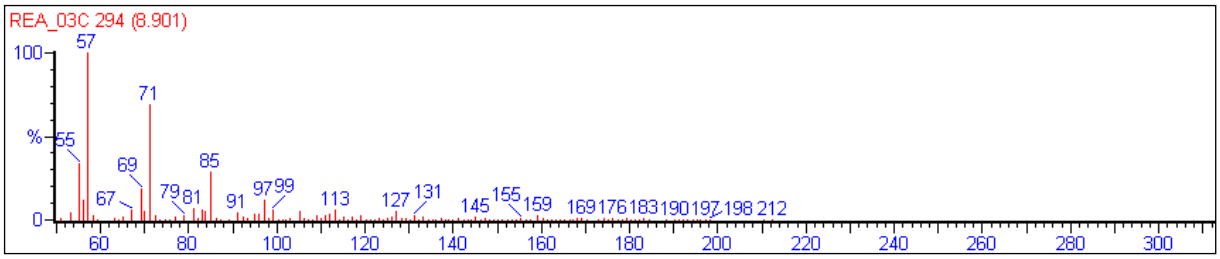

Peak at 9.334: Aliphatic hydrocarbon C_{13}

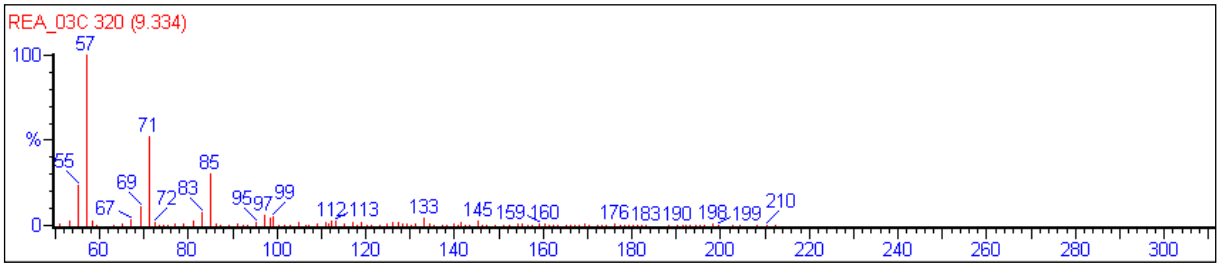

Peak at 10.217: Aliphatic hydrocarbon iso-C_{14}

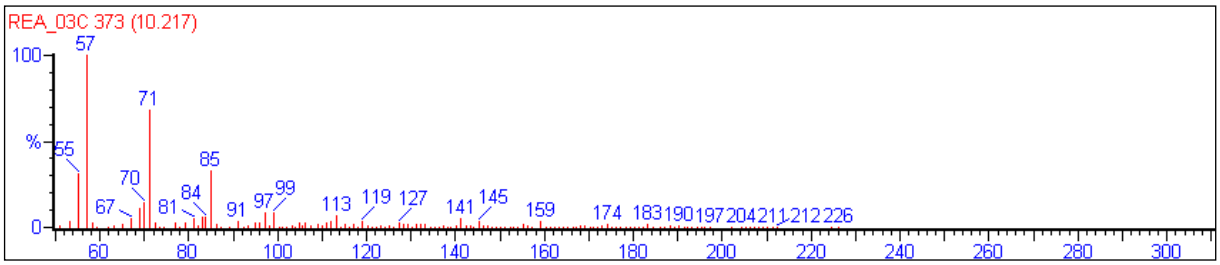

Peak at 10.851: Aliphatic hydrocarbon C_{14}

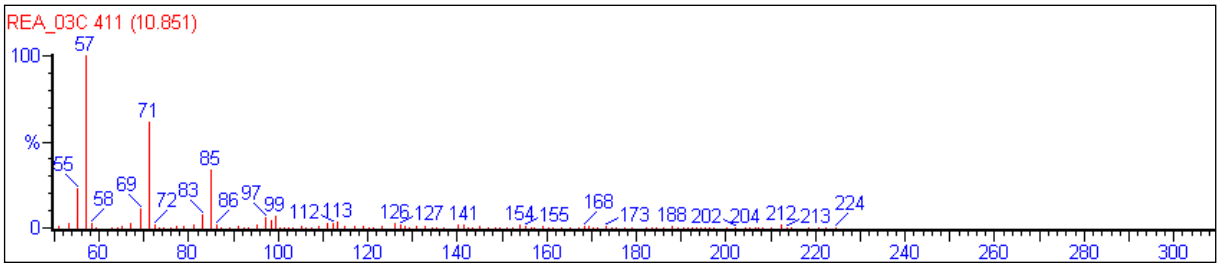

Peak at 11.718: Aliphatic hydrocarbon C_{15}

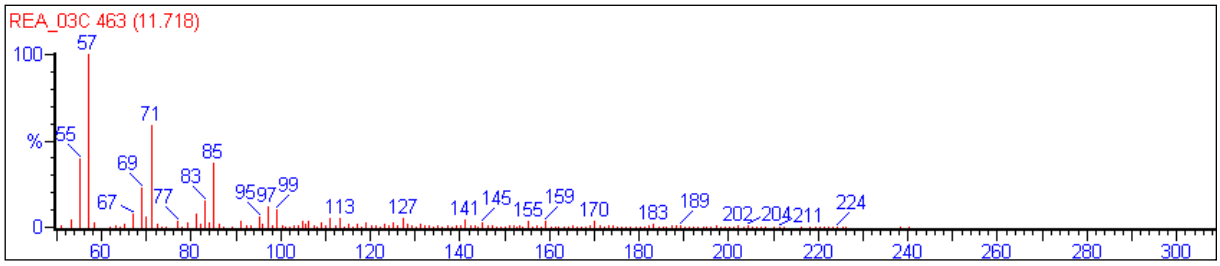

Peak at 12.251: Aliphatic hydrocarbon C_{16}

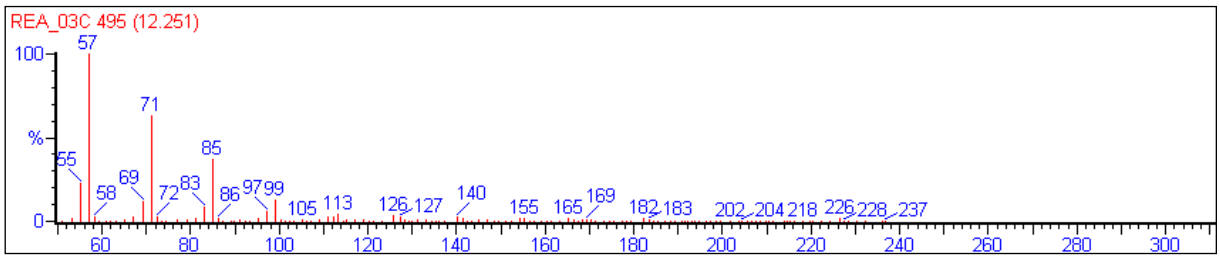

Peak at 12.851: Aliphatic hydrocarbon C_{17}

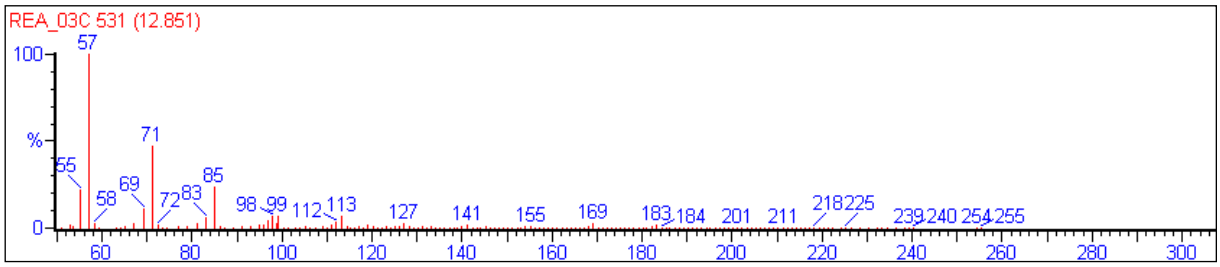

Peak at 13.584: Aliphatic hydrocarbon C_{18}

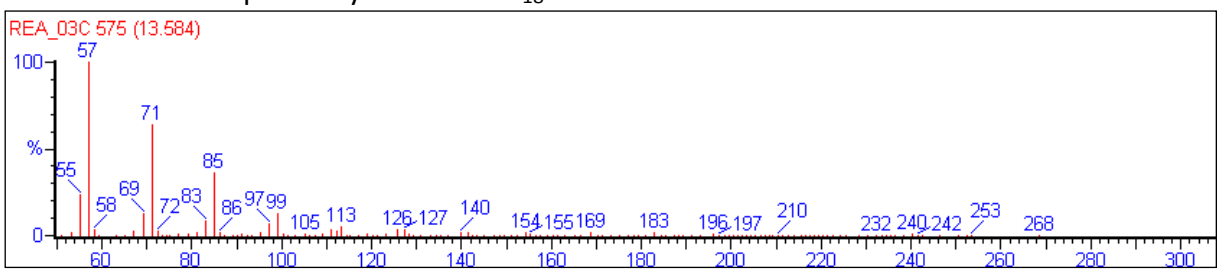

Peak at 14.184: Aliphatic hydrocarbon iso-C_{19}

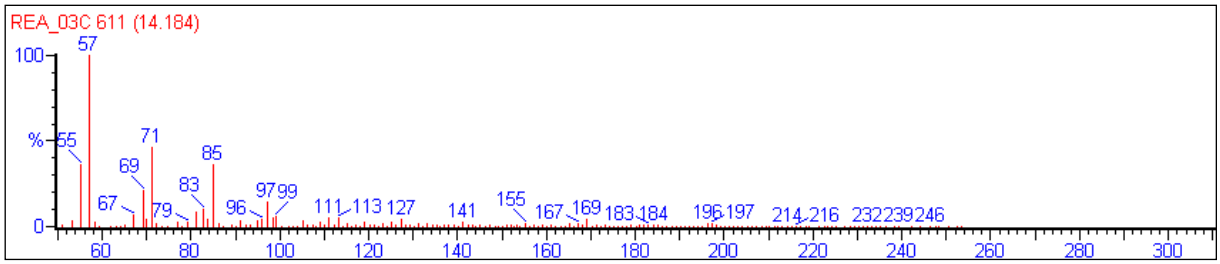

Peak at 14.834: Aliphatic hydrocarbon C_{19}

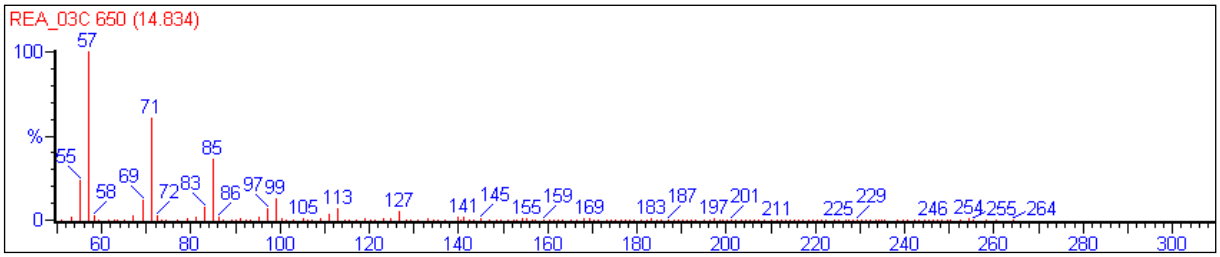

Peak at 14.901: Aliphatic hydrocarbon C_{20}

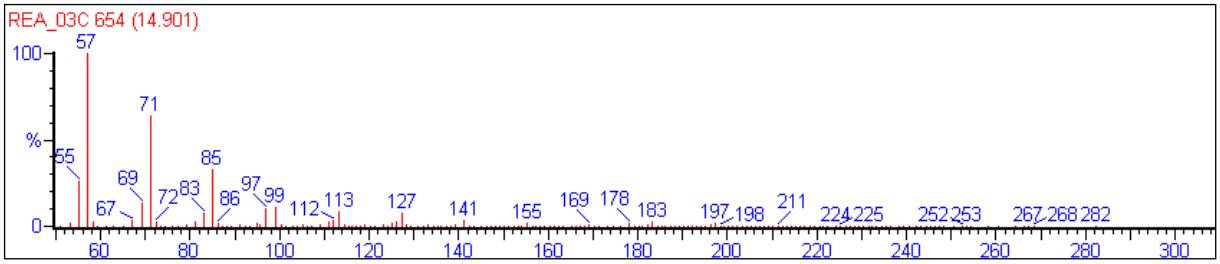

Peak at 16.018: Aliphatic hydrocarbon C_{21}

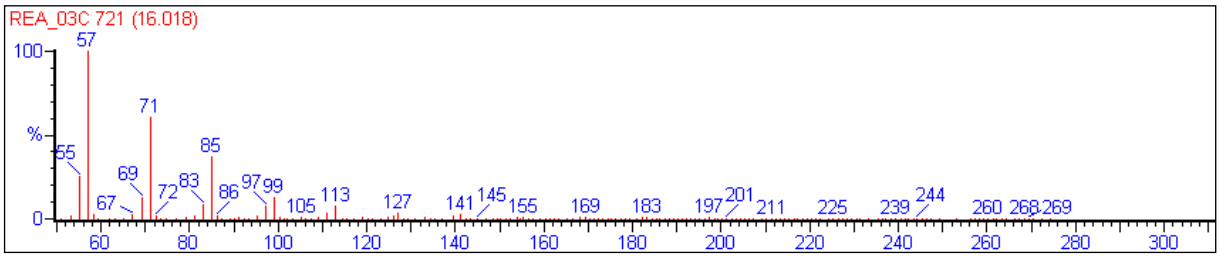

Peak at 17.135: Aliphatic hydrocarbon C_{22}

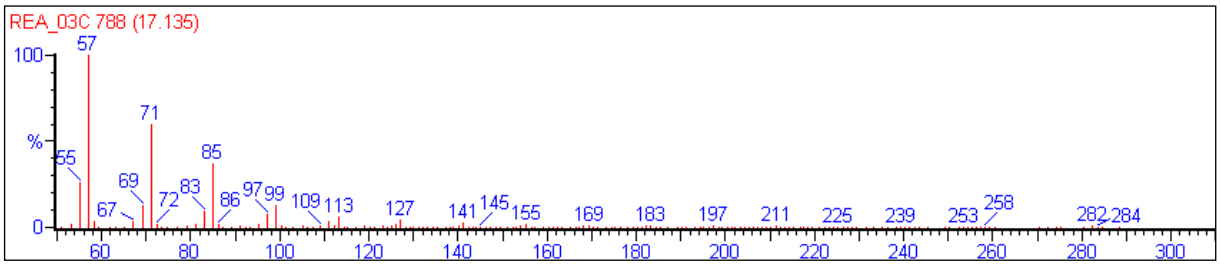

Peak at 18.218: Aliphatic hydrocarbon C_{23}

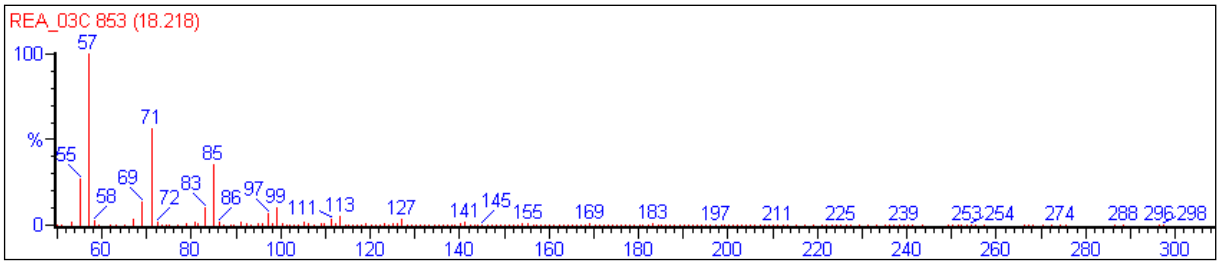

Peak at 19.235: Aliphatic hydrocarbon C_{24}

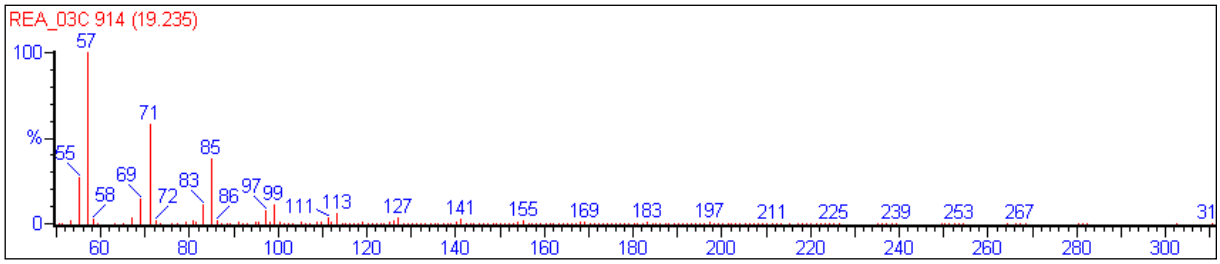

Peak at 20.218: Aliphatic hydrocarbon C_{25}

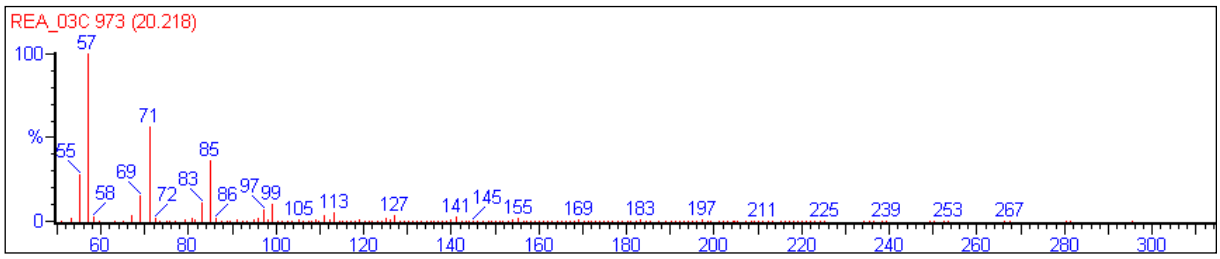

Peak at 21.235: Aliphatic hydrocarbon C_{25}

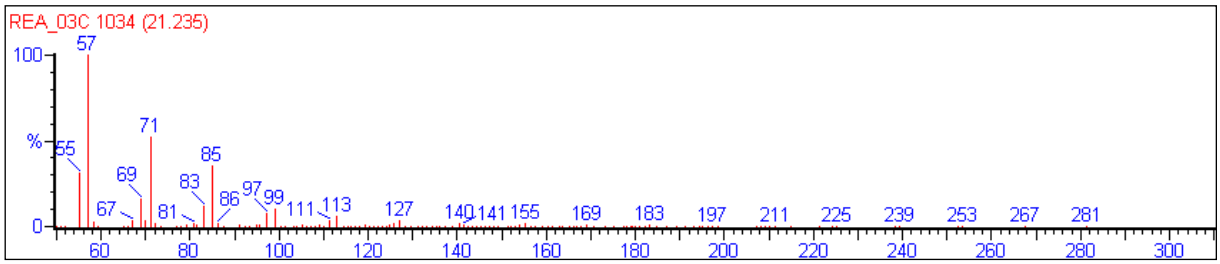

Peak at 22.352: Aliphatic hydrocarbon C_{26}

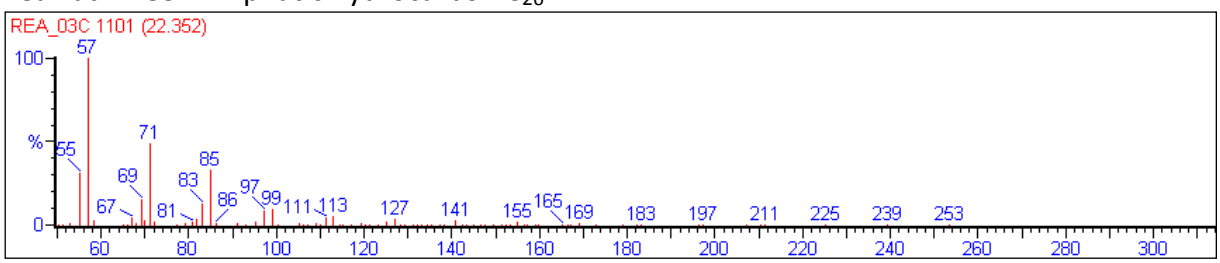

The hydrocarbons present are all long-chain aliphatic from 11 carbon atoms for the first peak to 27 for the last peak of the Gaussian distribution. It is possible to note that for lighter compounds (those that firstly exit the column from C_{11} to C_{14}) both the normal and the corresponding isomer are present: in general isomers are the more volatile compounds so in this case the firsts peak of the couples. For instance, the peak at time 7.201 corresponds to the isomer of dodecane (C_{12}) and the peak at 7.701 to the normal dodecane. For higher molecular weight the masses reported in the spectra correspond to the loss of a fragment-C_2H_4 or-C_2H_5 followed by progressive loss of-CH_2.
Starting from the ion at m/z 113 (corresponding to C_8) loss of hydrogen is observed with the formation of the ion at m/z 111 from which are progressively lost fragments-CH_2.

The soil obtained after the extractions and the original real sample were then analysed with ESEM (Environmental Scanning Electron Microscope) in order to verify, with a comparison between them, the efficiency of the extractions (if some pollutants remained) and to show the morphology of the samples.

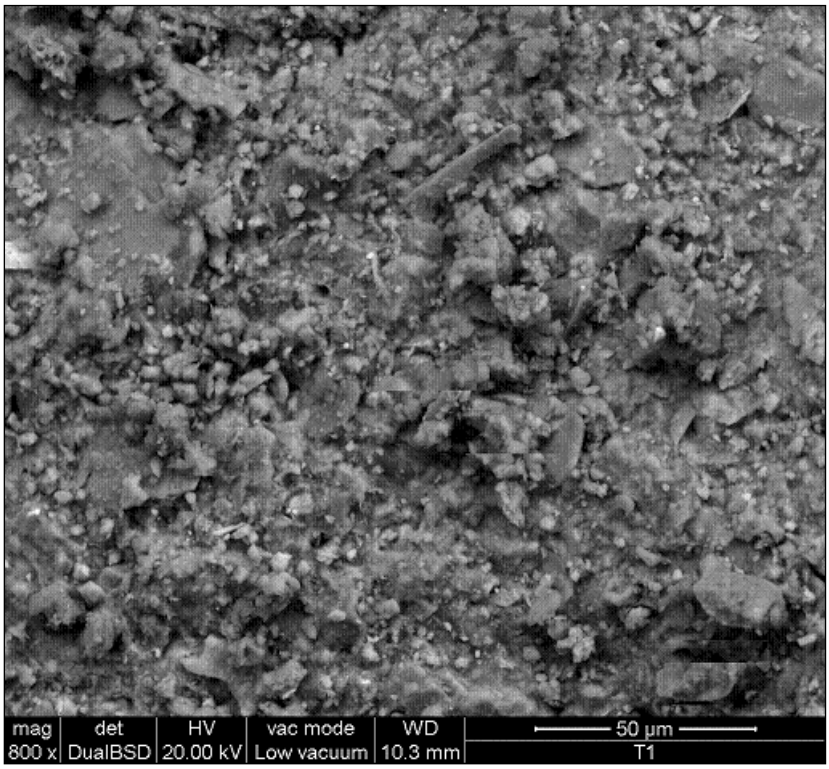

Figure 29: SEM of real polluted soil (RE.AL soil sample): morphology

Table 6: Quantification of elements in real soil sample by SEM

Elem	Wt %	At %	K-Ratio	Z	A	F
C K	15,87	25,47	0.0295	10.839,00	0.1776	10.004,00
O K	40,02	48,22	0.0986	10.483,00	0.2434	10.004,00
NaK	0,39	0,33	0.0014	0.967	0.3851	10.028,00
MgK	2,36	1,87	0.0118	0.9862	0.5211	10.051,00
AlK	7,06	5,04	0.0411	0.9531	0.6284	10.066,00
SiK	17,86	12,26	0.1135	0.9773	0.6729	10.013,00
SrL	0,95	0,21	0.0063	0.7712	0.8944	10.014,00
P K	0,16	0,10	0.0009	0.9419	0.6335	1.002,00
ZrL	0,00	0,00	0,00	0.776	0.8032	10.019,00
ClK	0,00	0,00	0,00	0.9189	0.8022	10.061,00
K K	1,95	0,96	0.0159	0.9194	0.9063	10.131,00
CaK	6,86	3,30	0.0581	0.9383	0.9301	10.049,00
BaL	1,33	0,19	0.0094	0.6859	10.594,00	10.072,00
FeK	4,15	1,43	0.0336	0.8432	0.9909	1.004,00
CuK	0,37	0,11	0.0029	0.8093	0.9961	10.012,00
HgL	0,66	0,06	0.0039	0.5894	10.327,00	1.001,00
Total	100,00					

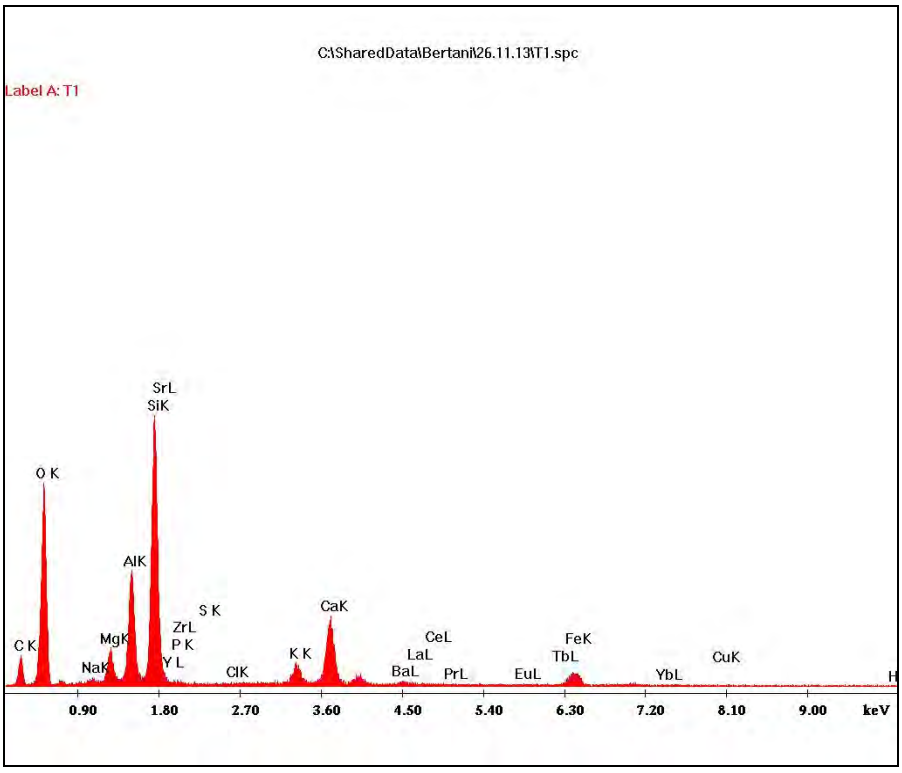

Figure 30: spectrum of elements in real soil sample by SEM

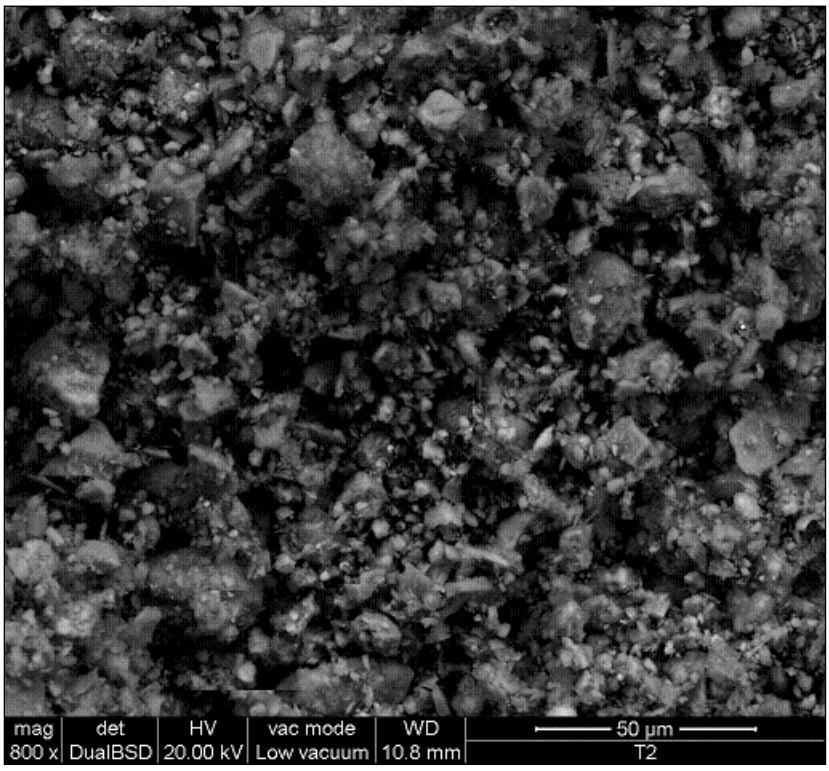

Figure 31: SEM of soil sample after 3 extractions: morphology

Table 7: Quantification by SEM of the elements in soil sample after 3 extractions

Elem	Wt %	At %	K-Ratio	Z	A	F
C K	11,35	19.31	0.0234	10.933	0.1935	10.005
O K	41,86	53.45	0.1045	10.573	0.2423	10.003
NaK	0,52	0.47	0.0019	0.9752	0.3703	10.025
MgK	2,93	2.47	0.0144	0.9946	0.503	10.043
AlK	6,61	5	0.0381	0.9612	0.6122	10.055
SiK	13,74	9.99	0.0885	0.9856	0.6698	10.017
SrL	1,25	0.29	0.0085	0.7777	0.8906	10.018
P K	0,21	0.13	0.0012	0.9499	0.659	10.025
ZrL	0,14	0.03	0.0009	0.7826	0.8341	10.026
ClK	0,03	0.02	0.0002	0.9267	0.8026	10.076
K K	1,84	0.96	0.0153	0.9274	0.9016	10.172
CaK	10,22	5.21	0.0876	0.9465	0.9258	10.043
BaL	1,26	0.19	0.0089	0.6921	10.446	10.061
FeK	4,44	1.62	0.0365	0.8512	0.9859	10.042
CuK	0,53	0.17	0.0042	0.8175	0.9937	10.053
HgL	3,06	0.31	0.0183	0.5962	10.318	10.015
Total	100,00	100				

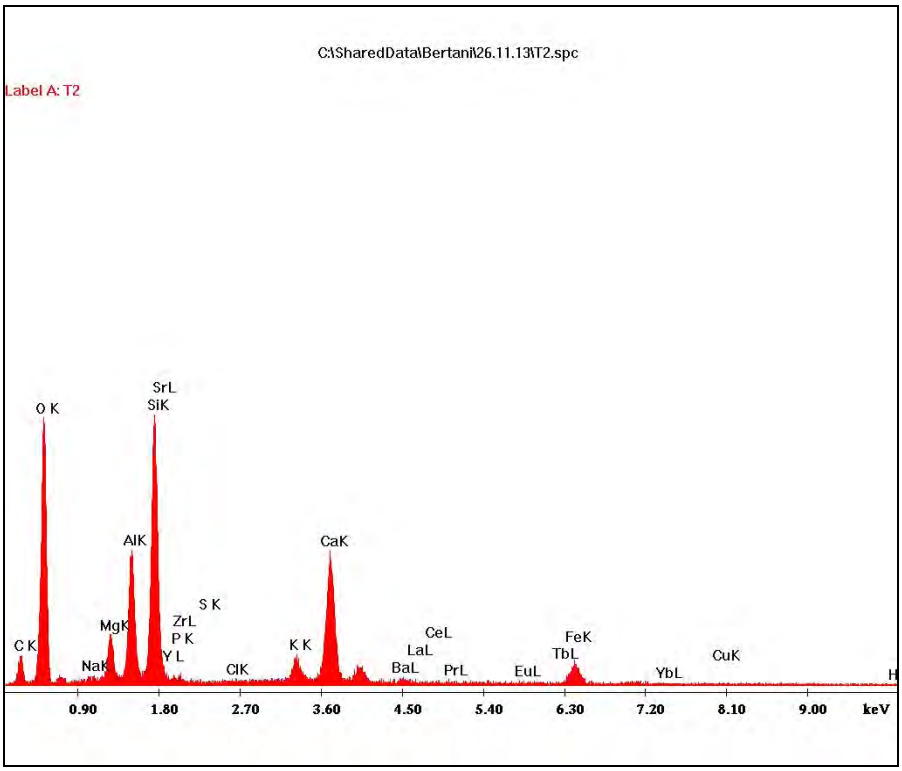

Figure 32: spectrum of elements of soil sample after 3 extractions by SEM

SEM analysis has confirmed that the extraction is successful because the percentage of carbon is decreased from 15,87% to 11,35%. The remaining percentage is due to carbon compounds that occur naturally in soils like humic acids and $CaCO_3$.

The remained soil was studied also with XRD device. The XRD equipment operation is described in chapter 5. The result is reported in figure 33 and the main bands with the respective intensity in table 8.

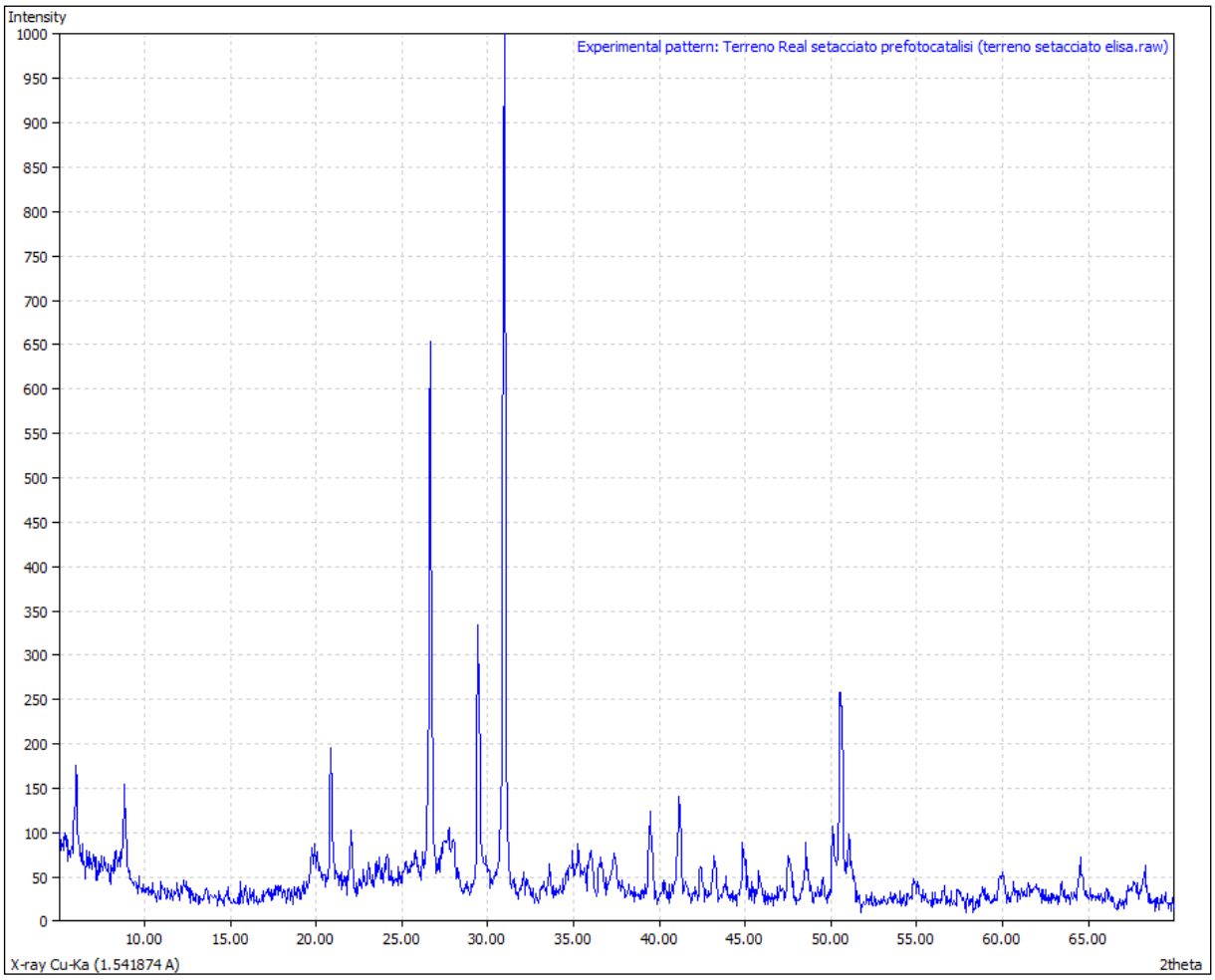

Figure 33:X-ray diffractometer (XRD) pattern of real soil sample

Table 8 XRD peaks of real soil sample after 3 extractions

2theta	**intensity**
6	164
8.85	154.55
19.89	86.94
20.85	195.99
22	101.88
26.65	651.45
29.44	328.77
30.94	996.96
39.45	124.96
41.14	141.07
50.48	254.25
50.57	252.68

It results that the soil sample was a mixture and comparing the bands with the library it is possible to underline the main bands present, characteristics of oxides, phosphates, silicates and carbonate. In figure 34 is reported as example the analogy of some silicates with the bands of the soil sample (blue line) and in figure 35 the analogy of some carbonate.

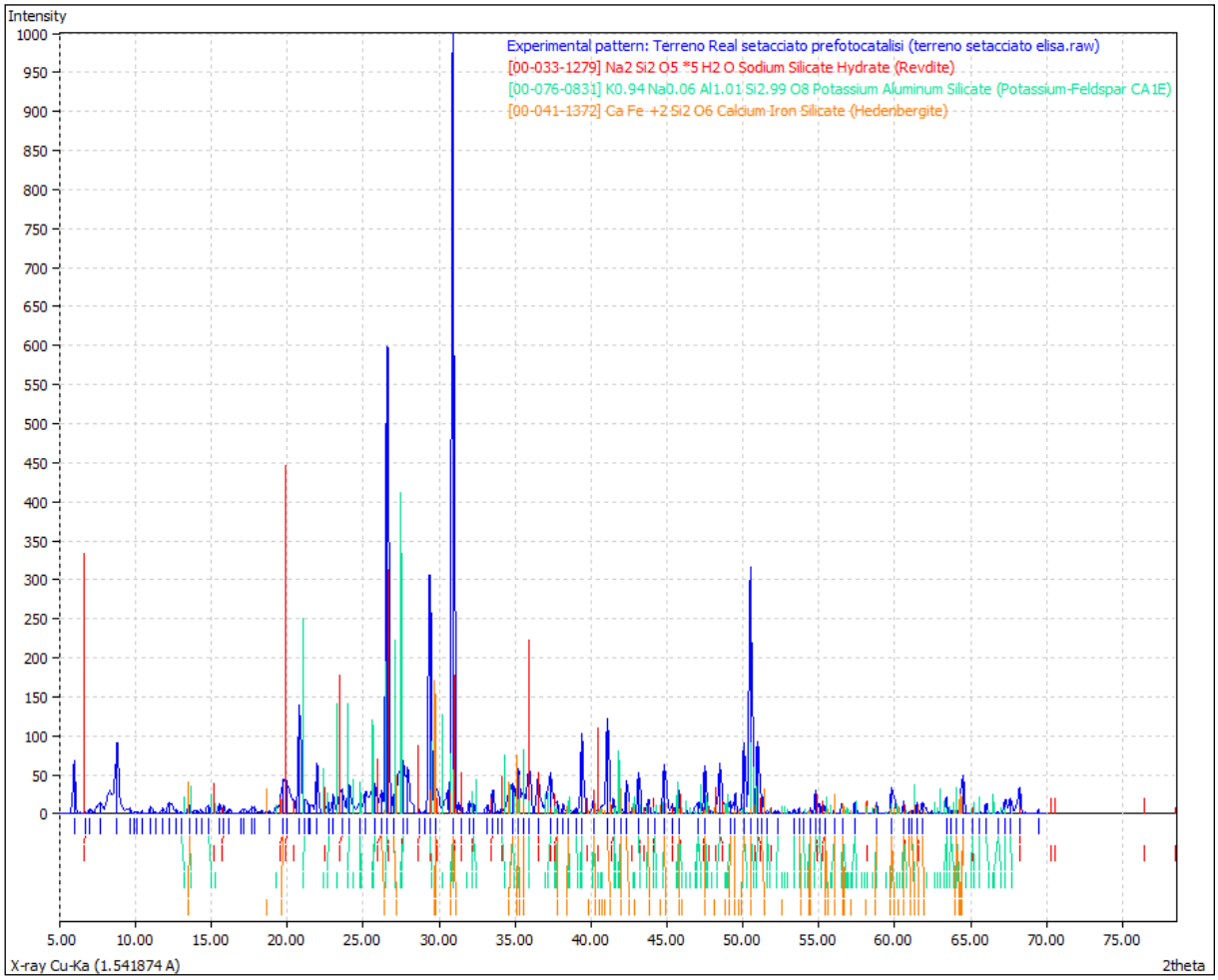

Figure 34: X-Ray diffractometer(XRD) pattern of real soil and the overlay of different silicates graphs.

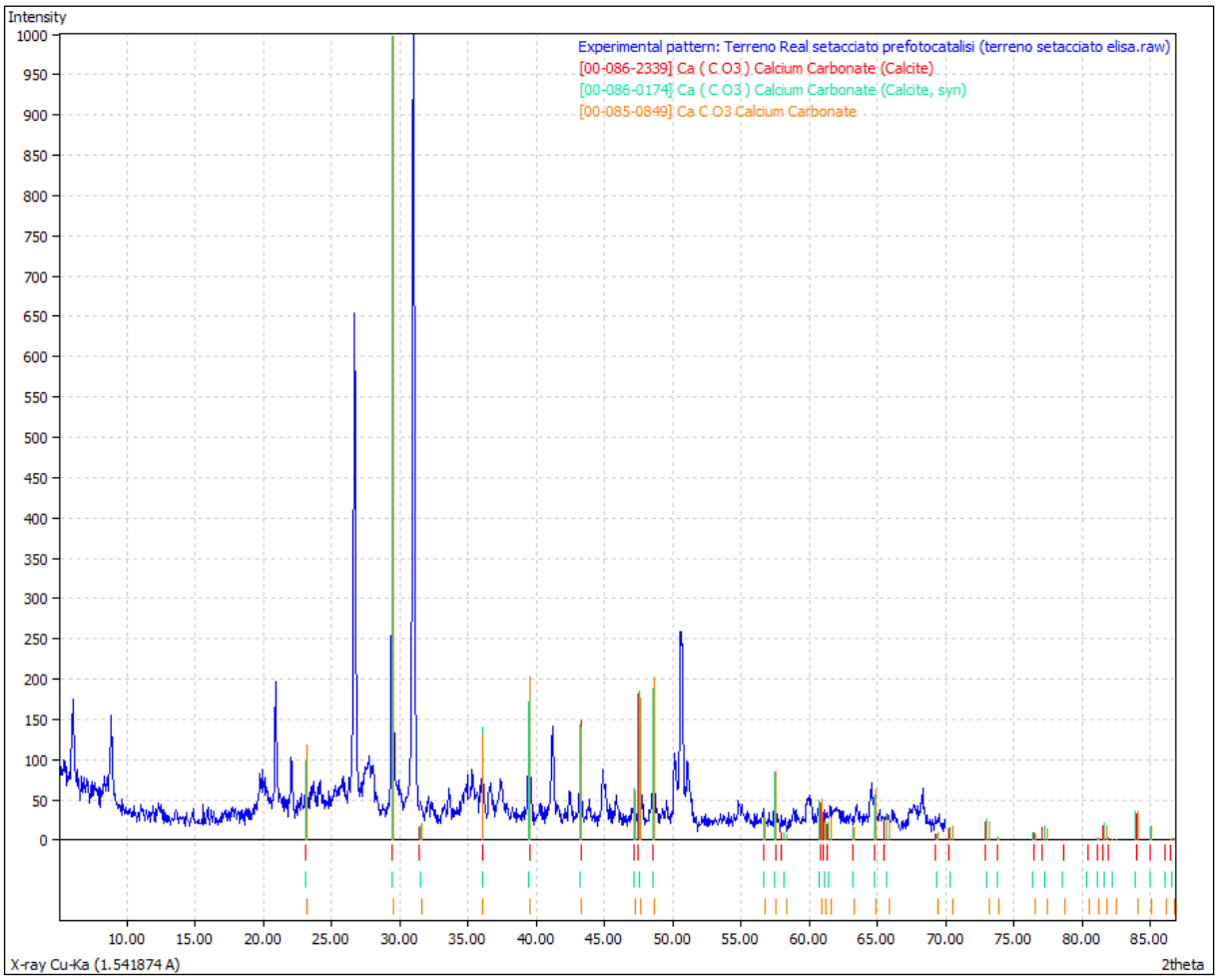

Figure 35: X-Ray diffractometer (XRD) pattern of real soil and the overlay of different carbonates graphs.

7. THE PHOTOCATALYTIC LABORATORY EXPERIMENTS

7.1 EXPERIMENTAL DESIGN

The study was divided in two parts: the first part regarding the experiments in aqueous suspension and the second one regarding those in heterogeneous phase on soil surfaces.

The distinction allows to analyze different types of photocatalysis linked to different difficulties degrees on the degradation of contaminants.

The experiments in aqueous suspension was conducted to verify the efficiency of the experimental conditions (catalyst, features of the lamps, distance from the sample) analysing at first the photodegradation of a tracer dye (Rhodamine-b) and then the degradation of a known mixture of different hydrocarbons in solution. These tests were made because from the literature it is known that photocatalysis of these compounds leads to good results in terms of degradation. Two first tests of photocatalysis on soil in suspension were also carried out.

Meanwhile the second part of the experimental work was made on solid phase: at first photocatalytic tests on clean soil artificially polluted in laboratory and subsequently tests on the real soil sample given by RE.AL Service spa were implemented. Different experiments were carried on in order to find the best set of parameters that lead to the best degradation under the laboratory conditions.

The description of the photocatalytic experiments and the subsequently discussion of the results are presented in next paragraphs.

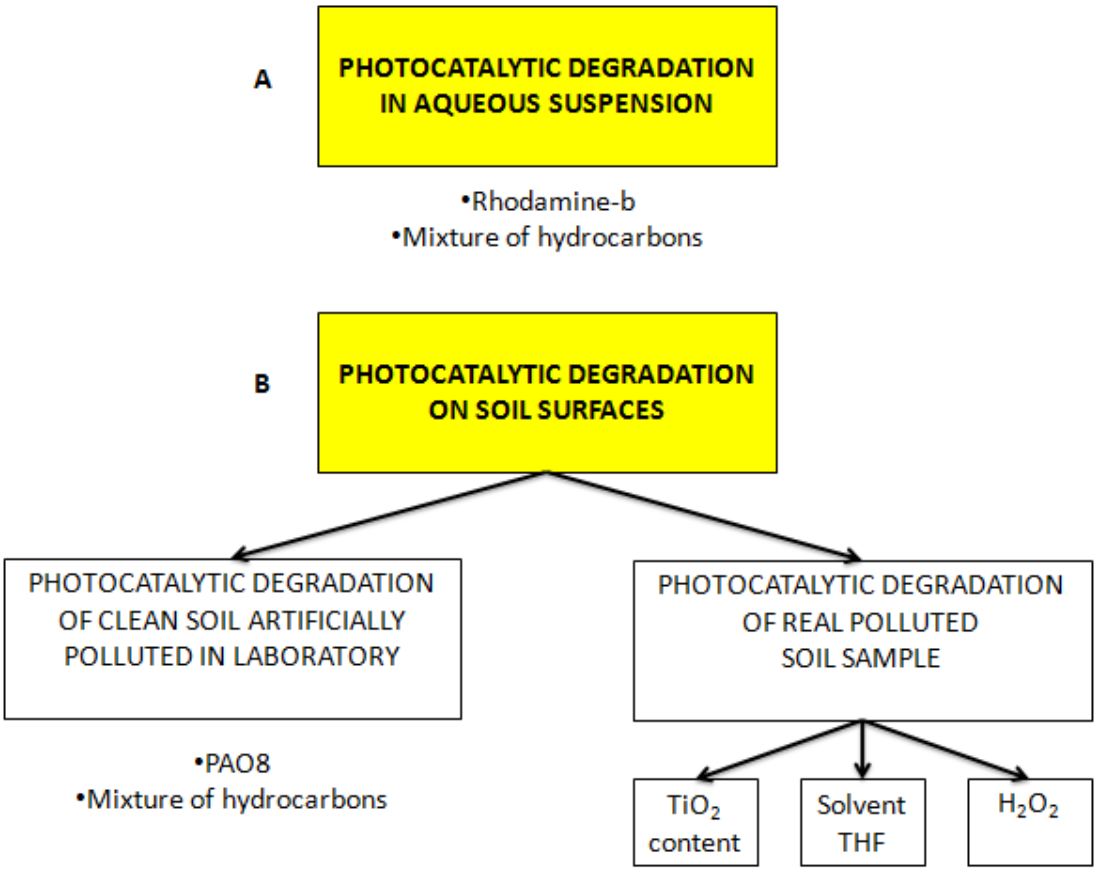

Figure 36: scheme of the experimental study

7.2 PHOTOCATALYTIC EXPERIMENTS IN AQUEOUS SUSPENSION

Photocatalytic experiments in aqueous suspension were performed in laboratory scale. The equipment consisted in a quartz box where a beaker containing the suspension was placed (figure 37). In parallel two UV lamps were placed as a lid of the box, the distance between them was 80mm while the distance from the sample was 15cm. Figure 38 reported the technical features of the lamps: wavelength of UV lamps used throughout all the experiments was 310nm with an UV irradiation of 90µW/mm^2.

Figure 37: images of the equipment for photocatalytic degradation in aqueous suspension

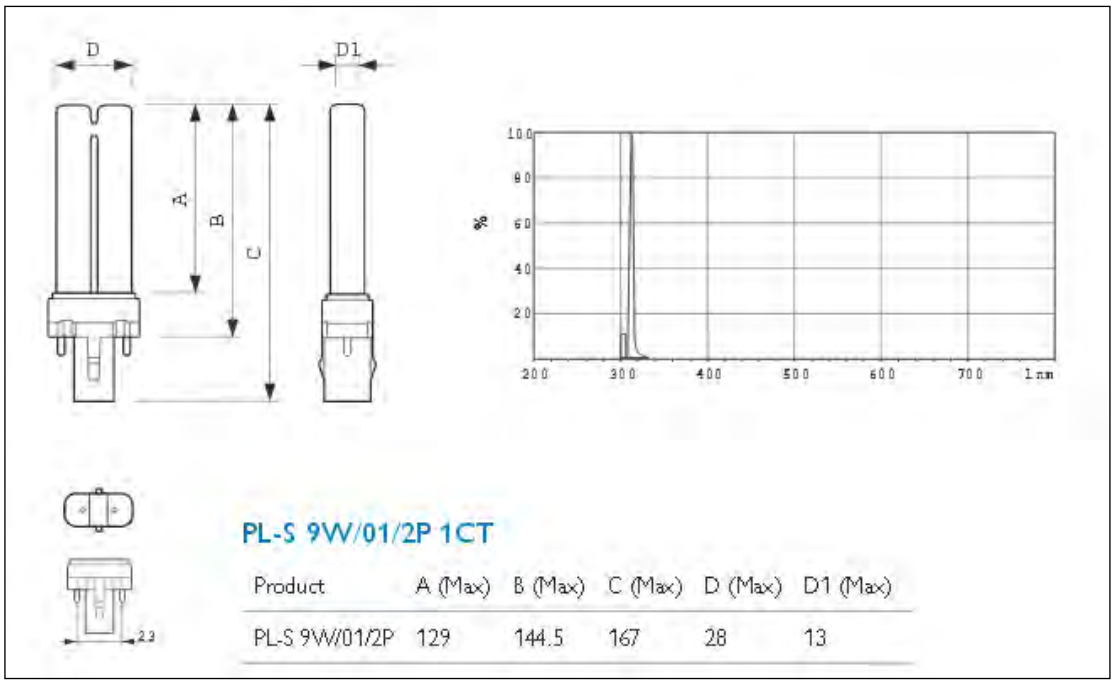

Figure 38: technical features of UV lamps.

7.2.1 Photocatalytic degradation of Rhodamine-b

100ml Rhodamine-b solution 10^{-4}M

100mg TiO_2

mixing with a magnetic stirrer

UV irradiation

Residence time 2h

Sampling of 1ml each 5min

The purpose of this experiment was evaluate the feasibility and efficiency of photocatalysis under the operational conditions (UV lamps wavelength and intensity): it is known from literature that Rhodamine-b solution can be degraded with photocatalysis so it was tried to implement a photodegradation in order to ensure the system could have worked. A 100ml of Rhodamine-b solution 10^{-4} M was placed in a beaker with 100g of catalyst TiO_2. The sample was placed in a quartz box located under UV lamps. The UV lamps had a wavelength of 310nm and the distance from the sample was 15cm. A continuous mixing was ensured by a magnetic stirrer. The experiment lasted 2 hours and every 5 minutes a sample of 1ml was collected.

Figure 39: images of the equipment for photocatalytic degradation of Rhodamine-b in aqueous suspension

The final result has demonstrated the efficiency of the system in fact Rhodamine-b was photodegraded as evidenced by the gradual change of color from pink to white shows in figure 40.

Figure 40: photodegradation of Rhodamine-b: gradual change of colour in function of the UV exposition time.

In order to verify the efficiency of the photocatalysis two blank experiments were performed: the first blank sample without UV irradiation and the second one without TiO_2. The blank experiments run for 2 hours and every 30 minutes 1ml of solution was collected. The results are shown in figure 41: as expected there was no degradation of Rhodamine-b.

<u>BLANK 1:</u>

100ml of Rhodamine-b solution 10^{-4} M

100mg TiO_2

mixing with a magnetic stirrer

test carried on in a dark room

Residence time 2h

<u>BLANK 2:</u>

100ml Rhodamine-b solution 10^{-4} M

no TiO_2

mixing with a magnetic stirrer

UV irradiation

Residence time 2h

Figure 41: blank samples with no degradation and no changing in colour

The samples, collected every 5 minutes, were filtered in order to remove TiO_2 and then 0.5 ml of each samples were picked up with a syringe and diluted with 3ml of water. On these quantities UV analysis was implemented. Setting the wavelength of the instrument at 553nm (the wavelength of maximum absorption of Rhodamine-b shows in figure 42) the absorbance of the samples was measured and the results are reported in table 9 and figure 43.

A calibration line (figure 44) was constructed with the absorbance analysis of different standards of Rhodamine's solutions: the result is a straight line passing through the origin of the axes thus absorbance and concentration are directly proportional, and the Lambert-Beer law has occurred. Using the equation of the straight line, the values of the concentration of Rhodamine-b for each sample of the experiment were calculated and reported in figure 45.

The decrement of the concentration, taking into account the instrumental error, expresses the good photodegradation of Rhodamine-b under the laboratory conditions.

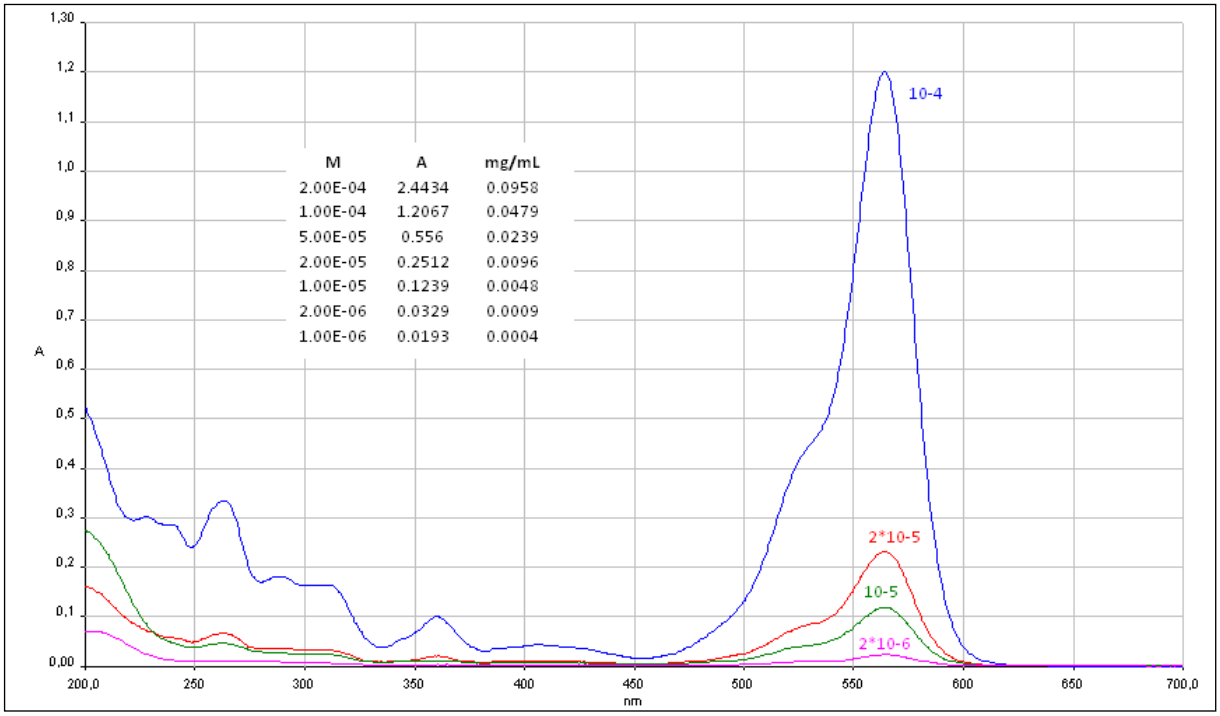

Figure 42: UV spectra of different standards concentrations of Rhodamine-b

Table 9: Rh-b absorbances and concentrations of the different samples taken every 5minutes.

Time of sampling (min)	A Absorbance	Rh-b conc (mg/ml)
0	1.1746	0.04634079
5’	0.7434	0.029328915
10’	0.5348	0.021099144
15’	0.4795	0.018917426
20’	0.3353	0.01322839
25’	0.259	0.010218172
30’	0.2205	0.008699254
35’	0.1547	0.006103286
40’	0.1484	0.005854736
45’	0.0532	0.002098868
50’	0.0511	0.002016018
55’	0.035	0.001380834
60’	0.0203	0.000800884
65’	0.0049	0.000193317
70’	0.0021	8.285E-05
75’	0.0189	0.00074565
80’	0.0119	0.000469484
85’	0.0098	0.000386634
90’	0.0105	0.00041425
95’	0.0224	0.000883734
100’	0.0028	0.000110467
105’	0.0119	0.000469484
110’	0.0133	0.000524717
115’	0.0098	0.000386634
120’	0.0182	0.000718034

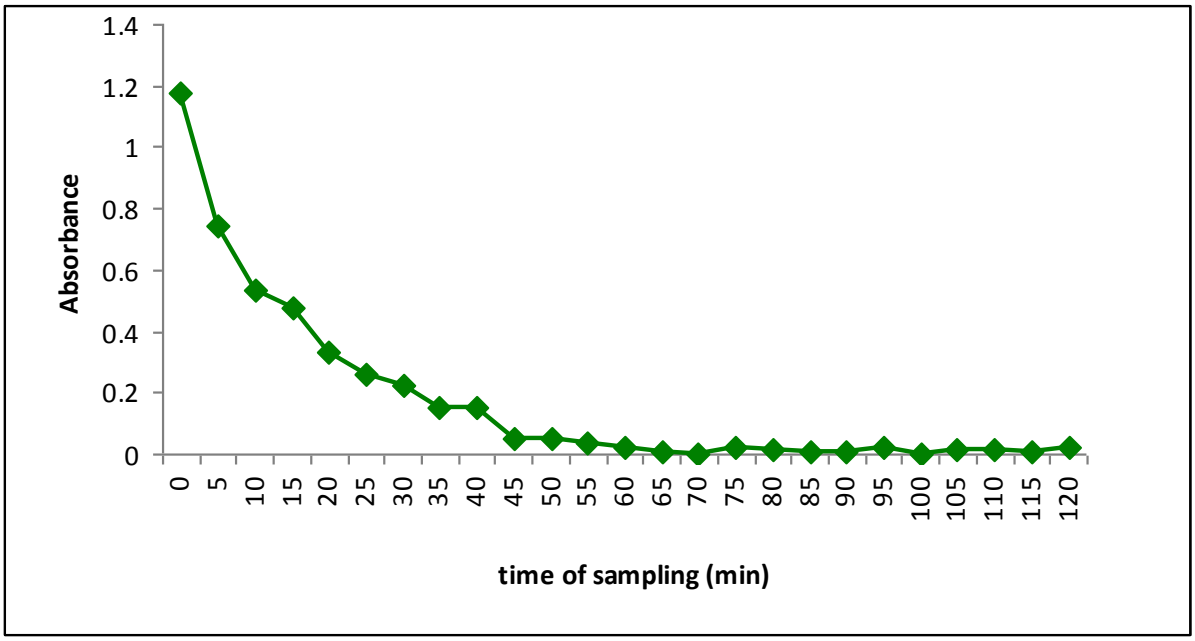

Figure 43: degradation of Rh-b: absorbence Vs time

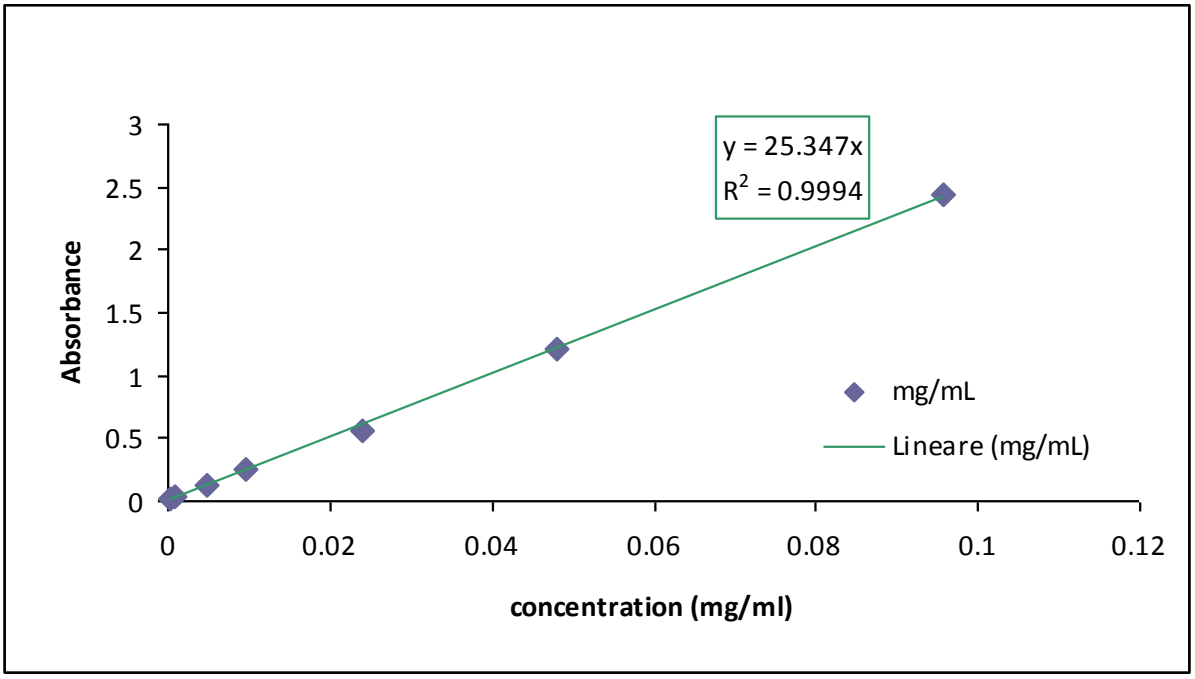

Figure 44: calibration line of Rh-b

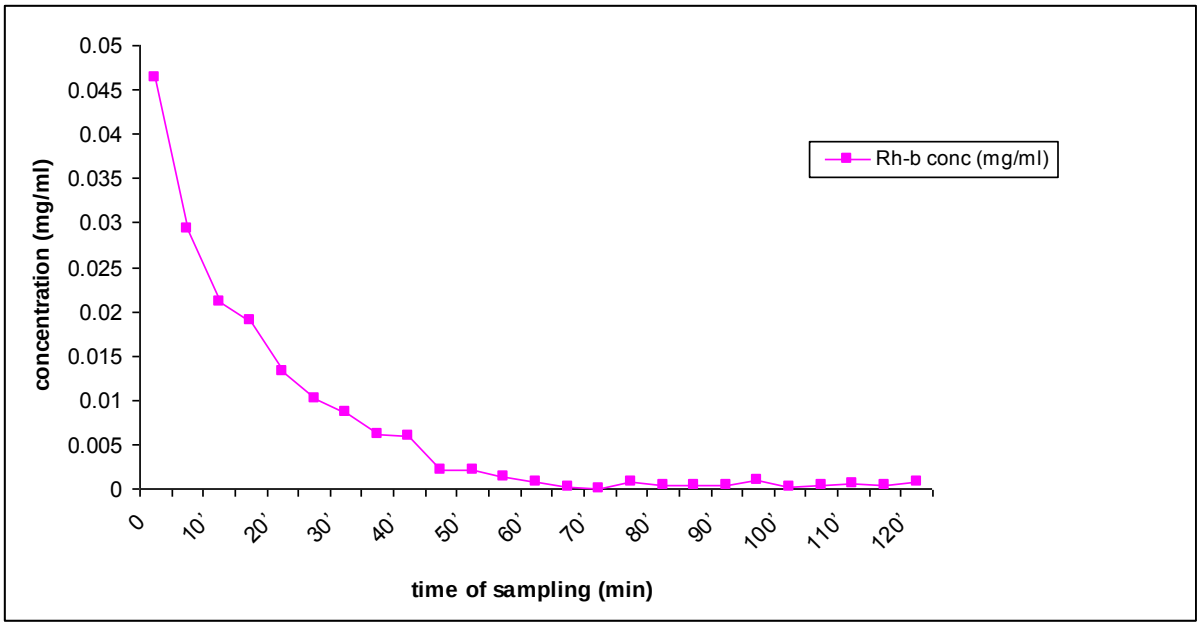

Figure 45: degradation of Rh-b: concentrations Vs time

7.2.2 Photocatalytic degradation of a mixture of hydrocarbons

10ml heptane

10ml hexane

10ml octane

10ml toluene

10ml cyclohexane

10ml isooctane

10ml THF

10ml H_2O

2g TiO_2

Residence time: 27h

The objective of the experiment was to investigate the photocatalysis of a known mixture of hydrocarbons. The mixture was made in laboratory and was composed by different hydrocarbons, 10 ml of each one: toluene, heptane, hexane, octane, cyclohexane and isooctane. To these, 10ml of THF, to create a homogeneous solution, 10 ml of H_2O and 2g of TiO_2 were added. The sample was placed in a quartz box located under UV lamps. The UV lamps had a wavelength of 310nm and the distance from the sample was 15cm. A continuous mixing was ensured by a magnetic stirrer. The UV lamps were turned on after 2 hours of mixing in a dark room.

*Figure 46***:** *images of the equipment for photocatalytic degradation of a mixture of hydrocarbons in aqueous suspension*

Samples were taken before starting photo-irradiation, at 12 and 27 h from the exposition to UV light and then analysed with GC-MS.

The chromatograms before and at the end of photocatalysis are reported in figure 47.

Operatively 0.2µL of product are taken and injected directly into column, under the following conditions:

Mode: Split

Carrier: He (1cc/min)

Column: DB5-HS Agilent J&W (5% diphenyl-, 95% dimethilsiloxane)

Rampa: 60-280 °C at 2°C/min, Isot 15min

Sample: 0.2 µl pure sample

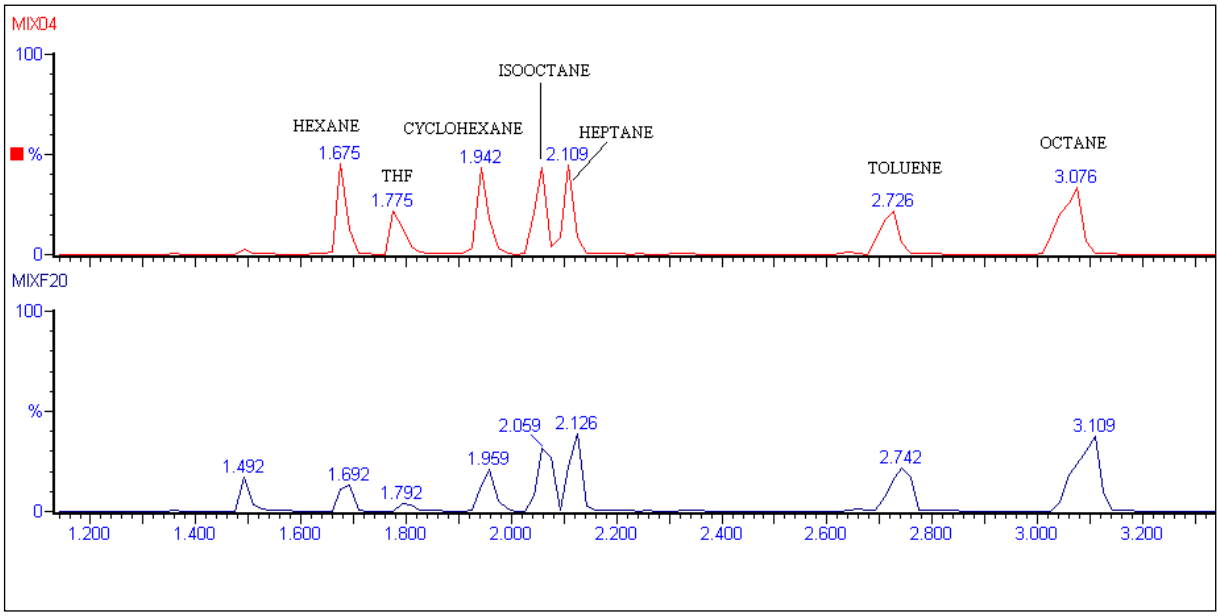

Figure 47: chromatograms of a mixture of hydrocarbons prephotocatalysis (red line) and postphotocatalysis (blue line)

7.2.3 Photocatalytic degradation of real sample in aqueous suspension

Two tests of photocatalytic degradation in aqueous suspension were carried on.

A. 100g soil sample (RE.AL service spa)
   2%TiO_2
   100ml H_2O
   Residence time: 16h
   No addition of H_2O

B. 100g soil sample (RE.AL service spa)
   5%TiO_2
   100ml H_2O
   Residence time: 50h
   Mixing every 30 min
   Addition of 20 ml of H_2O when the sample was dried

Both the tests resulted inefficient for the degradation of hydrocarbons present in the soil samples. Comparing the results of these 2 experiments with the results of the experiments carried on soil surfaces instead of in aqueous suspension it is possible to say that the reasons of the non efficient photodegradation could be the bigger quantity of soil used and the bigger distance between the UV lamps and the samples for which into the soil less power had arrived because it was absorbed by the air.

7.3 HETEROGENEOUS PHOTOCATALYTIC DEGRADATION ON SOIL SURFACES

Photodegradation studies on soil surfaces were carried out on a laboratory scale. They were performed in a box. In parallel 2 UV lamps were fixed in the top of the box and the distance between them was 80mm. Wavelength of UV lamps used throughout all the experiments was 310nm with an UV irradiation of 90µW/mm^2. Figure 48 shows the equipment used and figure 49 the technical features of the lamps.

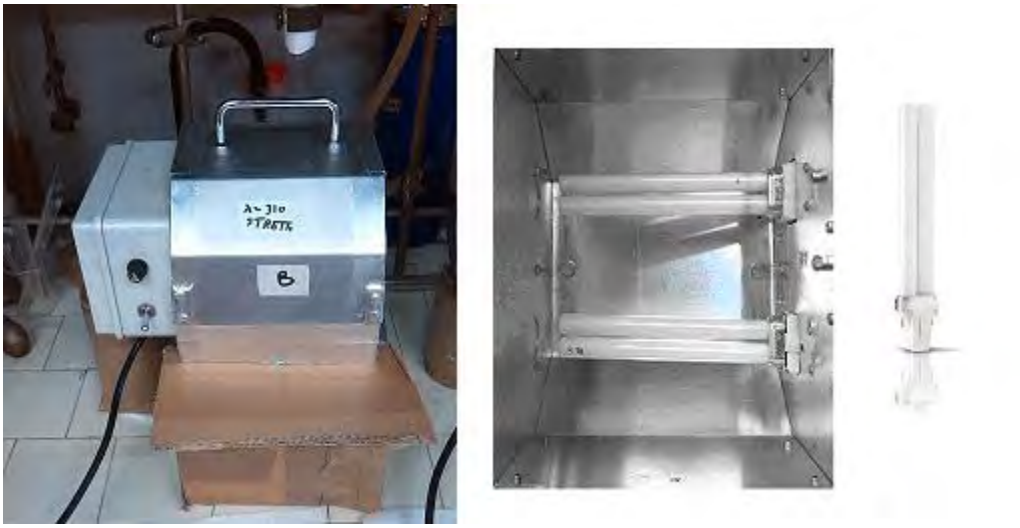

Figure 48: images of the equipment and UV lamps used for photocatalytic tests.

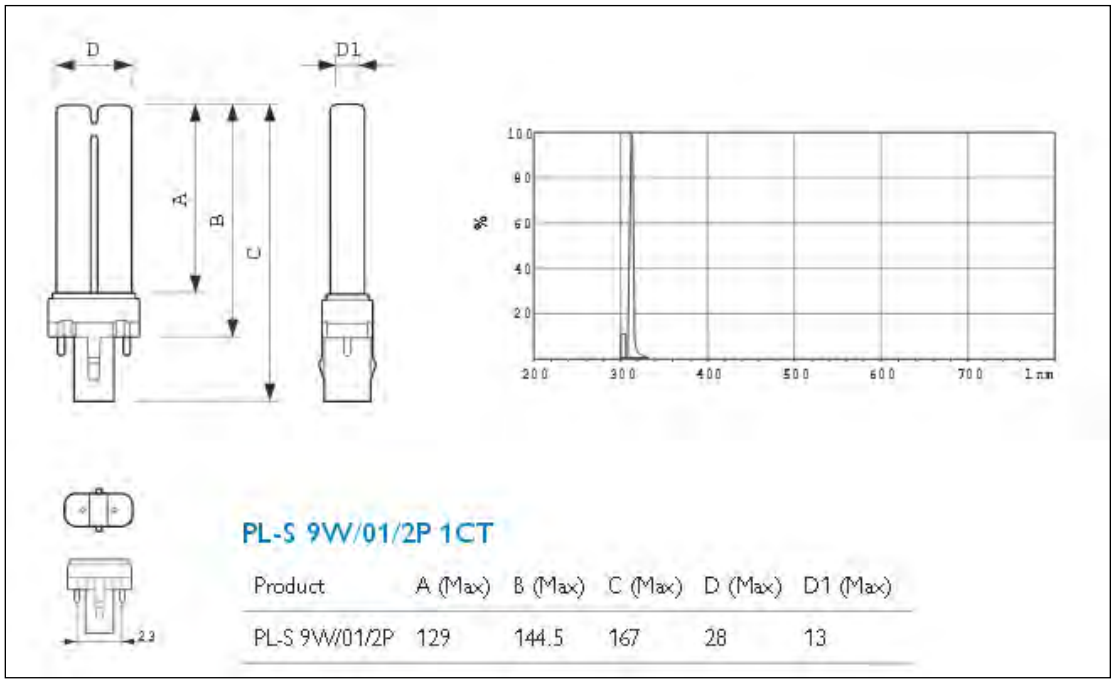

Figure 49: techincal features of UV lamps.

In the experiments on soil surfaces Petri dish containing the sample was placed on a support adaptable to the desirable distance from the lamps: the chosen distance was about 30mm. Figure 50 shows an example of Petri dish and the support used to adjust the distance between soil and lamps.

Figure 50: Petri dish and the support of the sample

7.3.1 Photocatalytic degradation of clean soil artificially polluted in laboratory

These experiments were done in order to evaluate the photocatalytic efficiency on soil artificially polluted in laboratory and compare the results with the ones present in literature (chapter 3).

Surface soil sample was collected from an ecological and clean soil. After being air-dried the soil sample was passed through a sieve with a pore size of 1mm. To confirm the sterility of the soil an extraction with hexane was made and then the result was analysed with GC-MS that confirmed the absence of any kind of pollutants.

Two tests were implemented: one with clean soil polluted by a poly-alpha-olefin and the other with clean soil polluted by a mixture of hydrocarbons.

7.3.1.1 Photocatalytic degradation of clean soil artificially polluted with PAO8

5g clean soil

2ml PAO8

5ml H_2O

5% TiO_2

Residence time: 52h

Two samples of 5g of clean soil were spiked with 2ml of PAO8 and stored in a dark room for 2 hours. One sample was used as a reference and the second one was placed under photo-irradiation. PAO8 is an industrial mixture of alpha-olefins, commonly used as a synthetic lubricant. The number 8 corresponds to the degree of viscosity expressed in cSt at 100 ° C.

Figure 51: PAO8

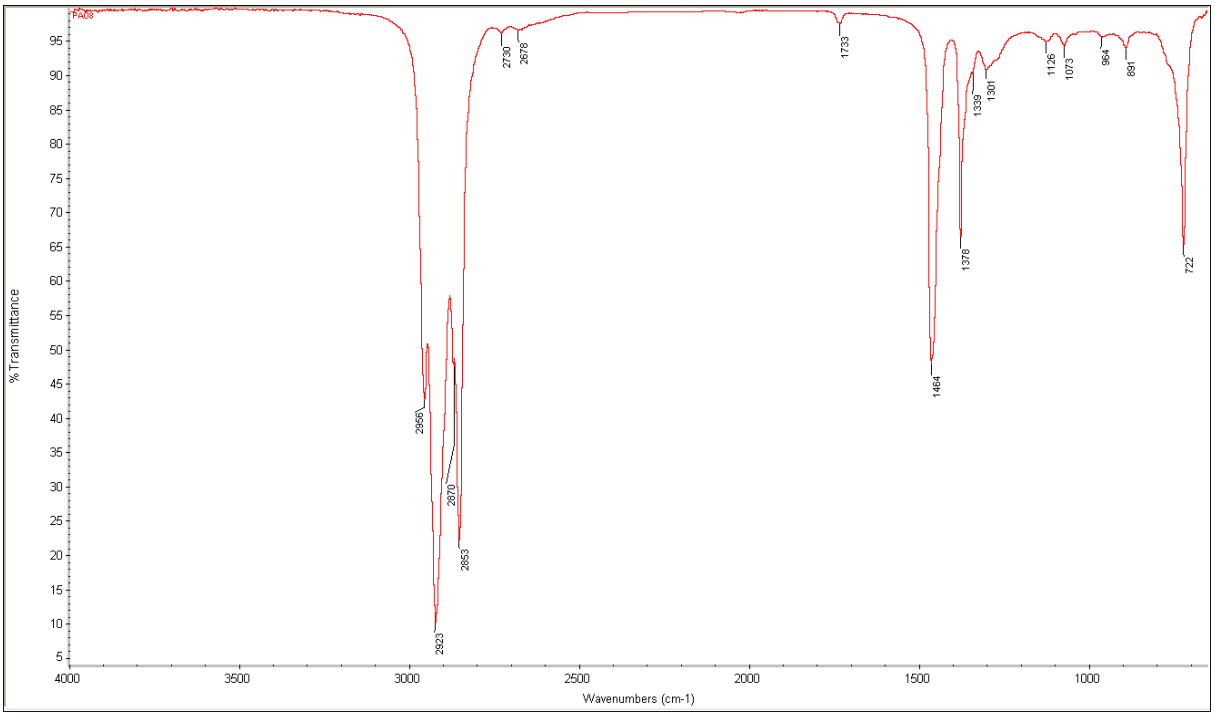

Figure 52: FT-IR of PAO8

In figure 53 the FT-IR spectra of the beginning clean soil and of the soil after PAO8 artificial pollution are reported.

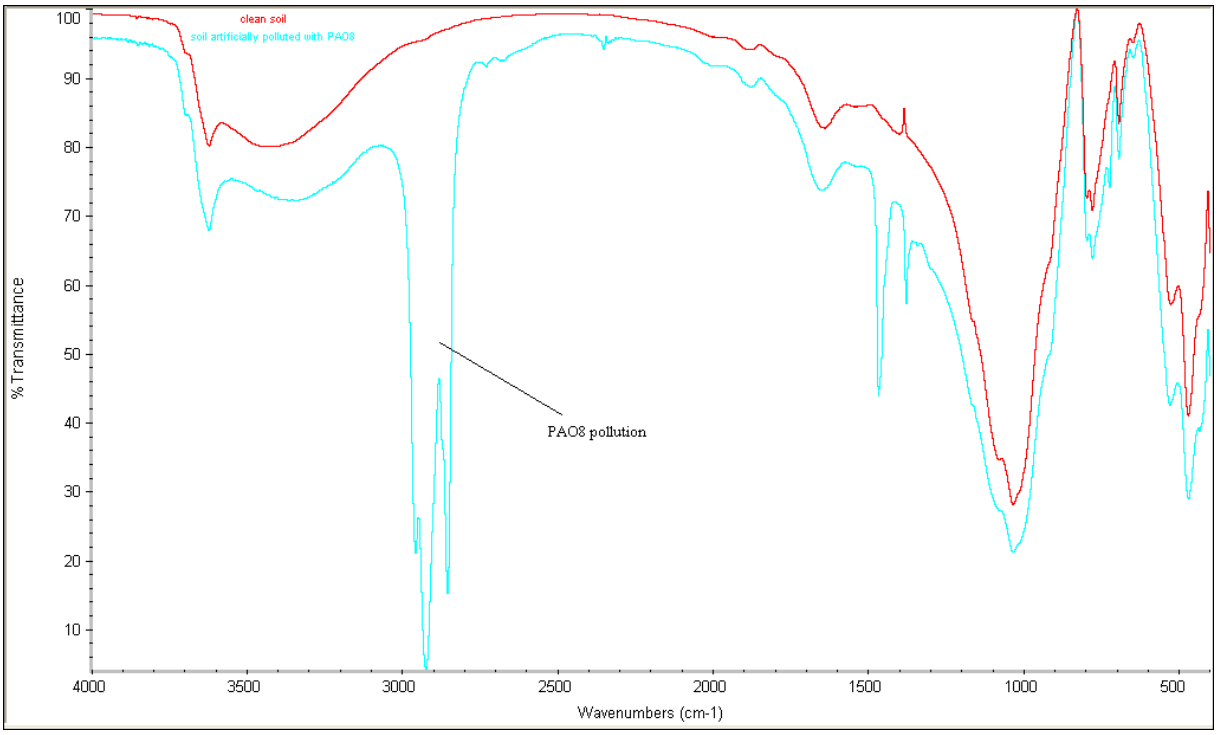

Figure 53: FT-IR spectra of clean soil (red line) and artificially polluted soil with PAO8 (blue line) before UV irradiation

The catalyst load was made by adding 5% of TiO_2 to the PAO8 contaminated soil and 5ml H_20 was added to acquire the desired amount of humidity. A Petri dish containing the sample was placed under the UV lamps. The distance from the lamp was 30mm and the UV wavelength was 310nm.

The sample was continuously monitored in order to add 10ml of H_2O each time it was dried and then mix it. The total residence time was 52 hours.

Quantification of PAO8 in the irradiated and non-irradiated soil samples (reference test) were obtained by the following method: the soil samples after the irradiation were transferred into round bottom flasks and mixed with 100ml of hexane. Each sample was extracted in hexane for 24 hours. The mixtures were then filtered with a Whatman round filter (pore size 4-7 µm) to separate the soils from the liquids. The latter ones were dried by Rotavapor to remove the solvent. The residues were re-dissolved in 10 ml of hexane and analysed with Carlo Erba GC-MS. Operatively 0.2µL of product are taken and injected directly into column, under the following conditions:

Mode: Splitless

Carrier: He (1cc/min)

Column: DB5-HS Agilent J&W (5% diphenyl-, 95% dimethilesiloxane)

Rampa: 80-280 °C at 10°C/min, Isot 15min

Sample: 0.2 µl

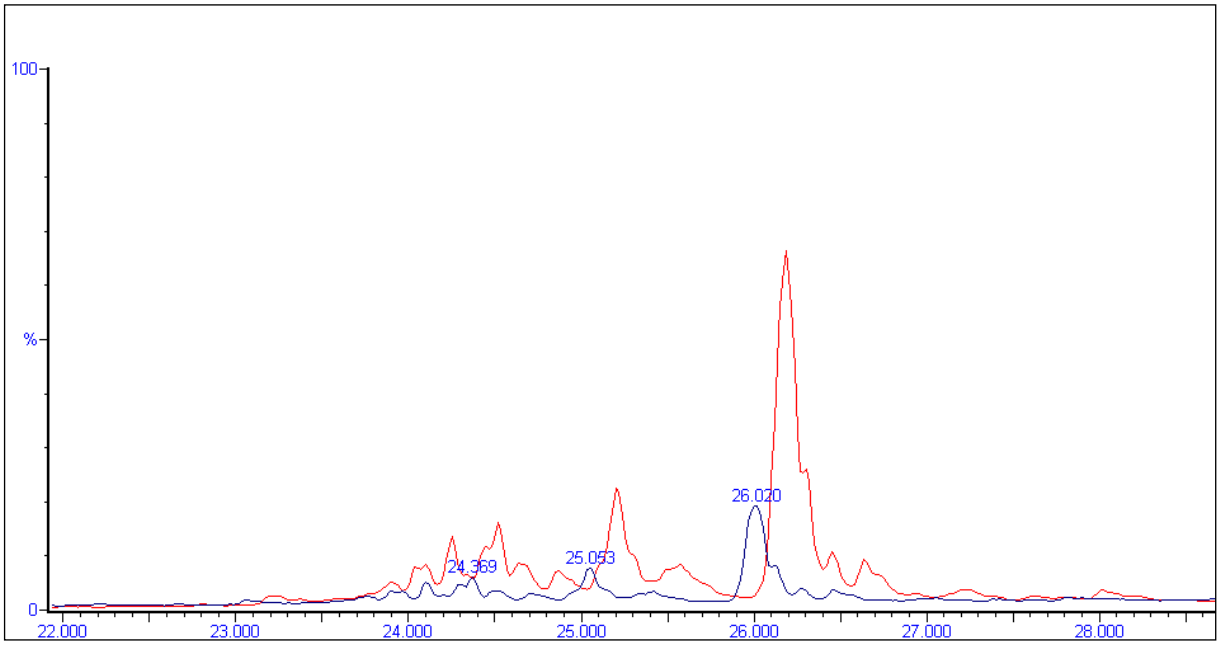

Figure 54: chromatograms of the PAO8 polluted samples with no UV irradiation (red line) and after photocatalytic experiment (blue line)

Figure 55: FT-IR of the PAO8 polluted sample with no UV irradiation (red line) and the sample after photocatalytic experiment (blue line)

7.3.1.2 Photocatalytic degradation of clean soil artificially polluted with a mixture of hydrocarbons

5g clean soil

5 ml of a mixture of hydrocarbons

5ml H_2O

5% TiO_2

Residence time: 47h

Differently from the previous test, the contaminants used in this case were a mixture of hydrocarbons composed by: toluene, heptane, hexane, octane, cyclohexane, isooctane, 10ml of each one.

5g of clean soil were spiked with 5ml of the hydrocarbon mixture. The soil was placed in a Petri dish, 5% of TiO_2 and 5ml of H_2O were added before turning on the UV lamps. The distance from the lamp was 30mm and the UV wavelength was 310nm. The total residence time was 47 hours.

Quantification of the degradation of hydrocarbons in the irradiated soil sample was obtained by the following method: the soil samples were transferred into round bottom flasks and mixed with 100ml of hexane. Each sample was extracted in hexane for 24 hours. The mixtures were then filtered with a Whatman round filters (pore size 4-7 µm) to separate the soils from the liquids. The latter ones were analysed with Carlo Erba GC-MS. Operatively 0.2µL of product are taken and injected directly into column, under the following conditions:

Mode: Split

Carrier: He (1cc/min)

Column: DB5-HS Agilent J&W (5% diphenyl-, 95% dimethilesiloxane)

Rampa: 60-280 °C at 2°C/min, Isot 15min

Solvent Delay: 1.8min

Sample: 0.2 µl

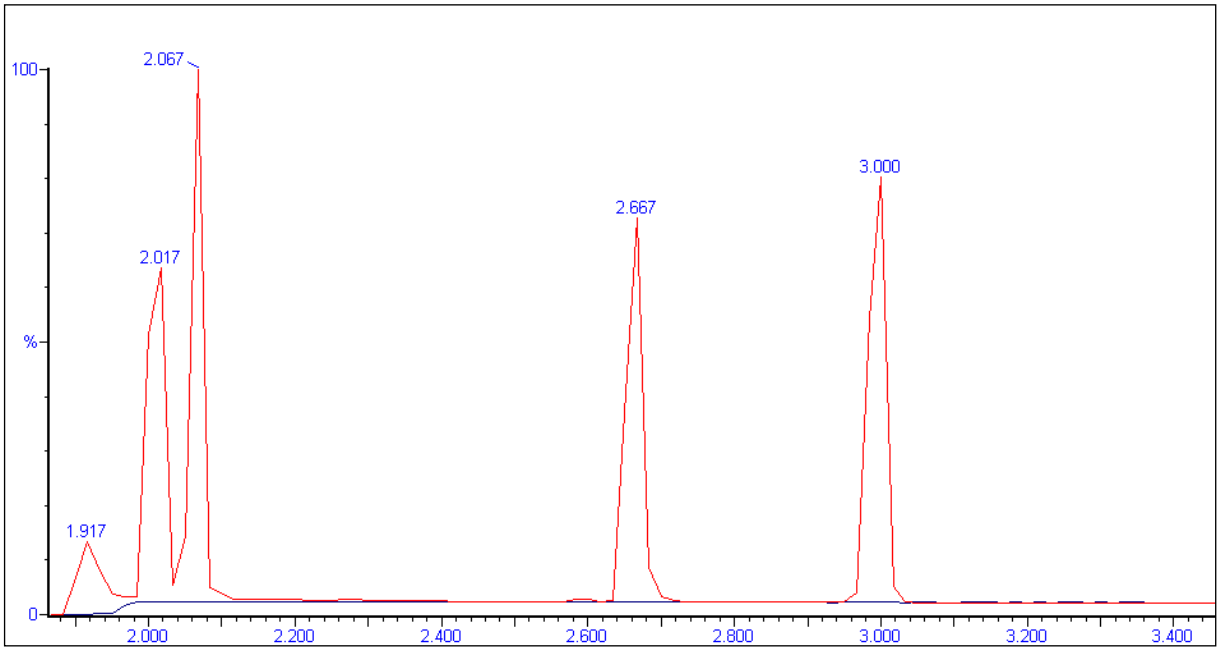

Figure 56: *chromatograms of the hydrocarbons polluted samples with no UV irradiation (red line) and after photocatalytic experiment (blue line)*

7.3.2 Photocatalytic degradation of real polluted soil sample

Different experiments were performed on the soil sample given by RE.AL Company in order to evaluate the efficiency of the photodegradation on real polluted soil surfaces and optimize the process under the experimental conditions described at the beginning of this chapter 7.3.

Therefore several photocatalytic experiments were implemented changing each time the main parameters: the content of TiO_2 and the possible use of substances, in this study THF and H_2O_2, in order to improve the degradation.

The soil sample was got by RE.AL service spa. The characterization of the sample is reported in chapter 6.

The final results in term of degradation were obtained by the following method: the soil samples after the irradiation were transferred into round bottom flasks and mixed with 100ml of hexane. Each sample was extracted in hexane for 24 hours. The mixtures were then filtered with Whatman round filters (pore size 4-7 µm) to separate the solid from the liquid phase. The latter was dried by Rotavapor to remove the solvent. The residues were re-dissolved in 10 ml of acetone and analysed with Carlo Erba GC-MS. Operatively 0.2µL of product are taken and injected directly into column, under the following conditions:

Mode: Splitless
Carrier: He (1cc/min)
Column: DB5-HS Agilent J&W (5% diphenyl-, 95% dimethilsiloxane)
Rampa: 80-280 °C at 10°C/min, Isot 15min
Solvent Delay: 4min
Sample: 0.2 µl

Two blank experiments were used as controls for the measurement of non-photocatalytic contaminant loss.

One consisted in a Petri dish containing 5 g of polluted soil sample with no addition of catalyst placed under irradiation and the second one in a Petri dish containing 5 g of polluted soil sample with 5% of TiO_2 posed in a dark room.

Temperature was measured to be at maximum 31° C in the samples subjected to irradiation.

7.3.2.1 Photocatalytic degradation of real polluted soil sample with 5% TiO_2

5g soil sample (RE.AL service spa)

5ml H_2O

5% TiO_2

Residence time: 47h

Photodegradation experiment was conducted in a box: 5g of soil sample provided by RE.AL Company were spread in a Petri dish distant 30mm from UV lamps. After adding 5% of TiO_2 and 5ml of H_2O the lamps were turned on. The sample was continuously monitored in order to add 10ml of H_2O each time it was dried and then mix it. The total residence time was 47 hours.

The results of analysis are shown by the chromatogram reported in figure 57 and the FT-IR in figure 58.

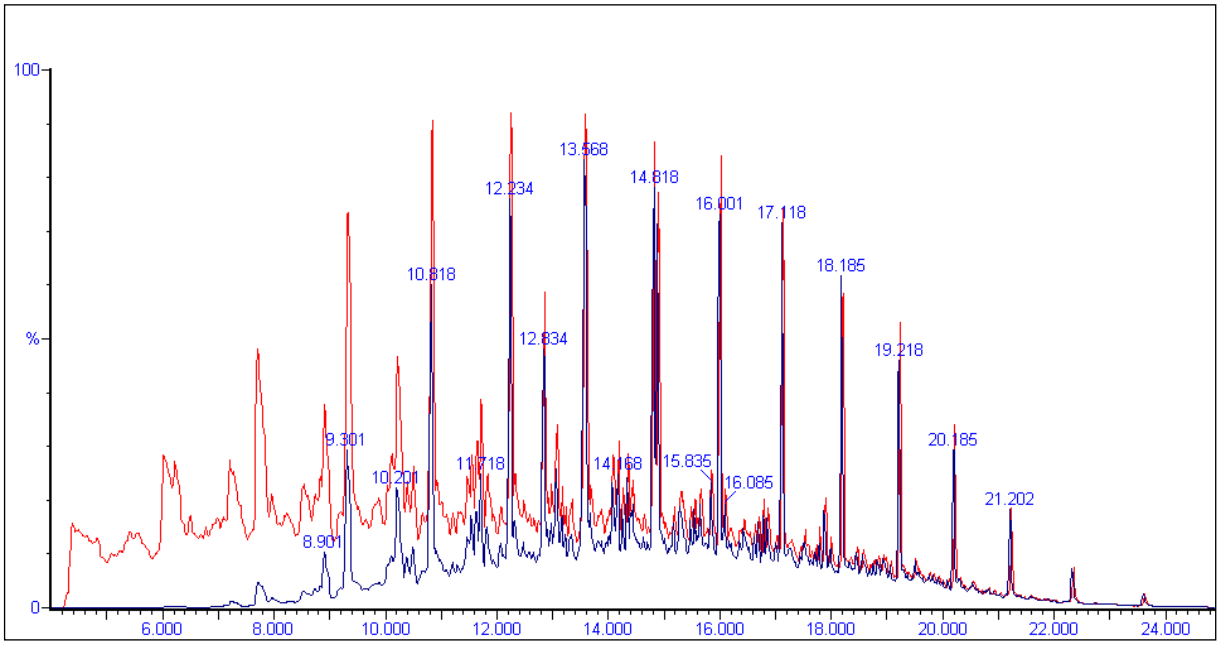

Figure 57: chromatograms of the RE.AL soil samples prephotocatalysis (red line) and after photocatalytic experiment with 5% of TiO_2 (blue line)

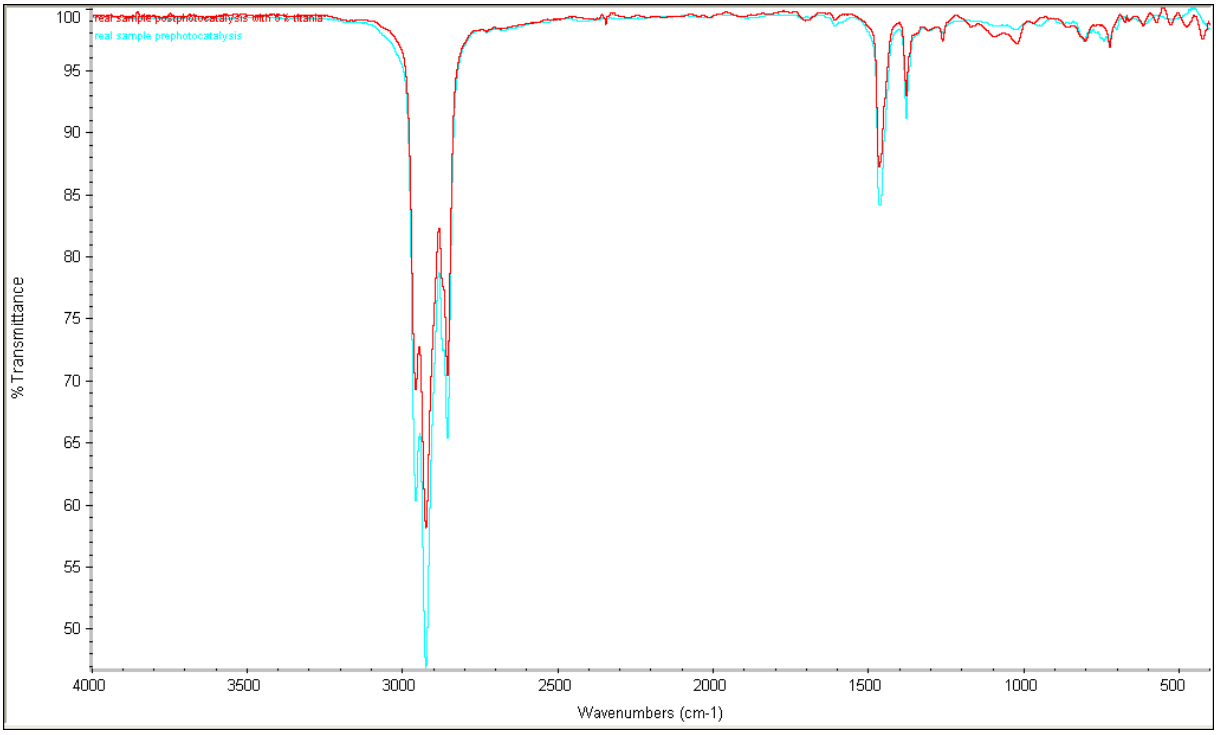

Figure 58: FT-IR of the RE.AL soil samples prephotocatalysis (blue line) and the sample after photocatalytic experiment with 5% of titania (red line)

7.3.2.2 Photocatalytic degradation of real polluted soil sample with 2% TiO_2

5g soil sample (RE.AL service spa)

5ml H_2O

2% TiO_2

Residence time: 47h

The type of experiment and the conditions were the same as the previous one except that the content of TiO_2 in this case was 2%.

5g of soil sample were spread in a Petri dish distant 30mm from UV lamps. After adding 2% of TiO_2 and 5ml of H_2O, the lamps were turned on. The sample was continuously monitored in order to add 10ml of H_2O each time it was dried and then mix it. The total residence time was 47 hours.

The chromatogram of GC-MS analysis is reported in figure 59.

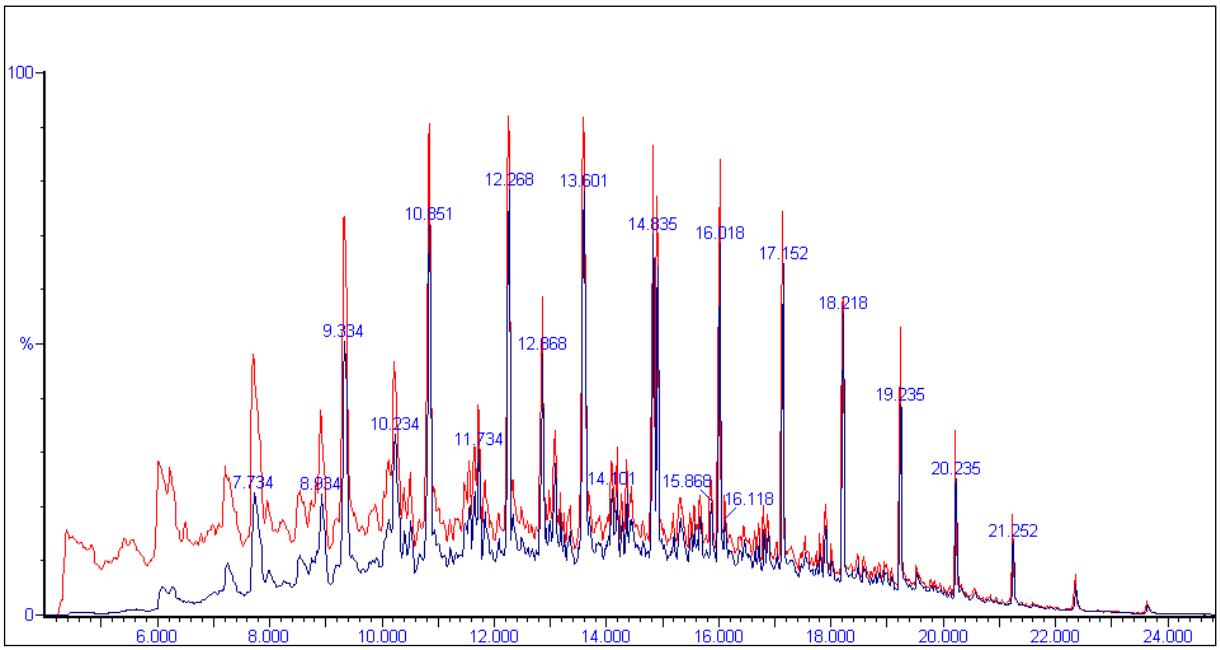

Figure 59: *chromatograms of the RE.AL.soil samples prephotocatalysis (red line) and after photocatalytic experiment with 2% of titania (blue line)*

7.3.2.3 Photocatalytic degradation of real polluted soil sample with THF

5g soil sample (RE.AL service spa) + 20ml THF (Tetrahydrofuran) mixed for 1h

20ml of H_2O

5% TiO_2

Residence time: 51h

The type of experiment and the conditions were the same as the previous tests except that in this case the use of a solvent like THF was studied in order to analyze if there would been an improvement in the efficiency of the photocatalytic degradation.

5g of soil sample (given by RE.AL service spa) were mixed for 1 hour with 20ml of THF. After the addition of 20ml of H_2O and 5% of TiO_2, the whole was spread in a Petri dish and placed under photo-irradiation for 51h. The sample was continuously monitored in order to add 20ml of H_2O/THF mixture (1:1) each time the soil was dried and then mix it.

The results of analysis are shown by the chromatogram reported in figure 60 and the FT-IR in figure 61.

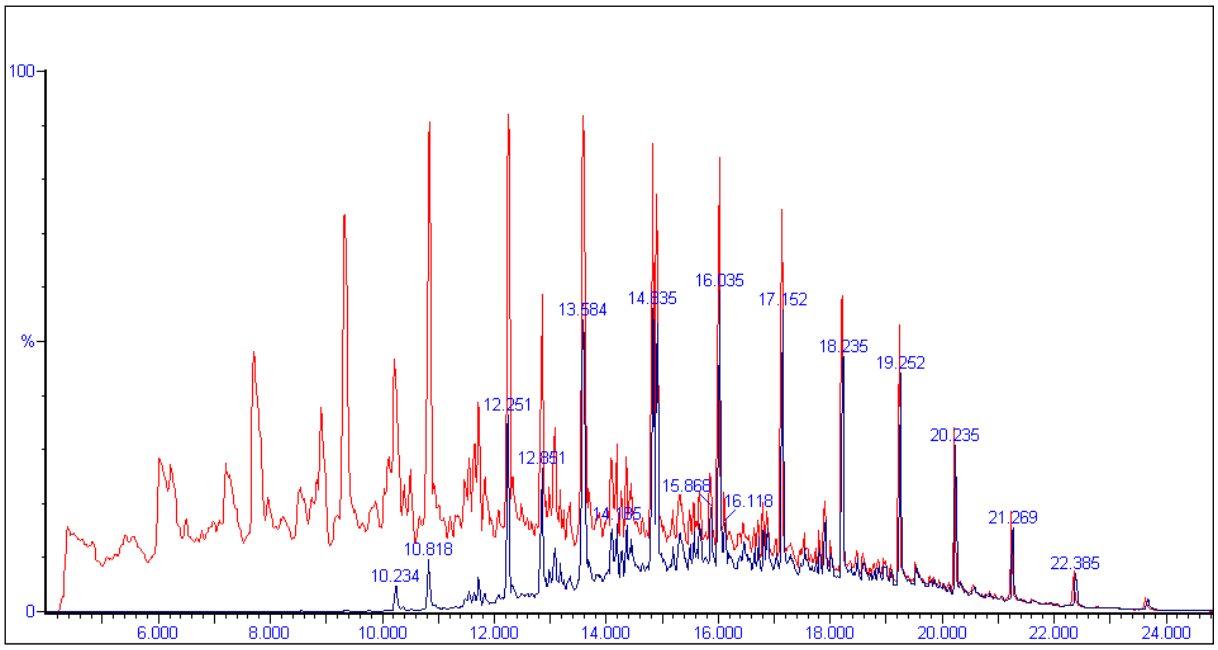

Figure 60: chromatograms of the RE.AL soil samples prephotocatalysis (red line) and after photocatalytic experiment with the addition of THF (blue line)

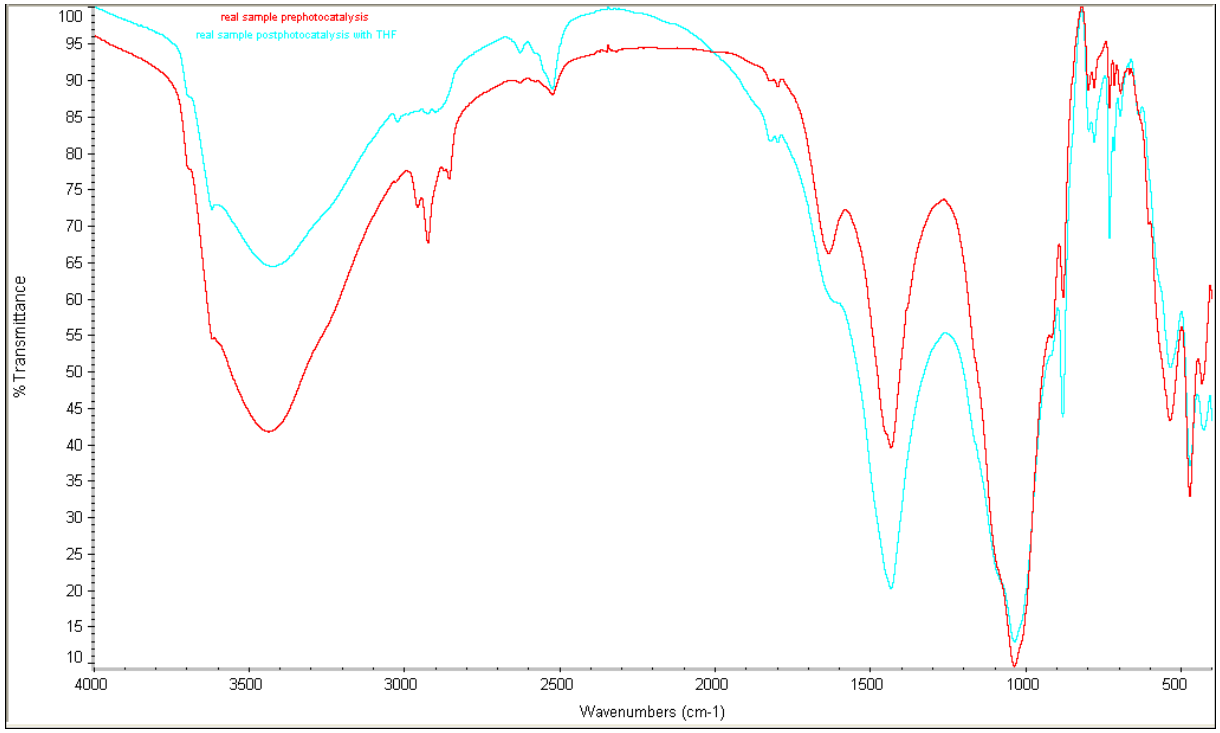

Figure 61: FT-IR of the RE.AL soil samples prephotocatalysis (red line) and the sample after photocatalytic experiment with the use of THF (blue line)

7.3.2.4 Photocatalytic degradation of real polluted soil sample with H_2O_2

5g soil sample (RE.AL service spa)

5ml H_2O_2

5% TiO_2

Residence time: 47h

The type of experiment and the conditions were the same as the previous tests except that in this case water was replaced with H_2O_2 with the aim of assessing whether the use of hydrogen peroxide could promote the degradation.

5g of soil sample (given by RE.AL service spa) were spread in a Petri dish. After the addition of 5% TiO_2 and 5ml of H_2O_2, the sample was placed under UV lamps. Each time it was dried, 10ml of H_2O_2 were added and the whole was mixed. The residence time was 47h.

The results of analysis are shown by the chromatogram reported in figure 62 and the FT-IR in figure 63.

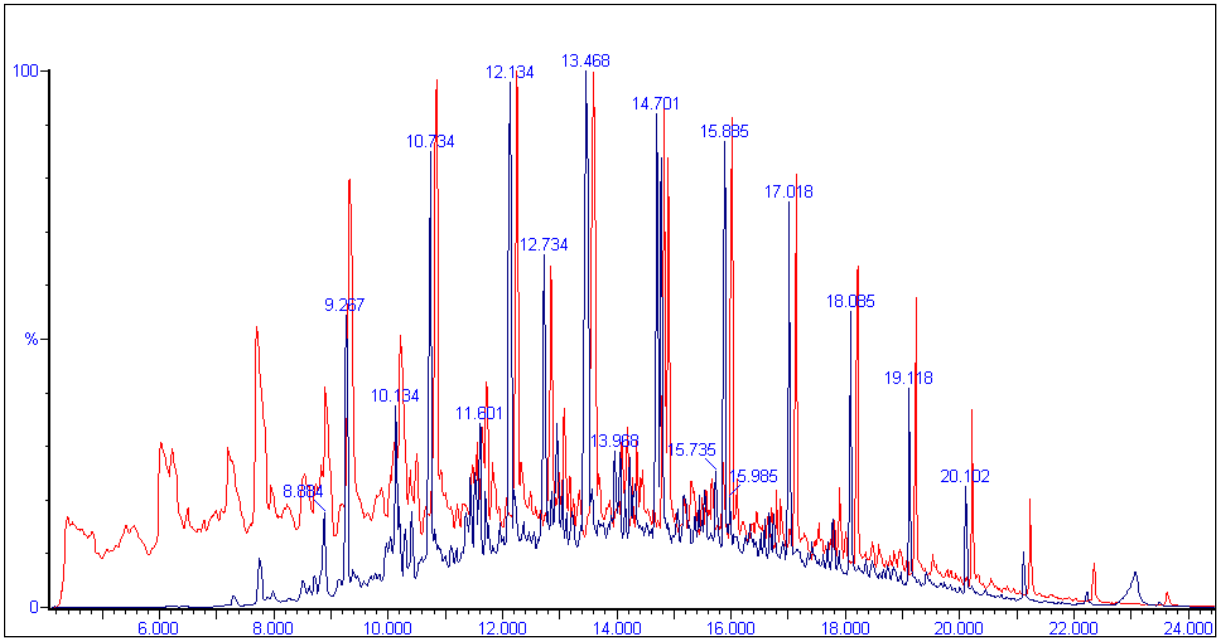

Figure 62: *chromatograms of the RE.AL soil samples prephotocatalysis (red line) and after photocatalytic experiment with the use of H_2O_2 instead of water (blue line)*

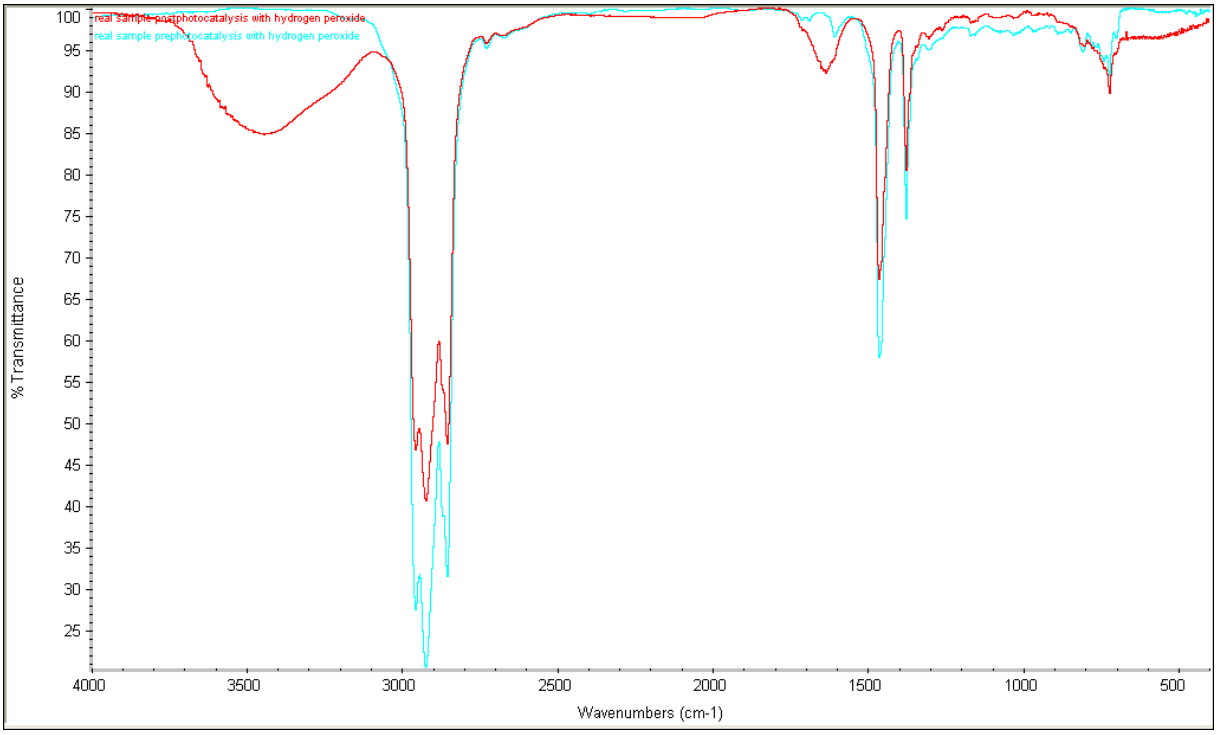

Figure 63: FT-IR of the RE.AL soil samples prephotocatalysis (blue line) and the sample after photocatalytic experiment with the use of H_2O_2 (red line)

8. DISCUSSION OF THE RESULTS

8.1 DISCUSSION OF THE RESULTS OF PHOTOCATALYTIC DEGRADATION IN AQUEOUS SUSPENSION

The results of the experiments on aqueous suspension confirm that the system has worked under the laboratory conditions. Rhodamine-b and a known mixture of hydrocarbons were degraded under those UV lamps.

8.1.1 Rhodamine-b

The standard method use to verify the efficiency of a photocatalytic system is the implementation of a photocatalytic test of Rhodamine-b. UV/TiO_2 process can be used successfully for the treatment of Rhodamine-b in aqueous suspension (Aliabadi, 2011).
Rhodamine-b degradation is reported in figure 64 and it confirm the success of the test.

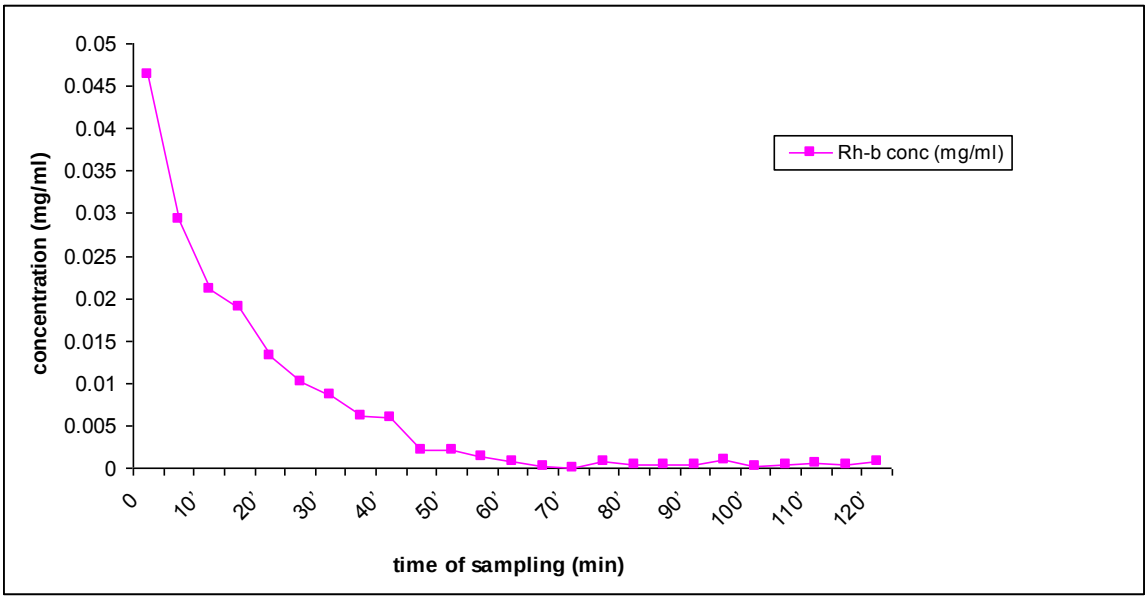

Figure 64: degradation of Rh-b: concentrations Vs time

8.1.2 Mixture of hydrocarbons

To analyze the hydrocarbon degradation in aqueous suspension the areas of each peak in chromatogram before and after photo-irradiation were calculated and compared with the area of octane's peak, that was the less degraded so it was assumed as constant. Comparing

the ratios before and after photocatalysis, the percentage of degradation of hexane, cyclohexane, isooctane, heptanes and toluene are 72.9%, 53.7%, 20.8%, 20.4% and 6.6% respectively. Table 10 and figure 65 show the result of the degradation of hydrocarbon mixture.

Table 10: degradation % of different hydrocarbons after UV irradiation in aqueous suspension. Octane's amount has been considered constant.

hydrocarbon	degradation %
hexane	72,9
cyclohexane	53,7
isooctane	20,8
heptane	20,4
toluene	6,6

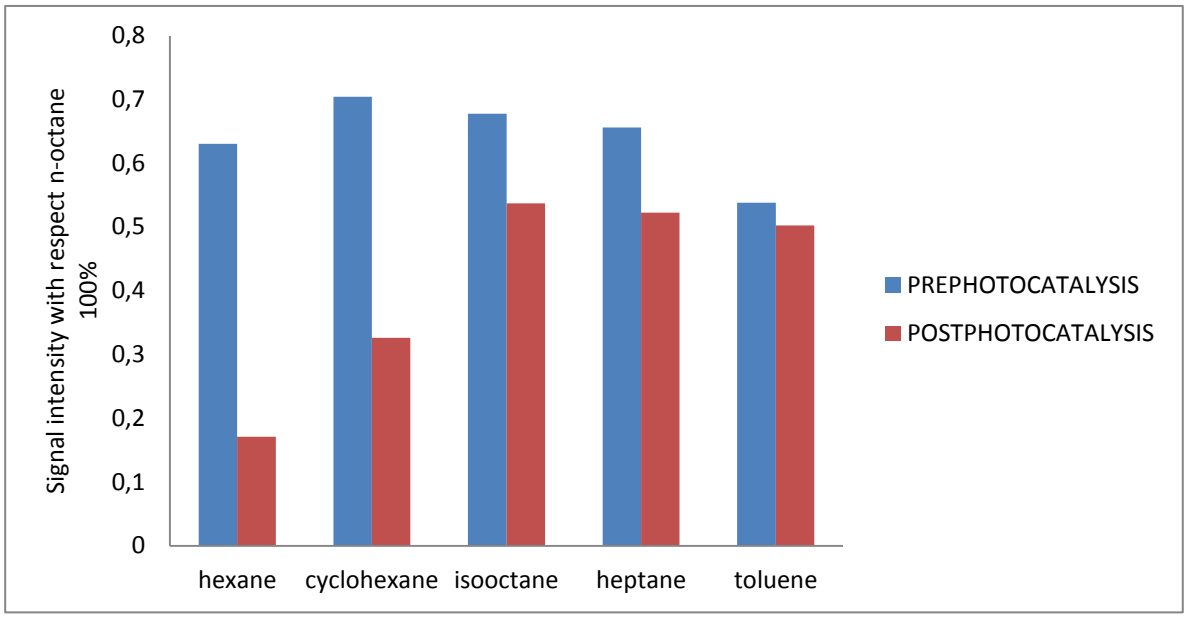

Figure 65: photodegradation of each hydrocarbon in aqueous suspension: the signal intensity is referred to the intensity of n-octane that is considered been 100%.

8.2 DISCUSSION OF THE RESULTS OF PHOTOCATALYTIC DEGRADATION ON SOIL SURFACES

The analysis of scientific papers in the literature showing the following key points:

- the few examples in the literature are all based on contaminated soil in laboratory;
- the degradation is not complete: although the removal is efficient, a 20 - 40% of contaminants are retained into the soil;
- the degradation of organic compounds results extremely difficult: it never leads to complete degradation of the pollutants.

8.2.1 Clean soil polluted with a mixture of hydrocarbons

In clean soil artificially polluted with a mixture of hydrocarbons the result show that hydrocarbons are completely degraded by photocatalysis under the laboratory conditions described in chapter 7.

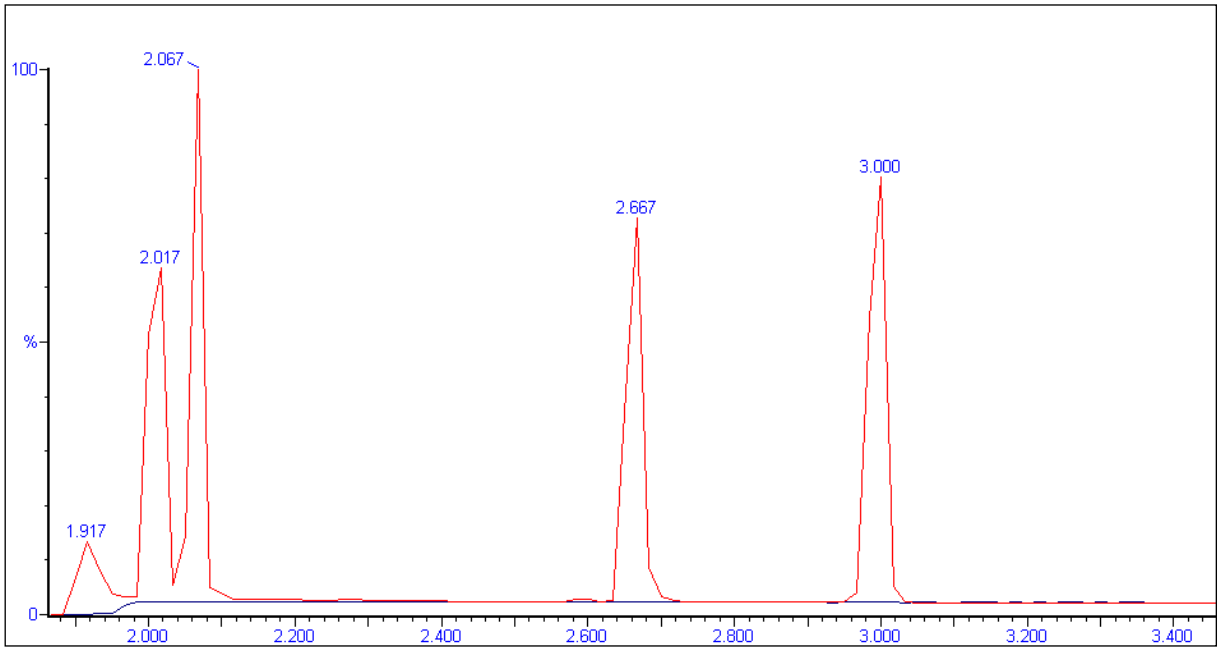

Figure 66: chromatograms of the hydrocarbons polluted samples with no UV irradiation (red line) and after photocatalytic experiment (blue line)

To be sure that hydrocarbons were not evaporated, the temperature of the soil inside the photoirradiated box was measured and compared with boiling temperature of each compounds: the measured temperature in soil exposed to UV irradiation was about 31°C

while the boiling temperatures of the present hydrocarbons are higher and reported in table 11.

Table 11: boiling temperatures of different hydrocarbons

hydrocarbon	Boiling temperature °C
hexane	69
cyclohexane	81
isooctane	99
heptane	98,4
toluene	110,6
octane	125,7

8.2.2 Clean soil polluted with PAO8

As the chromatogram report in figure 67 shows, the quantity of PAO8 in the soil sample decreases.

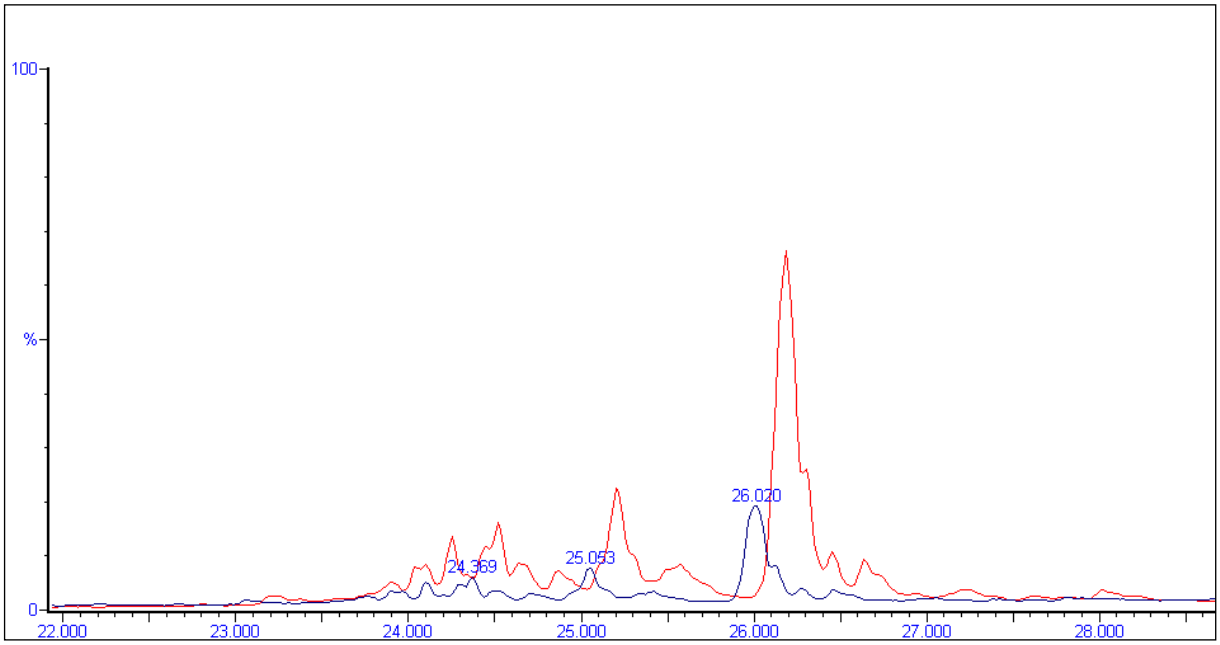

Figure 67: chromatograms of the PAO8 polluted samples with no UV irradiation (red line) and after photocatalytic experiment (blue line)

A selective disappearance of some components is detected; in particular the degradation appears to be greater on the components of the mixture with a lower retention time.

Overall, considering the total ion current, the intensity was changed from 2.66×10^6 to 7.74×10^5. This agrees with the result of Hamerski et al.: the degradation of the oil is only partial.

8.2.2 Real polluted soil

As regards real contaminated soil given by RE.AL Company, different experiments were performed in order to evaluate the efficiency of photocatalytic degradation on real polluted soil surfaces changing each time the test's conditions.

First of all, two blank experiments were used as controls for the measurement of non-photocatalytic contaminant loss.

One consisted in a Petri dish containing 5 g of polluted soil sample with no addition of catalyst placed under irradiation and the second one in a Petri dish containing 5 g of polluted soil sample with 5% of TiO_2 posed in a dark room. The result of the second blank showed no contaminants loss while the first one showed a reduction of lighter compounds. As shown in figure 68 there was a degradation of the first peak but the others contaminants remained unchanged.

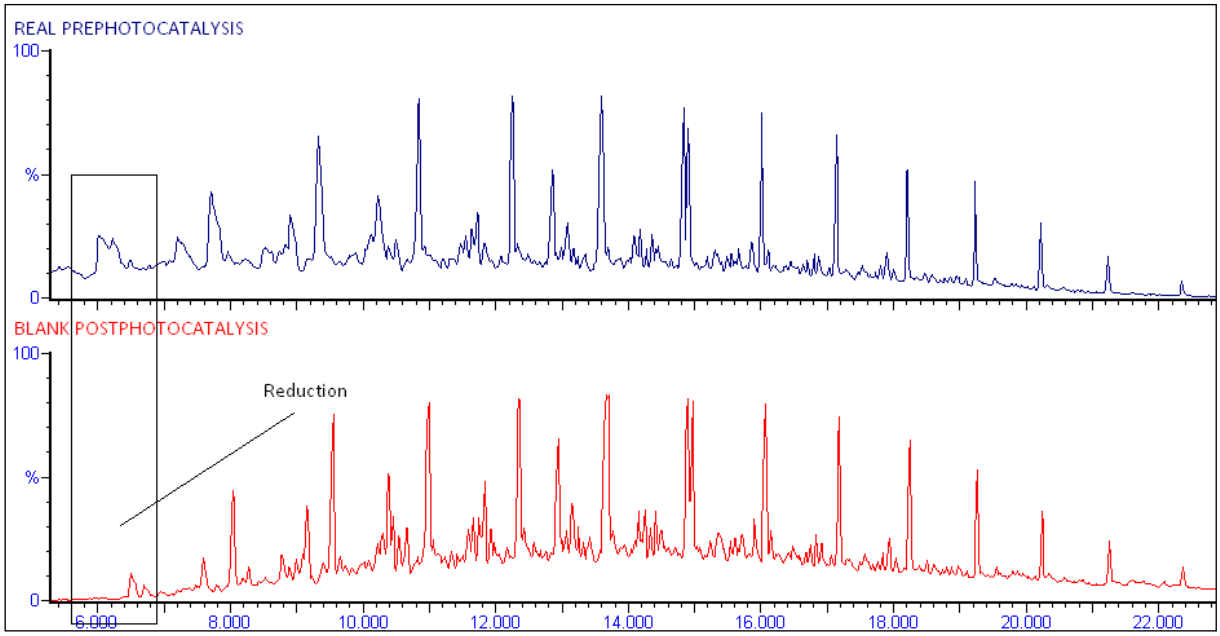

Figure 68: chromatograms pre and postphotocatalysis of blank experiment with no TiO_2 under UV irradiation. The chromatogram of blank test in dark room with TiO_2 is not reported because identical to that regarding the prephotocatalysis soil sample.

Temperature within the box was measured in this case too and compared with boiling temperatures of the contaminants present in the polluted soil and characterized with the steps described in chapter 6. Temperature in the test was always about 31°C and the lower boiling temperatures of the lighter compounds present in the mixture are 195 °C for undecane and 216.2 °C for dodecane.

Therefore TiO_2 in the absence of light and light in the absence of TiO_2 have no effect on the degradation of contaminants present into the soil.

During the experimental work the following parameters have been evaluated:

A. TiO_2 content: two tests are performed with 2 and 5% of TiO_2 respectively.
B. The presence of a solvent capable of dissolving both the hydrocarbons and water reducing the heterogeneity of the reactions: THF was selected.
C. Increment of the oxidizing capacity of the photocatalytic system with the introduction of hydrogen peroxide.

A. TiO_2 content

First tests were performed changing the content of the photocatalyst from 5% to 2%. Many studies have demonstrated that the rates of photocatalytic degradation of organic pollutants on soil surfaces are strongly affected by the dosage of the TiO_2 used (Dong, 2010).
Dong et al. in the scientific paper titled "Photocatalytic degradation of phenantrene and pyrene on soil surfaces in the presence of nanometer rutile TiO_2 under UV irradiation" state that the optimal catalyst dosage is 2% of TiO_2. In this thesis work there are two results:

- A significant reduction of the contaminants up to C_{13} with 2% TiO_2 and to C_{14} with 5% TiO_2 is observed (table 13).
- The degradation increases with 5% of TiO_2 compared to 2%: this result agrees with what is written in the literature for which, increasing the content of TiO_2 from 0 to 2%, degradation increases. In the case study 5% is the best value. For instance considering the peak corresponding to n-C_{13} the percentage of degradation with 2% of TiO_2 is 23.82, with 5% is 59.13 (table 13).

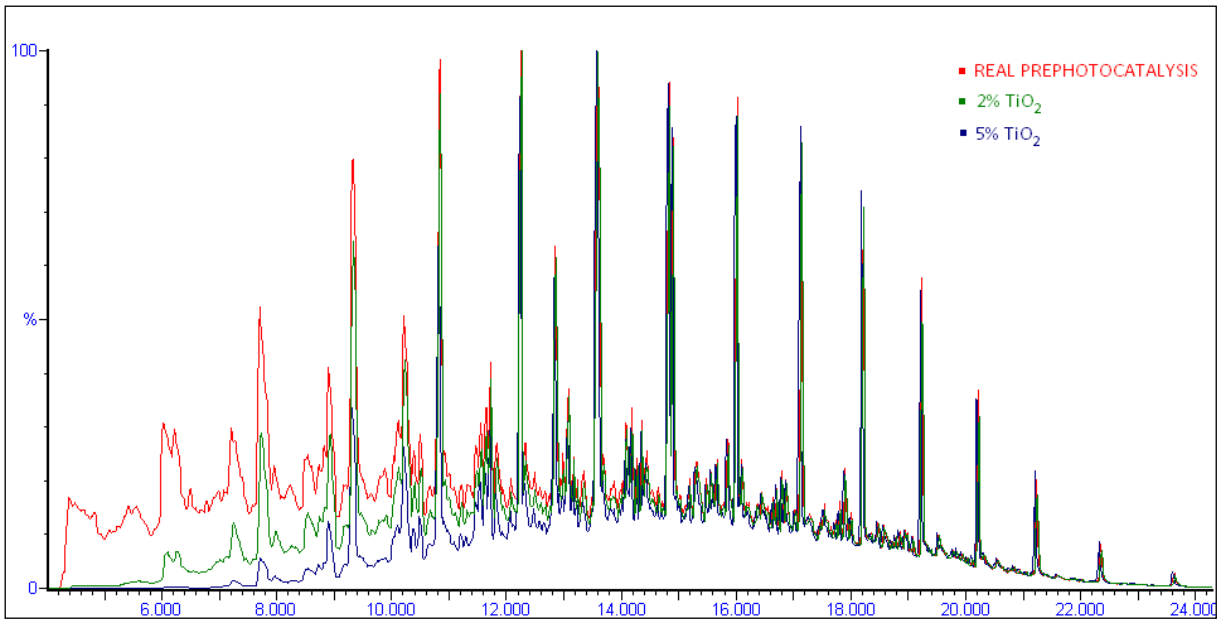

Figure 69: comparison between the chromatograms of prephotocatalysis, postphtocatalysis with 5% of TiO_2 and the one with 2% of TiO_2.

B. Presence of THF

In the presence of THF the percentage of degradation increases significantly for all compounds up to C_{17} and causes, even if limited, degradation even up to C_{20}.

The result is shown in figure 70 where the chromatogram resulted by the photodegradation with THF is compared with that of the soil prephotocatalysis. The use of a solvent, in this case THF, facilitates the hydrocarbon degradation because the solvent reduces the heterogeneity of the reactions.

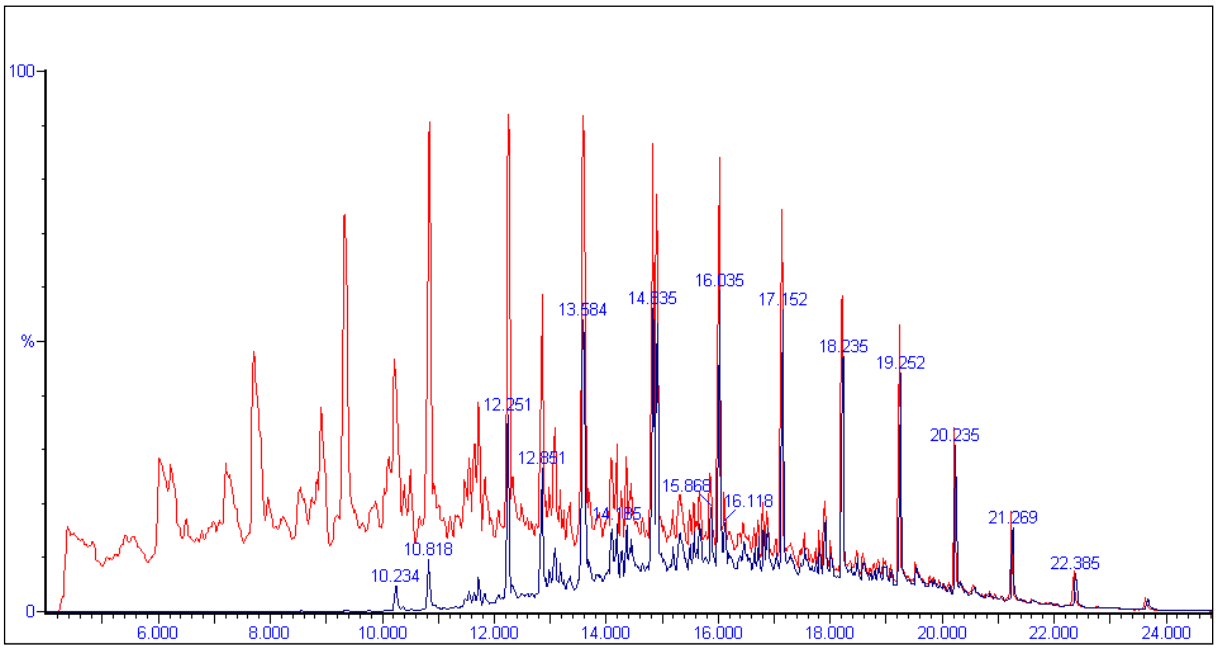

Figure 70: chromatograms of the soil samples prephotocatalysis (red line) and after photocatalytic experiment with the addition of THF (blue line)

In figure 71 is shown the comparison between the chromatograms of photocatalytic tests under different conditions: 2%TiO_2, 5%TiO_2 and THF.

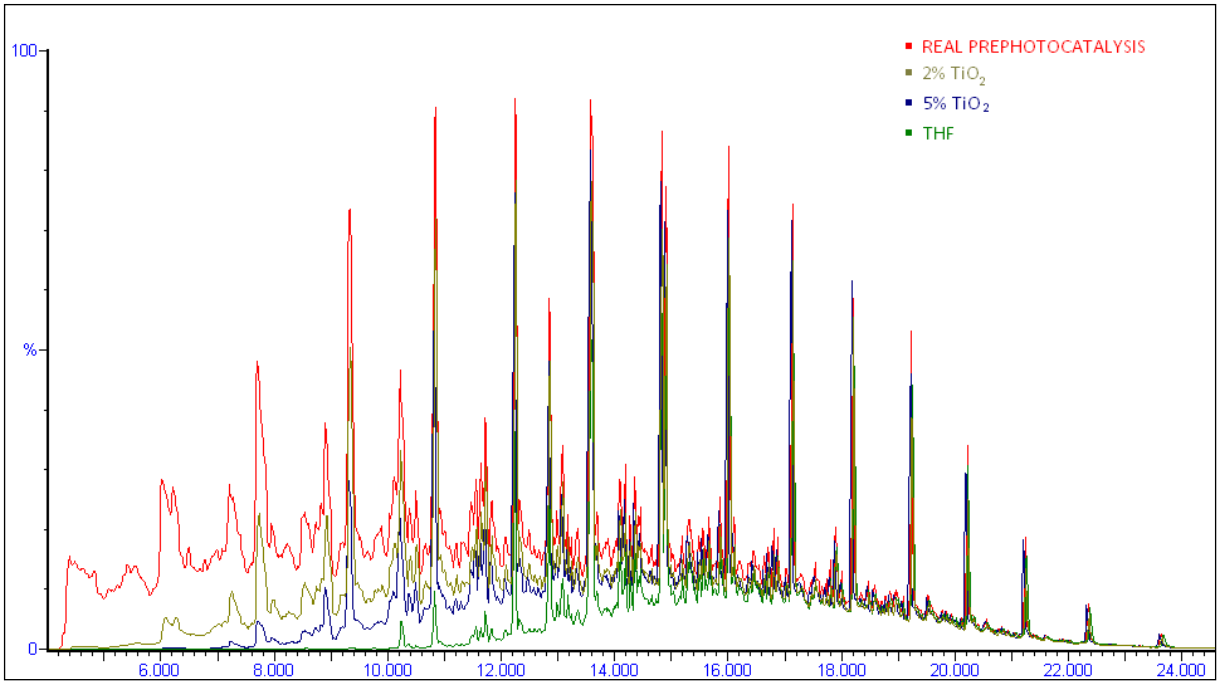

Figure 71: comparison between different photocatalytic degradations implemented under different conditions: 2%TiO_2 5%TiO_2 and THF

C. Use of H_2O_2

The use of hydrogen peroxide in presence of 5% of TiO_2 instead of water has been tested as suggested in literature.

The effect appears lowered when compared with the experiment done with 5% TiO_2 without H_2O_2 (figure 72). Degradation is complete for C_{11} and C_{12}, is slightly higher for n-C_{13} and C_{14}iso. Almost unchanged for n-C_{14}.

Dong et al. state that the addition of H_2O_2 sped up the photocatalytic degradation of phenantrene and pyrene on soil surfaces in the presence of nanometer rutile TiO_2. Instead in the thesis work, the use of hydrogen peroxide has not lead to an increase in photocatalytic efficiency in fact, as the chromatograms, reported in figure 72, show, the degradation of hydrocarbons in photocatalysis with 5% of TiO_2/UV/H_2O and in photocatalysis with 5%TiO_2/UV/H_2O_2 are more or less the same. McGeever (1983) found that H_2O_2 addition (up to 3x10-3 M) decreased the degradation rate of perchloroethylene in the UV/TiO_2 system. Tanaka et al. (1990) investigated the effect of H_2O_2 addition on the photocatalytic degradation of organochlorine compounds and organophosphorus insecticides: addition of low H_2O_2 concentrations ($5x10^{-5}$ to 10^{-2} M) increased the degradation rate while high concentrations of H_2O_2 (>10^{-2} to $5x10^{-1}$ M) reduced the rate.

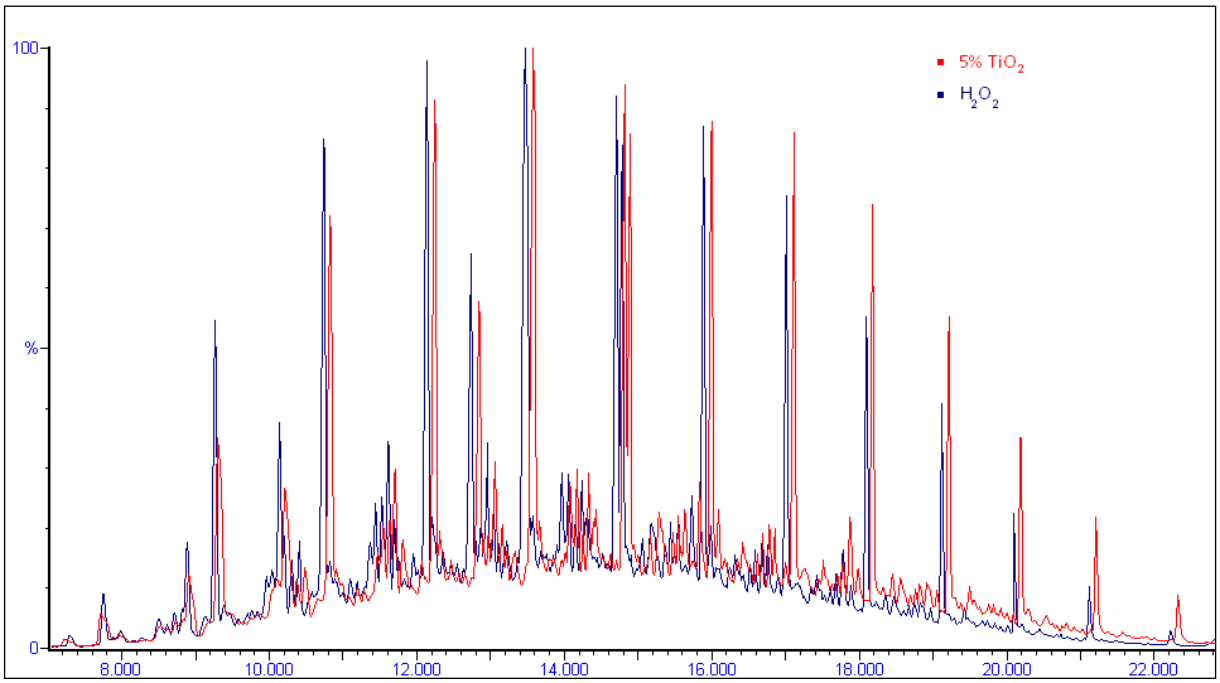

Figure 72: *comparison between the chromatograms of phtocatalysis with 5% of TiO_2 and the one with H_2O_2 instead of water.*

A quantitative analysis was made calculating the areas of the peaks in chromatograms and comparing the ratio between each peak with the peak at the retention time of 16.018 corresponding to C_{21}, which seems to remain unchanged in all the tests so it is considered constant.

The results are reported in tables 12-13 and in graphs 73-74-75-76-77-78.

Table 12: results of photodegradation in different conditions. All the amount are referred to the signal intensity of C_{21} that is considered constant. The values are the ratio between the intensity of each signal and the intensity of C_{21}.

peak	INITIAL SOIL	2% TiO_2	5% TiO_2	H_2O_2	THF
C11	1,015	/	/	/	/
C12	1,595	0,867	/	/	/
C13	2,146	1,635	0,877	0,860	/
iso-C14	1,104	0,995	0,602	0,463	0,118
C14	1,821	1,649	1,337	1,341	0,215
C16	1,480	1,327	1,230	1,385	0,675
C17	0,906	0,846	0,812	0,906	0,481
C18	2,189	2,018	1,958	2,102	1,610
C19	1,147	1,108	1,100	0,960	1,052
C20	0,974	0,981	0,882	0,890	0,932

Table 13: results of photocatalysis in different conditions. The percentage of degradation are calculated referring all the amount of contamninants to the signal intensity of C_{21} that is considered constant.

% OF DEGRADATION					
peak	**INITIAL SOIL**	**2% TiO_2**	**5% TiO_2**	**H_2O_2**	**THF**
C11	1,015	100	100	100	100
C12	1,595	45,60	100	100	100
C13	2,146	23,82	59,13	59,93	100
iso-C14	1,104	9,91	45,48	58,11	89,28
C14	1,821	9,48	26,57	26,36	88,22
C16	1,480	10,32	16,86	6,42	54,41
C17	0,906	6,61	10,38	0,00	46,91
C18	2,189	7,85	10,58	3,97	26,47
C19	1,147	3,44	4,09	0,00	8,29
C20	0,974	-0,69	9,52	1,48	4,31

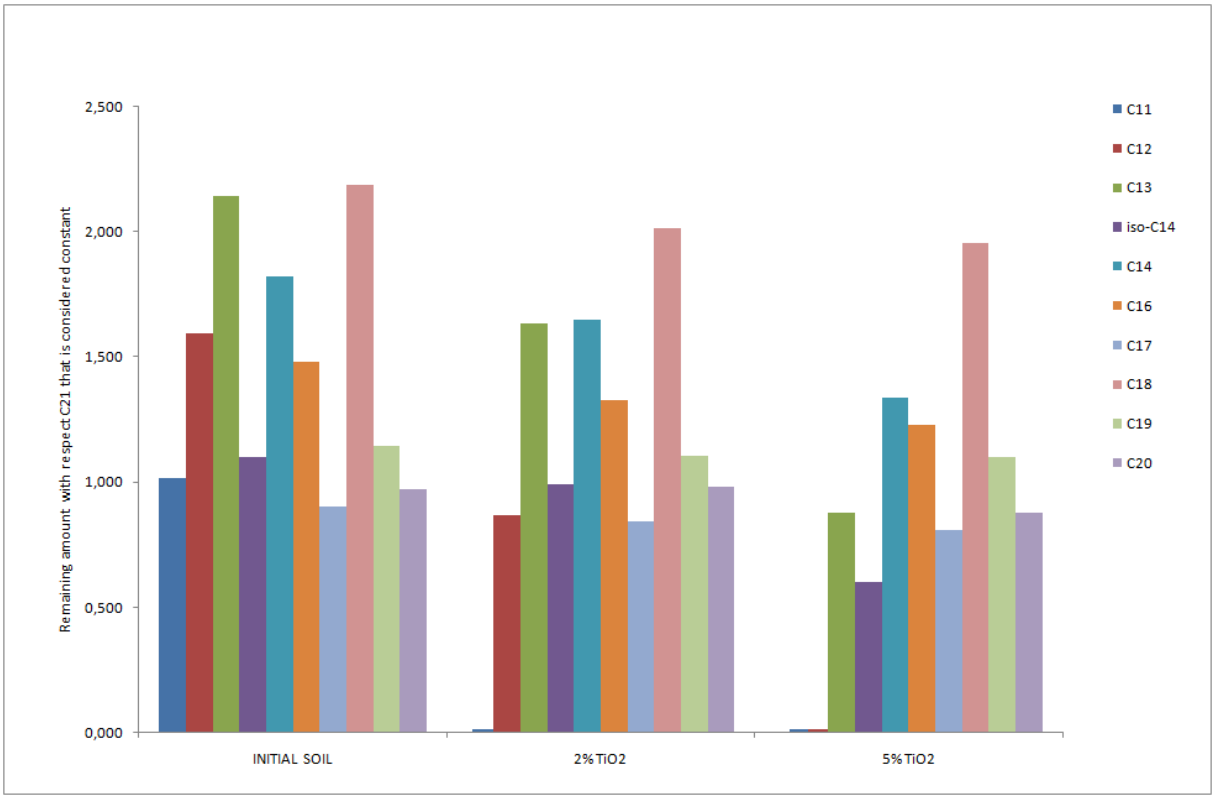

Figure 73: result in the degradation of the rise from 2 to 5% of the TiO_2 content. All the amounts are referred to the signal intensity of C_{21} that is considered constant

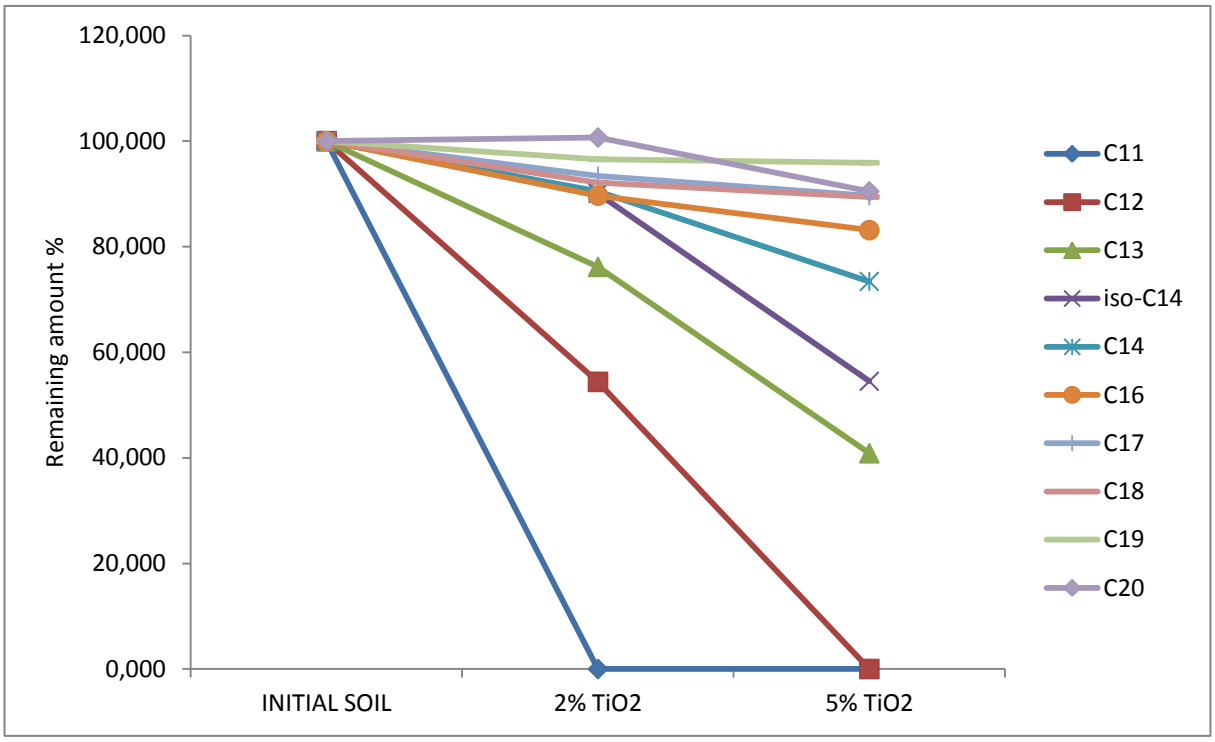

Figure 74: result in the degradation of the rise from 2 to 5% of the TiO_2 content: remaining amount (%)

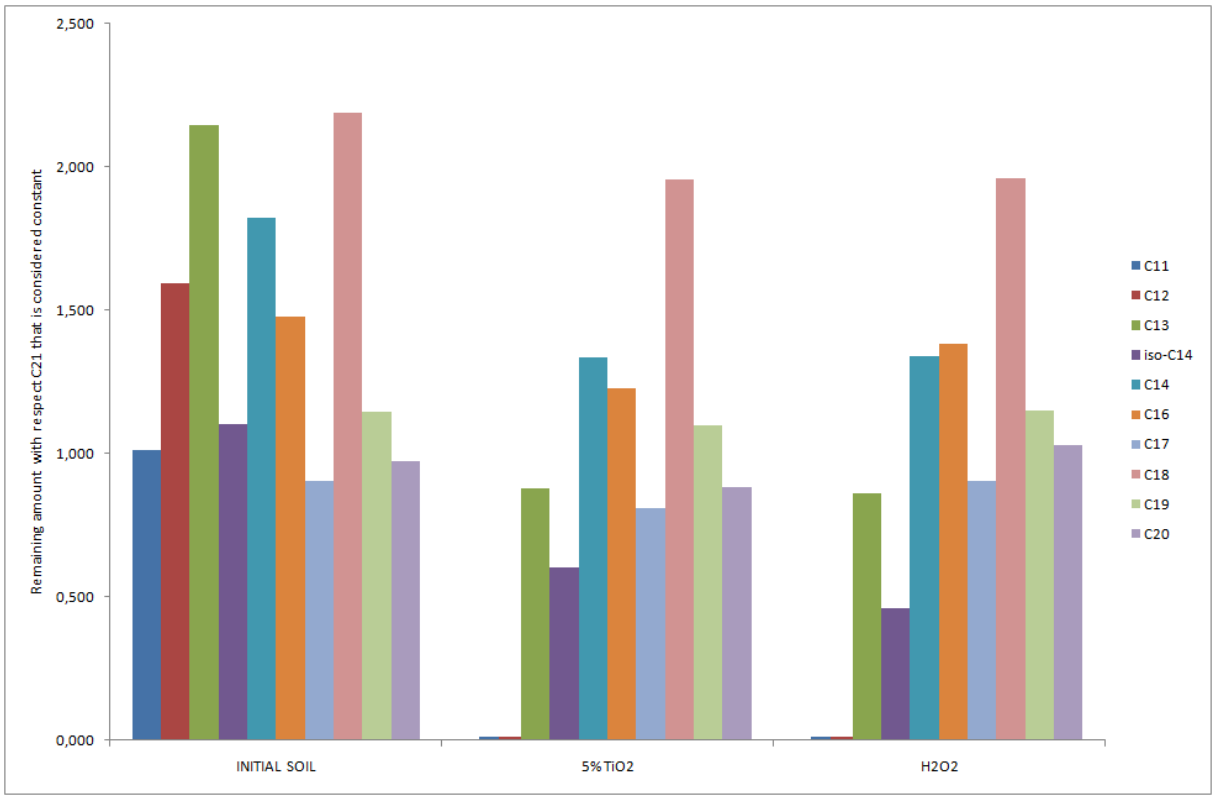

Figure 75: effect in the degradation of the use of hydrogen peroxide instead of water. All the amounts are referred to the signal intensity of C_{21} that is considered constant

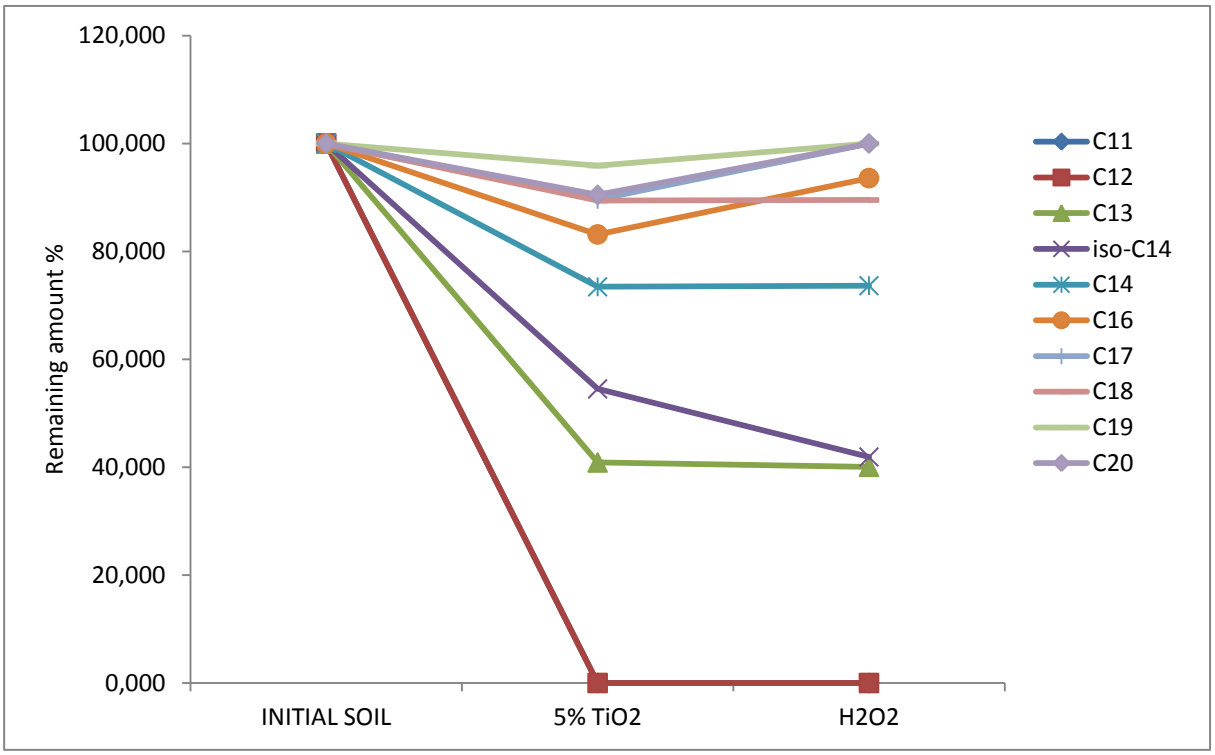

Figure 76: effect in the degradation of the use of hydrogen peroxide instead of water: remaining amount (%)

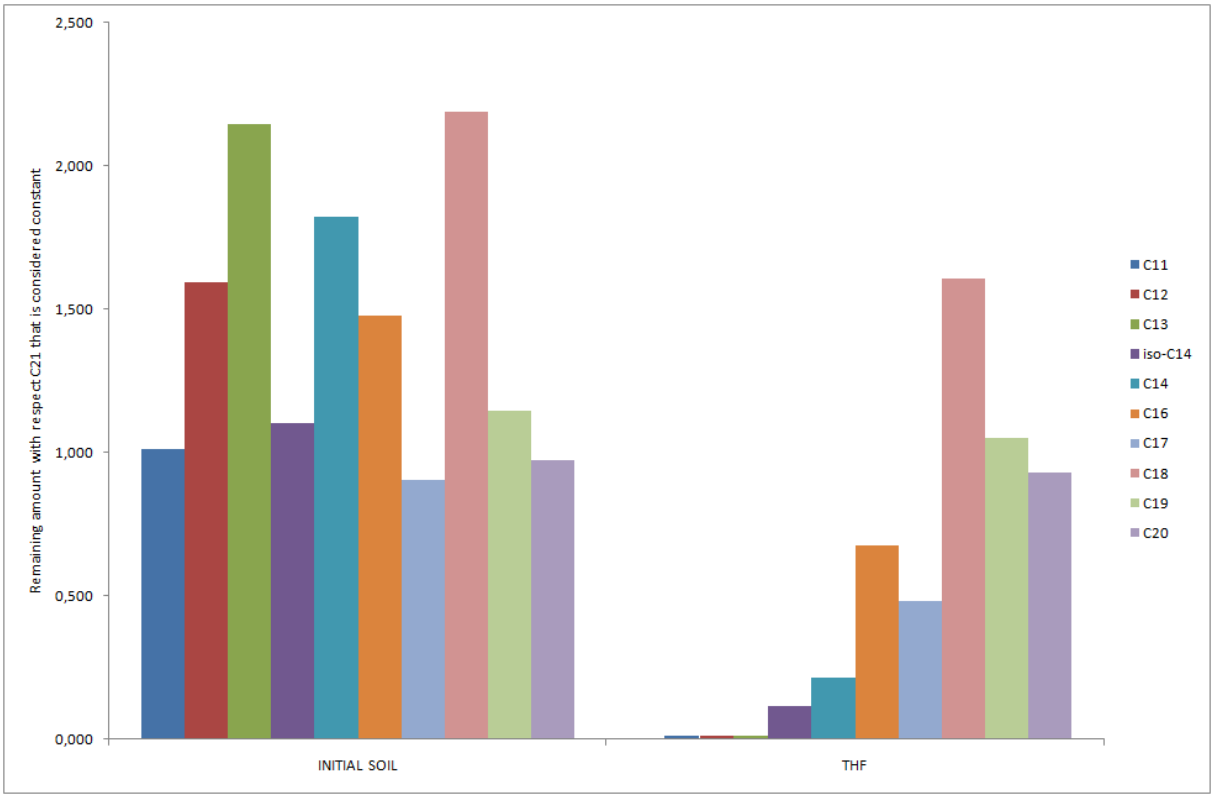

Figure 77: effect in the degradation of the use of THF. All the amounts are referred to the signal intensity of C_{21} that is considered constant

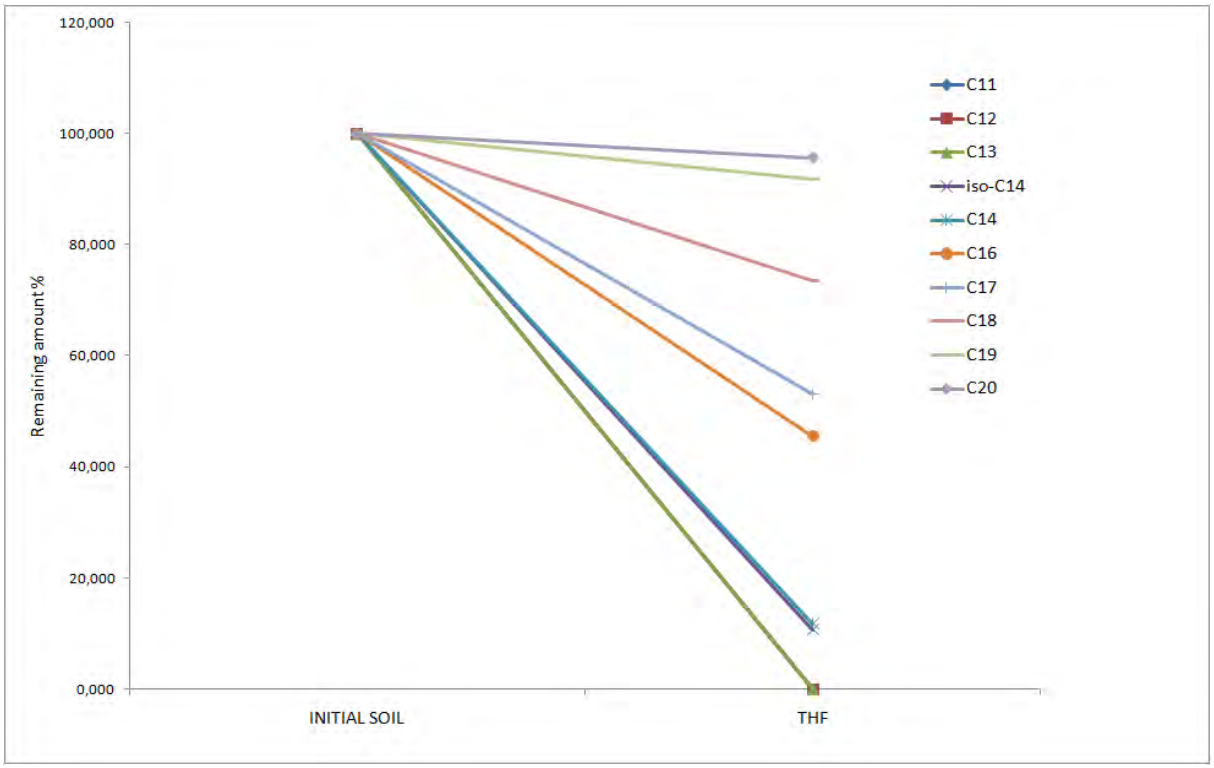

Figure 78: effect in the degradation of the use of THF: remaining amount (%)

9. CONCLUSIONS AND SUGGESTIONS

The experimental study described in chapter 7 and the analysis of the results compared to those reported in the literature lead to the following conclusions:

- From the literature and from experimental data it is observed that the photocatalytic degradation of hydrocarbon pollutants in the soil is a complex process, practically not efficient for hydrocarbons heavier than C_{20}.
- It was observed that increasing the percentage of TiO_2, the efficiency of degradation increases up to C_{14}.
- The effect of the presence of hydrogen peroxide seems to be not significant under the experimental conditions.
- The presence of a solvent, such as THF, able to solubilise the water and hydrocarbons simultaneously, has a remarkable effect on the efficiency of photodegradation. In particular, the compounds C_{11}, C_{12} and C_{13} are degraded completely, C_{14} are degraded to about 90%, C_{16} and C_{17} are degraded to about 50%; the degradation processes also occur on heavier compounds up to C_{20}.

This preliminary work suggests to carry on the study analysing the following topics:

- Still increase the percentage of TiO2 to find the optimum value or use in addition other semiconductor oxides such as Fe_2O_3.
- Examine the photocatalytic effect of pH, which is a parameter that has not been considered here. In the literature a relationship between the nature of the substance to be degraded and the pH value is reported.
- Investigate in depth the effect of hydrogen peroxide (different volumes and different percentages).
- Evaluate the effect of other solvents (acetone, alcohols) able to make water and hydrocarbons compatibles. It will be helpful to examine the behaviour of these solvents in the conditions of photocatalysis to take into consideration the fact that they can produce catalytically active species.
- Study the substances formed during the degradation. However comparing the GC-MS of the initial extracts with those of the postphotocatalytic products, the presence of

new signals is not detected; it can be interpreted as an indication that aliphatic hydrocarbons with the photocatalytic process leads mainly to the formation of CO_2.

REFERENCES

Aliabadi M., Sagharigar T., 2011. *Photocatalytic removal of rhodamine-b from aqueous solutions using TiO_2 nanocatalyst.* Journal of applied environmental and biological sciences 1(12) 620-626

Battiston S., 2010. *Preparazione e caratterizzazione di compositi C/TiO_2 per lo sviluppo di materiali fotoattivi nanostrutturati.*

Brezová V., Blazková A., et al., 1997. *Phenol decomposition using Mn+/TiO_2 photocatalysts supported by the sol-gel technique on glass fibres.* Journal of Photochemistry and Photobiology A: Chemistry 109(2): 177-183.

Carp O., Huisman C.L., et al., 2004. *Photoinduced reactivity of titanium dioxide.* Progress in Solid State Chemistry 32(1-2): 33-177.

Choi W., Termin A., et al., 2002. T*he role of metal ion dopants in quantum-sized tio_2: correlation between photoreactivity and charge carrier recombination dynamics*. The Journal of Physical Chemistry 98(51): 13669-13679.

Dong D., Gu J., Kong L., Zheng Y., Li X., 2010. *Photocatalytic degradation of phenanthrene on soil surfaces in the presence of nanometer anatase TiO_2 under UV-light;* Chemical Engineering Journal Volume 158, Issue 3, 378–383.

Dvoranová D., Brezová V., et al., 2002. *Investigations of metal-doped titanium dioxide photocatalysts.* Applied Catalysis B: Environmental 37(2): 91-105.

Gräetzel M., 1983. *Energy resources through photochemistry and catalysis.* New York, Academic Press.

Hamerski M., Grzechulska J., Morawski A. W., 1999. *Photocatalytic purification of soil contaminated with oil using modified TiO_2 powders.* Solar Energy Volume 66, Issue 6, Pages 395–399.

Herrmann J. M., Tahiri H., et al., 1997. *Characterization and photocatalytic activity in aqueous medium of TiO_2 and Ag-TiO_2 coatings on quartz*" Applied Catalysis B: Environmental 13(3-4): 219-228.

Higarashi M., Wilson F., 2002. *Remediation of pesticide contaminated soil using TiO_2 mediated by solar light.* Catalysis Today 76 201-207.

Hoffmann M. R., Martin S. T., et al., 1995. *Environmental applications of semiconductor photocatalysis.* Chemical Reviews 95 (1): 69-96.

Kaneko M., Okura I., 2002. *Photocatalysis: Science and Technology.*

Kudo A, Miseki Y., 2009. *Heterogeneous photocatalyst materials for water splitting.* Chemical Society Reviews 38(1): 253.

McGeever C. E., 1983. *Effect of hydrogen peroxide on photocatalysis of perchloroethylene in aqueous suspensions of titanium dioxide.*

Moon J., Takagi H., et al., 2001. *Preparation and characterization of the Sb-doped TiO_2 photocatalysts.* Journal of Materials Science 36(4): 949-955.

Ohtani B., Mahaney P., O.O., Li D., Abe R., 2010. *What is Degussa (Evonik) P25? Crystalline composition analysis, reconstruction from isolated pure particles and photocatalytic activity test.* Journal of Photochemistry and Photobiology A : Chemistry, 216(2-3): 179-182.

Rocca A., Leopardi A., 2004. *I materiali fotocatalitici.*

Tanaka K., Hisanaga T., Harada K., 1990. *Photocatalytic degradation of organochloride compounds in suspended TiO_2.* Journal photochem. Photobiol A : Chem. 54, 113-118.

Teodorescu, V. S., Blanchin M.G., et al., 1999. *XTEM study of Al doped TiO_2 anatase epitaxial films deposited on MgO by pulsed laser deposition.* Journal of Materials Science 34(22): 5469-5476.

Tobaldi D.M., 2009. *Materiali ceramici per edilizia con funzionalità fotocatalitica.*

Turolla A, 2010. *Elettrofotocatalisi eterogenea su biossido di titanio: modellizzazione del reattore e studio delle cinetiche.*

Wang Y., H. Cheng, et al., 1999. *Preparation, characterization and photoelectrochemical behaviors of Fe(III)-doped TiO_2 nanoparticles.* Journal of Materials Science 34(15): 3721-3729.

Wanga Y., Liua C.S., Lia F.B., Liua C.P., Liangb J.B., 2008. *Photodegradation of polycyclic aromatic hydrocarbon pyrene by iron oxide in solid phase*; Journal of Hazardous Materials Volume 162, Issues 2–3, 716–723.

Yamashita H., Harada M., et al., 2001. *Application of ion beam techniques for preparation of metal ion-implanted TiO_2 thin film photocatalyst available under visible light irradiation: metal ion-implantation and ionized cluster beam method.* Journal of Synchrotron Radiation 8(2): 569-571.

Zhanga L., Peijun L., Zongqiang G., Xuemei L., 2008. *Photocatalytic degradation of polycyclic aromatic hydrocarbons on soil surfaces using TiO_2 under UV light;* Journal of Hazardous Materials Volume 158, Issues 2–3, 478–484.

AKNOWLEDGEMENT

Ringrazio i miei relatori professor Roberto Raga per i suoi consigli e la sua supervisione e la professoressa Roberta Bertani per la sua costante presenza e disponibilità.

Un ringraziamento particolare va a coloro che mi hanno sopportata in questi 6 mesi di laboratorio: Fabio, Flavio e Paolo che mi hanno accolta e aiutata.

I ringraziamenti più sentiti vanno alla mia famiglia che mi è sempre stata vicina e che lo sarà sempre: questo successo è anche vostro.

Grazie ad Ale che mi è sempre accanto e che mi ha aiutato in mille situazioni. Grazie perchè nonostante tutto siamo ancora qua a sopportarci, a litigare, a volerci bene, a sorriderci.

Ringrazio tutti i miei amici! Tutti coloro che mi hanno accompagnato in questi anni attraverso momenti belli e momenti brutti: ci siamo divertiti, abbiamo faticato, abbiamo riso e anche pianto ma lo abbiamo fatto insieme. Grazie perchè ognuno di voi è stato e sarà fondamentale. Vi voglio bene.